P2X PURINERGIC RECEPTORS IN CHEMOAFFERENT NEURONS

EXPRESSION OF P2X PURINOCEPTOR SUBUNITS IN THE RAT CAROTID BODY CHEMOAFFERENT PATHWAY: REGULATION BY CHRONIC HYPOXIA.

By

MONA PRASAD, B. SC. H.

A Thesis
Submitted to the School of Graduate Studies
in Partial Fulfillment of the Requirements
for the Degree

Master of Science

McMaster University

MASTER OF SCIENCE (2001) McMaster University
(Biology) Hamilton, Ontario

TITLE: Expression of P2X Purinoceptor Subunits in the Rat Carotid Body Chemoafferent pathway: Regulation by Chronic Hypoxia.

AUTHOR: Mona Prasad, B. Sc. (McMaster University)

SUPERVISOR: Dr. Colin A. Nurse

NUMBER OF PAGES: xiii, 109

ABSTRACT

Hypoxic chemotransmission in the rat carotid body (CB) is mediated in part by ATP acting on P2X purinoceptors. Here we use RT-PCR, cloning, and sequencing techniques to show P2X2 and P2X3 receptor expression in petrosal neurons (PN). Confocal immunofluorescence indicated co-localization of P2X2 and P2X3 protein in many petrosal neurons and CB afferent terminals *in situ*.

Petrosal and nodose neurons share a similar developmental origin (i.e. the ectodermal placodes) and GDNF is a required survival factor for both the neuronal groups. However, in the present study the profiles of P2X receptor subunit expression in the petrosal and nodose neurons differed from each other. The PNs showed a slight increase in the expression of P2X2 and P2X3 mRNA by P-21, whereas in nodose neurons the corresponding expression levels peaked by P-9, but fell significantly by P-21. However, in both cases the expression levels for the P2X2 mRNA were higher than those of P2X3 mRNA and the expression profile for both the P2X subunits developed along a parallel time course.

Previous developmental studies have indicated that expression levels of various autoreceptors on type I cells (e.g. DA D2-receptors, A2a and A2b adenosine receptors) change during the first week of postnatal life, as the animal breathes normoxic air. In the present study, the possibility that oxygen tension might regulate P2X receptor expression on type I cells was examined. RT-PCR

was employed to compare expression levels of the P2X subunits in isolated type I cells grown under different O_2 tensions. Compared to normoxic (20% O_2) control, a two-fold increase in expression of P2X2 mRNA was observed in type I cell clusters grown under chronic hypoxia (6% O_2). Immunofluorescence studies also indicated an up-regulation in P2X2 and P2X3 protein expression in type I cells grown under CHox. Thus, ATP and P2X2/P2X3 purinoceptors play an important role under normal conditions and following exposure to chronic hypoxia.

ACKNOWLEDGEMENTS

I would like to thank Dr. Colin A. Nurse for being a brilliant supervisor for his support, guidance and encouragement. Secondly I would like to thank Cathy Vollmer for her patience and hard work in isolating/preparing cells for my never-ending experiments. I would also like to thank all members of my lab: Dr. Ian Fearon, Dr. Min Zhang, Mike Jonz and Veronica Campanucci for all their help and advice. Special thanks to my committee members: Drs. Ana Campos and Eva Werstiuk for their guidance. I would also like to thank Dr. Muller's lab for the use and supply of equipment, especially Dr. Mike Liang.

I would like to thank my parents for their endless support in my quest for knowledge, to my siblings: Rachna, Abby and Sanjay for their laughter and encouragement. Last, but not least to my friends for all the good times.

TABLE OF CONTENTS

INTRODUCTION 1

CELLS INVOLVED IN THE CHEMOTRANSDUCTION PATHWAY 4

Type I or Glomus Cells of the Carotid Body 4

Petrosal Ganglia 4

Nodose Ganglia 5

NEUROTRANSMITTERS INVOLVED IN THE CHEMOTRANSDUCTION PATHWAY 6

Acetylcholine 6

Dopamine 7

Adenosine 7

ATP 8

MODEL OF CHEMOTRANSDUCTION 10

A REVIEW OF MOLECULAR TECHNIQUES USED IN THIS STUDY 11

PCR: 11

RT-PCR 12

Quantitative RT-PCR using LightCycler 13

Cloning 14

AIMS OF THIS THESIS 16

PREFACE 18

CHAPTER 1 EXPRESSION OF P2X RECEPTOR SUBUNITS IN RAT CAROTID BODY CHEMOAFFERENT NEURONS 19

SUMMARY 19

INTRODUCTION 19

MATERIALS AND METHODS 23

Isolation of petrosal, and type 1 cells 23

Confocal Immunofluorescence 24

Reverse transcriptase polymerase chain reaction (RT-PCR) 26

Cloning and sequencing of P2X2 and P2X3 PCR products 29

RESULTS 30

RT-PCR Identification of P2X mRNA in Isolated Petrosal Neurons 30

Cloning and sequencing of P2X2 and P2X3 PCR products 33

Localization of P2X2 and P2X3 Subunits in isolated petrosal neurons by Confocal Immunofluorescence 33

DISCUSSION 39

CHAPTER 2 COMPARISON OF P2X PURINOCEPTOR SUBUNIT EXPRESSION IN PETROSAL AND NODOSE NEURONS DURING DEVELOPMENT USING QUANTITATIVE RT-PCR **43**

SUMMARY 43
INTRODUCTION 43
MATERIALS AND METHODS 46
Isolation of petrosal and nodose cells and RNA 46
Reverse transcriptase polymerase chain reaction (RT-PCR) 46
Quantitative RT-PCR using LightCycler 47
Confocal Immunofluorescence 49
RESULTS 50
Developmental changes in the expression of P2X subunits in the Petrosal and Nodose ganglia 50
Localization of P2X2 and P2X3 Subunits in isolated Nodose neurons by Confocal Immunofluorescence 58
Comparison of developmental profile of dopamine content in the carotid body with mRNA levels of P2X subunits in isolated petrosal neurons 58
DISCUSSION 61

CHAPTER 3 UP-REGULATION OF PURINERGIC RECEPTORS IN TYPE I CELLS DURING CHRONIC HYPOXIA **66**

SUMMARY 66
INTRODUCTION 67
MATERIALS AND METHODS 68
Isolation of type 1 cells and RNA 68
Reverse transcriptase polymerase chain reaction (RT-PCR) 69
Quantitative RT-PCR using LightCycler 70
Confocal Immunofluorescence 70
RESULTS 71
Detection of P2X2 and P2X3 mRNA in isolated CB type I cells by RT-PCR 71
Detection and quantitative analysis of P2X2 and P2X3 mRNA in isolated CB type I cells grown under chronically hypoxic conditions 73
Expression of P2X2 and P2X3 subunits in isolated glomus clusters cultured with cAMP and PKA blocker as revealed by Confocal Immunofluorescence 73
DISCUSSION 77

GENERAL CONCLUSION 82

REFERENCES 86

APPENDIX 1 EXPRESSION OF P2X SUBUNITS IN RAT ADRENAL MEDULLARY CHROMAFFIN CELLS 104

LIST OF FIGURES AND TABLES

INTRODUCTION

Figure 1: Diagram of the Carotid Body and Chemoafferent Pathway. 2

CHAPTER 1

Figure 1.1 The P2X purinergic receptor channels differ among themselves with respect to the rates of desensitization during prolonged agonist stimulation. 21

Figure 1.2 Map of pCR 4-TOPO vector (Invitrogen) used to sub-clone the P2X subunits. 22

Figure 1.3 Detection of mRNA for P2X2, P2X3 and β-actin in isolated petrosal neurons. 31

Figure 1.4 Primer fragment alignments for both P2X2 and P2X3 subunit with specific primers. 32

Figure 1.5 Sequence alignments for both P2X2 and P2X3 cloned subunit from the petrosal neurons. 34

Figure 1.6 Petrosal Neuron in culture immunostained with TH and P2X3 subunit. 35

Figure 1.7 Petrosal Neurons in culture immunostained with NF and P2X2/P2X3. 37

Figure 1.8 Expression of P2X2 and P2X3 subunits in tissue sections of petrosal ganglia and carotid body as revealed by Confocal Immunofluorescence. 38

CHAPTER 2

Figure 2.1 Overall Experimental Methods for the Quantitative RT-PCR using LightCycler System – Flowchart. 48

Figure 2.2 Melting Curve Analysis for ß –actin. 51

Figure 2.3 Melting Curve Analysis for P2X2 receptor subunit. 52

Figure 2.4 Melting Curve Analysis for P2X3 receptor subunit. 53

Figure 2.5 Quantitative analysis of the P2X2 and P2X3 mRNA expression in isolated petrosal neurons during postnatal development. 54

Figure 2.6 Quantitative analysis of the P2X2 and P2X3 mRNA expression in isolated nodose neurons during postnatal development. 55

Figure 2.7 Detection of mRNA for P2X2, P2X3 and β-actin in isolated petrosal and nodose neurons at developmental ages E-21, P-1, P-6, P-9 and P-21. 57

Figure 2.8 Expression of P2X2 and P2X3 subunits in tissue sections of nodose ganglia as revealed by Confocal Immunofluorescence. 59

Figure 2.9 Comparison of developmental profile of dopamine content in the carotid body with mRNA levels of P2X subunits in isolated petrosal neurons. 60

CHAPTER 3

Figure 3.1 Detection of mRNA for P2X2, P2X3 and β-actin in isolated CB type I cells. 72

Figure 3.2 Detection of mRNA for P2X2, P2X3 and β-actin in isolated type I cell clusters cultured in chronic hypoxia. 74

Figure 3.3 Quantitative analysis of P2X2 and P2X3 mRNA in isolated type I cell clusters grown in chronic hypoxia. 75

Figure 3.4 Expression f P2X2 and P2X3 subunits in isolated type I cell clusters cultured in chronic hypoxia as reveled by confocal immunofluorescence. 76

Figure 3.5 Expression f P2X2 and P2X3 subunits in isolated type I cell clusters cultured with cAMP and PKA blocker as reveled by confocal immunofluorescence. 78

GENERAL CONCLUSIONS

Figure 1 Schematic diagram of proposed schema for CB chemotransmission involving ATP, ACh, adenosine and DA. 85

APPENDIX 1

Figure A.1 Detection of mRNA for P2X2, P2X3 and β-actin in rat AMC and MAH cells. 106

Figure A.2 Expression of P2X2 and P2X3 subunits in cultured rat adrenal medullary chromaffin and MAH cells as revealed by Confocal Immunofluorescence. 107

LIST OF TABLES

CHAPTER 1

TABLE 1.1: List of Primer Sequences used in this study. 28

APPENDIX 1

Table A.1 Expression of P2X2 and P2X3 subunits in various cell types. 108

INTRODUCTION

Breathing is tightly regulated in mammals resulting in the maintenance of appropriate oxygen levels in the blood that is crucial for cell survival. The delivery of oxygen is required for energy production and the removal of carbon dioxide, a by-product of cellular metabolism, is essential in maintaining homeostatic control. In mammals the sensory cells responsible for the maintenance of oxygen levels in the blood are the peripheral arterial chemoreceptors (Gonzalez *et al.*, 1994). The main peripheral chemoreceptor is the carotid body (CB), a small sensory organ located at the bifurcation of the common carotid artery. The CB contains specialized chemoreceptor cells, i.e. glomus or type I cells, which sense arterial Po_2, Pco_2 and pH and release a variety of neurotransmitters. These in turn determine the action potential frequency in the sensory fibers of the carotid sinus nerve (CSN; Gonzalez *et al.*, 1994), which innervates the CB. Fibers from the carotid sinus nerve that are postsynaptic to the chemoreceptor cells have cell bodies in the petrosal ganglion. The central processes of these petrosal neurons carry chemosensory information towards the central pattern generator in the brainstem, which regulates changes in ventilation (Figure 1).

Several neurotransmitters, such as, acetylcholine, serotonin, and dopamine are known to be stored and released by type I cells (Gonzalez *et al.*, 1994). Burnstock *et al.* (1972) postulated that adenosine triphosphate (ATP) or a related nucleotide was the transmitter substance released by non-adrenergic nerves in the gut. In the past three decades extracellular ATP has been assigned the role of a neurotransmitter and/or

Figure 1: Diagram of the Carotid Body and Chemoafferent Pathway. The diagram illustrates the carotid body, the chemoafferent petrosal ganglion and adjacent nodose ganglion. Type I cells and blood vessels are indicted by *arrows*. The type I cells sense changes in PO_2, PCO_2 and pH and send chemosensory signals via the carotid sinus nerve and the petrosal ganglia to the respiratory center in the brainstem. **SCG**: Superior Cervical Ganglion, **CSN**: Carotid Sinus Nerve.

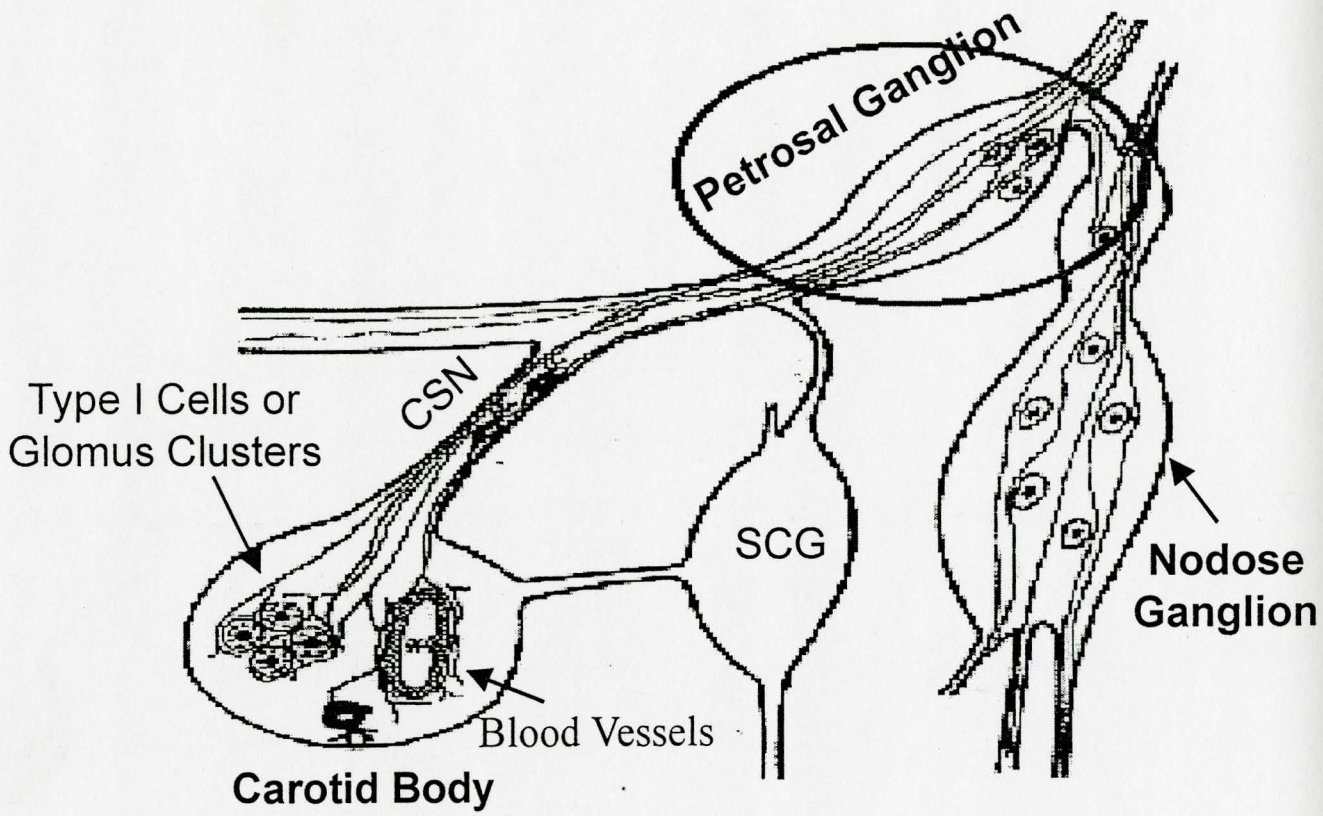
Petrosal Ganglion
CSN
Type I Cells or
Glomus Clusters
SCG
Nodose
Ganglion
Blood Vessels
Carotid Body

neuromodulator in various systems (Collo *et al.*, 1996; Zimmerman, 1994). ATP acts as a neurotransmitter in the central nervous system. ATP is produced when large biochemical molecules such as carbohydrate, fatty acids and protein are catabolized. The hydrolysis of one or more phosphate bonds from the ATP molecule releases free energy that is used for biochemical processes. In the past decade several ATP (purinergic) receptors have been identified and characterized pharmacologically, and seven different subunits have been cloned. Recently, a study carried out by Zhang *et al* (2000) demonstrated that ATP and ACh were co-released from rat CB type I cells onto chemoafferent petrosal neurons during hypoxic chemoexcitation. Immunocytochemical studies also demonstrated the presence of the P2X2 receptor subunit in these chemoafferent neurons (Zhang *et al*, 2000). The electrophysiological data, however, were not consistent with the presence of homomeric P2X2 receptors. Rather, the responses elicited when ATP was applied to functional petrosal neurons in co-culture (i.e. those that were responsive to a hypoxic stimulus) suggested the presence of heteromeric P2X2/P2X3 receptors. P2X3 receptor subunits were therefore proposed to heteropolymerize with the P2X2 subunits in the formation of functional purinoceptors in these neurons.

In this thesis, the expression of the P2X2 receptor subunit and the hypothesized P2X3 subunit was investigated using reverse transcriptase–polymerase chain reaction (RT-PCR) applied to the mRNA extracted from isolated chemoafferent (petrosal) neurons. Further studies were performed to elucidate the developmental expression pattern of these P2X receptor subunits over the first 3-weeks of postnatal life. This was

of interest since Donnelly and Doyle (1994) have shown that CB sensitivity to hypoxia undergoes postnatal maturation, reaching adult sensitivity in the rat around 3 weeks after birth. The expression of the P2X2 and P2X3 receptor subunits was also studied in isolated CB type I cell clusters grown under normoxic or chronically hypoxic conditions, using quantitative RT-PCR. Finally, complementary immunocytochemical studies were employed to correlate expression of these P2X receptor subunits at the protein level.

CELLS INVOLVED IN THE CHEMOTRANSDUCTION PATHWAY

Type I or Glomus Cells of the Carotid Body

The carotid body (CB) is formed by clusters of cells, surrounded by a dense network of capillaries. The blood supply to these capillaries originates from the common carotid artery (McDonald *et al*, 1983). The clusters of cells consist of two different cell types; i) type I or glomus cells, which are round or ovoid cells (diameter 10-12 μm) arranged in clusters, sense changes in Po_2, Pco_2 and pH (Gonzalez *et al*, 1994); and ii) the type II or sustentacular cells which are located mainly at the periphery of the clusters and are glial-like supporting cells (Gonzalez *et al*, 1994). The CB consists of about 40, 000 glomus cells in the rat and 5-30 glomus cells per cluster are encased with 2-3 type II cells (McDonald, 1981). The carotid sinus nerve or CSN is the branch of the glossopharyngeal nerve (nerve IX) that contains chemoreceptive axons, which innervate the CB (McDonald *et al.*, 1983). The type I cells release several neurotransmitters such as acetylcholine (ACh), adenosine triphosphate (ATP), dopamine (DA) and serotonin (5-

hydroxytryptamine; 5-HT). Some of these neurotransmitters, e.g. ACh and ATP have excitatory properties (Zhang *et al.*, 2000), whereas DA appears to have an inhibitory effect on CB chemotransmission (Herztberg *et al*, 1990; Gonzalez *et al.*, 1994).

Petrosal Ganglia

Fibers from the carotid sinus nerve that are postsynaptic to the glomus cells have cell bodies in the petrosal ganglion (PG). Central processes from the PG carry chemosensory information towards brainstem and modulate the increase in ventilation during hypoxia (Figure 1) The PG expresses receptors for ACh, DA, 5-HT, GABA (Gonzalez *et al.*, 1994; Zhong and Nurse, 1999; Zhang and Nurse, 2000, Zhong *et al.*, 1997), substance P (Prabhakar *et al.*, 1984), and NO (Prabhakar *et al.*, 1993). The current study will for the first time provide direct evidence that P2X ATP receptor subunits are also expressed in PG chemoafferent neurons.

Nodose Ganglia

Located adjacent to the petrosal ganglion is the nodose ganglion (NG), which supplies sensory innervation to the visceral organs. Approximately 2% of NG fibers innervate the CB (Finley *et al.*, 1992). As reported by Virgino *et al* (1998), all neurons in the nodose ganglion were immunoreactive for both P2X2 and P2X3 purinergic receptor subunits. Petrosal and nodose neurons share a similar developmental origin (i.e. the ectodermal placodes) and GDNF is a survival factor for both of these neuronal groups

(Erickson *et al.*, 2000). In this study, NG neurons were used as a positive control for studies on the developmental pattern of P2X subunit expression in the PG.

NEUROTRANSMITTERS INVOLVED IN THE CHEMOTRANSDUCTION PATHWAY

Acetylcholine

Acetylcholine (ACh) is a neurotransmitter synthesized from choline and acetyl-CoA through the action of the enzyme choline acetyltransferase (ChAT). At cholinergic synapses the influx of Ca^{2+} stimulates the exocytosis of presynaptic vesicles containing ACh, which is thereby released into the synaptic cleft. Recently, using a co-culture preparation of CB type I cells and petrosal neurons, strong evidence was provided for the co-release of ACh and ATP during hypoxic chemosensory signaling (Zhong *et al.* 1997, Nurse and Zhang, 1999). These neurotransmitters acted via nicotinic ACh (nAChR) and P2X purinergic receptors, respectively. ACh and nicotine have also been shown to augment CSN discharge that in turn increases ventilation when administered intravascularly *in vivo* (Gonzalez *et al.*, 1994). These findings, together with the demonstration that rat type I cells express cholinergic markers, e.g. ChAT, acetylcholinesterase and vesicular ACh transporter (Nurse and Zhang, 1999), support the notion that ACh is an important excitatory neurotransmitter in the rat CB.

Dopamine

Catecholamines are neurotransmitters formed from the amino acid tyrosine. Dopamine (DA) is the major catecholamine synthesized by CB type I cells (Gonzalez *et al.*, 1994). Hertzberg *et al* (1990) have proposed that dopamine (DA) is an inhibitory neurotransmitter / neuromodulator in the chemotransduction pathway. They postulated that the increase in CB sensitivity seen after birth is due, at least in part, to a decrease in the release of dopamine and thus the removal of the inhibitory mechanism (Hertzberg *et al.*, 1990). In some species, the CSN chemosensory discharge was attenuated by dopamine at low doses, but stimulated at higher doses (Gonzalez *et al.*, 1994; Bairam *et al.*, 1998). Dopamine D2-receptors and dopamine D1-receptors are expressed in both adult rat CB and petrosal ganglia (Bairam *et al.*, 1997; Gauda *et al.*, 1997; Bairam *et al.*, 1998). However, depletion of DA in rat CB following administration of the drug reserpine, had minimal effect on the hypoxic chemosensory discharge (Donnelley, 1996). Thus, DA is unlikely to act as an excitatory transmitter in rat CB chemotransmission.

Adenosine

Adenosine derived from ATP is neither stored in vesicles nor released as a classical neurotransmitter, i.e. via exocytosis. Extracellular ATP is degraded by ecto-nucleotidases on the cell membrane to produce adenosine (Cunha and Riberio, 2000). RT-PCR studies have shown that rat carotid body type I cells express adenosine A_{2a} and A_{2b}, but not A_1 and A_3 receptors (Kobayashi *et al.*, 2000). However, A_1 adenosine receptors are expressed in the petrosal ganglion (Gauda *et al.*, 2000). Rocher *et al.*

(1999) have proposed that the A_1 adenosine receptors in the petrosal ganglia have an inhibitory role in the CB chemotransmission.

ATP

Extracellular ATP is thought to serve as a neurotransmitter, neuromodulator, cytotoxin and mitogen in various systems (Collo *et al.*, 1996). ATP plays important roles in diverse tissue functions that include fast excitatory neurotransmission, developmental processes, pulmonary function, nociception, auditory and ocular function, the apoptotic cascade, astroglial cell function, metastasis formation, bone and cartilage disease and platelet aggregation/homeostasis (Burnstock, 2000; Burnstock and Williams, 2000; Dunn *et al.*, 2001). Purinergic receptors have become well-studied and important mediators for a broad range of intercellular signaling pathways in various tissues (Burnstock, 1997; North *et al.*, 1997). These receptors are comprised of two main groups, the ionotropic P2X receptors and the metabotropic (G-protein coupled) P2Y receptors. In the nervous system, purinergic excitatory synapses use ATP to mediate fast synaptic transmission via activation of P2X-receptor cation channels (Surprenant *et al.*, 1995; North and Surprenant, 2000). P2X receptors are members of a multigene family of ATP-gated ion channels and consist of at least seven receptor subunits, P2X1-P2X7 (Buell *et al.*, 1996; Collo *et al.*, 1996; Khakh *et al.*, 2001). In neural tissues, the expression of P2X2, P2X3, P2X4 and P2X6 subunits is especially common (Lewis *et al.*, 1995; Vulchanova *et al.*, 1997; Khakh *et al.*, 1999), and though homomeric channels can account for ATP responses in some cases, heteropolymerization of P2X subunits may occur in both the

central and peripheral nervous system (Lewis *et al.*, 1995; Collo *et al.*, 1996; Torres *et al.*, 1999). To date four functional heteromultimers including P2X2/3, P2X4/6, P2X1/5 and P2X2/6 have been identified (King *et al.*, 2000). Both P2X2 and P2X3 receptors are highly expressed in sensory neurons (Luo *et al.*, 1999; Dunn *et al.*, 2001). Although their exact subunit stochiometry is controversial, most of the evidence supports the idea that P2X receptors assemble as trimers (Khakh, 2001). The muscle nicotinic acetylcholine receptor (nAChR) is the best-characterized ionotropic receptor. Each subunit of the nAChR has four transmembrane domains (4TMD), and four different subunits combine to form pentameric hetero-oligomers (Torres *et al.*, 1999, A). Unlike the nAChR, the purinergic P2X receptors have two transmembrane domains (2TMD), yielding a topology that places their amino- and carboxyl termini in the intracellular compartment. Mutagenesis studies indicated that second transmembrane domain is a critical determinant of P2X subunit assembly (Torres *et al.*, 1999, B).

Several splice variants for each of the P2X subunits exist. For example, three splice variants of the P2X2 have been identified in guinea pig cochlea. Heterologous expression of the wild type P2X2 receptor isoforms (i.e. P2X2-1, P2X2-2 and P2X2-3) from the rat resulted in the formation of functional homomeric receptors with different characteristics when transfected into HEK293 or human embryonic kidney cells (Chen *et al.*, 2000).

P2X receptors are present both pre- and post- synaptically. Activation of presynaptic P2X receptors can modulate release of several neurotransmitters, whereas postsynaptically, interactions of these receptors with ATP elicit excitatory synaptic

currents (Khakh, 2001). The P2X receptor channels differ among themselves with respect to the rates of desensitization during prolonged agonist stimulation, and each P2X receptor subtype has distinct characteristics. For example, α,β-methylene ATP (αβmetATP) has an agonist action on homomeric P2X3 receptors, while homomeric P2X2 receptors are not affected by αβmetATP (Vulchanova *et al.*, 1997; Virginio *et al.*, 1998). The expression of P2X2/P2X3 subunit mRNA and protein will be studied in the PG, NG and CB type I cells in this thesis to elucidate the possible role of ATP and P2X receptors in carotid body chemotransmission.

MODEL OF CHEMOTRANSDUCTION

The CB senses a decrease in arterial Po_2 and the information is transmitted to the respiratory center in the brainstem, resulting in an increase in breathing pattern. At normal blood Po_2 (100 mmHg), Pco_2 (40 mmHg) and pH (7.4) the firing frequency of the chemoreceptor cells is < 2 impulses per second per fiber (Fidone *et al.*, 1986). The frequency is increased when blood Po_2 and/or pH decreases or when Pco_2 is increased.

Two hypotheses have been proposed to account for the mechanism by which type I cells transduce a hypoxic stimulus. One hypothesis assumes that a heme- containing and/or a redox-sensitive enzyme is the oxygen sensor and that a biochemical event associated with the heme protein triggers the chemotransduction cascade (Lahiri *et al.*, 2000). Biscoe *et al.* (1989) postulated that cytochromes in the mitochondria present in CB type I cells are the oxygen sensors. The second hypothesis suggests that a K^+ channel

protein is the primary oxygen sensor and that inhibition of this channel by hypoxia depolarizes the cell and opens voltage gated Ca^{2+} channels. The Ca^{2+} influx then triggers neurotransmitter release (Lopez-Barneo *et al.*, 1988, Prabhakar, 2000). Both hypotheses for chemosensory transduction require further testing, though it is also possible that a separate protein sensor (e.g. in mitochondria or plasma membrane) may signal K^+ channel inhibition via cytosolic factors, (e.g. ATP or reactive oxygen species; Prabhakar, 2000)

A REVIEW OF MOLECULAR TECHNIQUES USED IN THIS STUDY

PCR

The Polymerase Chain Reaction (PCR) was developed by Kary Mullis in the mid-1980s and has revolutionized molecular genetics. PCR enables the experimenter to produce an enormous number of copies of specific DNA sequences from a small amount of sample (Watson *et al.*, 1997). Essential components of PCR are: template DNA (the target DNA to be amplified), primers, deoxynucleoside triphosphates (dNTP's) – dATP, dGTP, dTTP, and dCTP, DNA polymerase (for PCR thermostable *Taq* polymerase is used), and magnesium chloride.

The PCR exploits certain features of DNA replication. First, the 3' hydroxyl can be provided by the primers, which are sequences of ~ 20 nucleotides. These can be constructed as desired by the researcher to complement any location on the target gene. Two primers, the upstream (left or forward) and the downstream (right or reverse) are

complementary to sites that flank the target sequence. Specific primers for target genes can be produced if the sequence of the gene is known, otherwise random sequenced primers can also be used to amplify DNA. Second, heat can be used to denature the double stranded DNA (dsDNA). The reaction mixture is heated to ~95°C to allow the strands to separate and then cooled rapidly to allow for primer annealing. Annealing temperature has to be optimal and can be calculated by determining the GC (guanine–cytosine) content of the primers, using the following equation: $T_M = 4$ (G+ C) + 2 (A + T), where T_M = melting temperature. The primers should have ~ 50% GC content for efficient priming (Sambrook *et al.*, 1989). The annealing temperature determines the accuracy of the primers' binding to the correct complementary sequences on the target gene; a high annealing temperature can increase the fidelity of the reaction (Kramer *et al.*, 1999). Third, the $MgCl_2$ concentration is critical in increasing hybridization stringency and preventing nonspecific primer-template interactions (Kramer *et al.*, 1999). Mg^{2+} is known to affect enzyme activity. In particular, improper dNTP's: Mg^{2+} concentration will reduce polymerase activity in the PCR. Magnesium ions also increase the melting temperature of dsDNA and form soluble complexes with dNTP's to produce a substrate that is recognized by the polymerase enzyme (Bustin *et al.*, 2000). The reaction mixture is placed in a thermocycler, a machine that can adjust the temperature of the reaction chamber quickly and uniformly at various time intervals (Robinson *et al.*, 1999). PCR goes through a programmed cycle that is repeated for ~ 35 cycles. After 32 cycles, one DNA fragment can be amplified to ~1,073, 741, 824 molecules (Watson *et al.*, 1997). The amplified DNA can be detected by agarose gel electrophoresis. Nucleic acids can be

visualized by adding ethidium bromide to the agarose solution before the gel polymerizes. Ethidium bromide is a dye that displays enhanced fluorescence when intercalated between stacked nucleic acid bases. Irradiation of ethidium bromide – treated gels by UV illumination results in orange-red bands where nucleic acids are present (Boyer *et al.*, 1993).

RT-PCR

Reverse transcriptase – polymerase chain reaction (RT-PCR) is a modification of the original PCR where the main difference lies in the enzyme and template being used (Watson *et al.*, 1997). A RNA polymerase known as reverse transcriptase (RT) is used to convert mRNA target into a complementary DNA (cDNA) strand (Watson *et al.*, 1997). In RT-PCR the templates used are mRNA molecules that have poly-(A) tails. The primers used for RT-PCR are usually made up of dTTPs, a chain of ~ 20 thymines, this is also known as oligo-dTs. The oligo-dTs primers anneal to the poly-(A) tail of the mRNA providing a 3' hydroxyl group for the RT enzyme. mRNA extracted from isolated cells are purified for the RT-PCR. RT-PCR is the most sensitive method for the detection of low-abundance mRNA, often obtained from limited tissue samples (Bustin *et al.*, 2000), as is the case for the petrosal neurons examined in this thesis. β-actin mRNA was one of the first RNAs to be used as an internal control, since it is expressed at moderately abundant levels in most cell types and encodes an ubiquitous cytoskeletal protein (Bustin *et al.*, 2000). RT-PCR, without the reverse transcriptase enzyme, was used as negative

controls in this study to ensure that the RNA samples were devoid of contaminating genomic DNA.

Quantitative RT-PCR using LightCycler:

The recent introduction of fluorescence-based kinetic RT-PCR procedures significantly simplifies the process of producing reproducible quantification of mRNA (Bustin *et al.*, 2000). The LightCycler (Roche Molecular Biochemicals, Mannheim, Germany) performs PCR in small-volume glass capillary tubes, contained within a rotor-like carousel, which is heated and cooled in an air-stream (Wittwer *et al.*, 1989). The carousel is rotated past a light-emitting diode (LED) as the light source. Blue light (470 nm) from the LED is focused on the respective capillary tips exciting the fluorophore (i.e. SYBR Green 1 dye molecules, which bind to double-stranded DNA and emit the fluorescence signal; Rasmussen *et al.*, 1998). A photodetection diode channel detects the emitted fluorescent light. The unbound dye exhibits little fluorescence in solution, but during the elongation step, increasing amounts of dye bind to the nascent double-stranded DNA. When measured in real-time, the amount of fluorescence signal observed during the elongation step is increased, and falls off when the DNA is denatured. Therefore, fluorescence measurements at the end of the elongation step of every PCR cycle reflect increasing amount of amplified DNA. The fluorescence data resulting from each reaction sample are determined entirely by the primers used. Consequently, in the presence of any double-stranded DNA, fluorescence is generated and this includes non-specific binding of the primers to each other, i.e. primer dimers. To overcome this problem a Melting

Curve Analysis (MCA) is carried out at the end of the PCR. The temperature is slowly raised in the thermal chamber and this causes the dsDNA to denature, releasing the SYBR Green 1 dye. During this process fluorescence is measured at frequent intervals (0.1°C) and the decrease in fluorescence is measured. Plotting fluorescence as a function of temperature generates a melting curve for the amplicon and a characteristic melting peak at the melting temperature (T_M) is obtained. The specific melting peak of an amplicon occurs at a higher temperature, and is distinguishable from amplification artifacts that occur at a lower melting temperature and over broader, non-specific peaks (i.e. primer dimers; Bustin *et al.*, 2000).

Cloning

Cloning allows for the amplification and recovery of a specific gene from a large, complex DNA sample such as a genome (Watson *et al.*, 1997). Plasmids are small circular double stranded extrachromosomal, independently replicating DNA molecules that can be isolated from *E. coil* colonies by the alkaline lysis mini prep protocol (Kramer *et al.*, 1999). These plasmids are used as vectors, i.e. vehicles that carry DNA into an organism for amplification. Sequencing of these plasmids, that carry cDNA of genes that are expressed in low quantities, is then feasible.

In this study, the TOPO TA Cloning Kit for Sequencing was used (Invitrogen). The pCR 4-TOPO vector is unique from other vectors, since it contains single 3' thymine (T) overhangs that can anneal to the single deoxyadenosine (A) overhangs. The latter (deoxyadenosine overhangs) are added on by *Taq* polymerase that has a non-template-

dependent terminal transferase activity (Invitrogen). Topoisomerase is covalently bound to both ends of the vector, which catalyses the ligation reaction. Once the poly-(A) overhangs from the PCR fragment bind to the poly-(T) overhangs of the vector, the topoisomerase (at room temperature) can form a phosphodiester bond that ligates the two components together. The ligated closed vector is then transformed into competent *E. coli* cells (Invitrogen), which have been chemically modified so that they have increased membrane permeability and are capable of taking up plasmid DNA (Watson *et al.*, 1997).

The pCR 4-TOPO plasmid contains antibiotic resistance genes for Ampicillin and Kanamycin. The transformed cells are grown in Luria Bertani (LB) broth containing the antibiotic ampicillin. Thus, cells that grow on this medium are selected for the recombined plasmids that contain the PCR fragment (*N.B.* cells that do not contain the plasmids will die in the presence of ampicillin). The site at which the PCR fragment is inserted encodes a lethal *E. coli* gene, *ccdB*. The disruption of this *ccdB* gene by the insertion of the PCR fragment facilitates the survival of the transformed cells. These two mechanisms built into the vector ensure that cells selected on the LB/Ampicillin medium contain the PCR fragment in the recombined vector.

AIMS OF THIS THESIS

Based on the evidence that ATP is an important neurotransmitter in rat CB chemotransmission, one aim of this thesis was to clarify the molecular identity and location of the ATP receptors expressed in the chemoafferent pathway. Chapter 1

describes the expression of the P2X2 and P2X3 receptor subunits using RT-PCR and cloning techniques on isolated petrosal neurons (PN). Data from these molecular techniques are corroborated at the protein level by immunostaining with specific antibodies against both P2X2 and P2X3 subunits. Chapter 2 compares the developmental pattern of P2X subunit expression in the petrosal ganglia and nodose ganglia over the first 3 weeks (postnatal). mRNA levels were measured by quantitative RT-PCR using a real-time PCR (LightCycler) system. Chapter 3 measures and compares the mRNA levels of both P2X2 and P2X3 subunits in type I cells that were incubated in i) a normoxic or ii) a chronically hypoxic environment. Immunofluorescent detection of P2X2 and P2X3 protein subunits were carried out on cultured type I cells incubated in i) a control normoxic environment; ii) a hypoxic environment; iii) a normoxic environment with dibutyryl cyclic AMP present in the growth medium; and iv) a hypoxic environment in the presence of KT5720, a selective PKA blocker in the growth medium.

PREFACE

The data in the following chapter have been used in part for a publication in the *Journal of Physiology* (London): "Expression of P2X2 and P2X3 purinoceptor subunits in carotid body chemoafferent neurons: Role in PO_2 and PCO_2 signaling." co-authored by Mona Prasad, Ian M. Fearon, Min Zhang, Michael Laing, Cathy Vollmer and Colin. A. Nurse (**currently in press**). The following credit goes to the individuals who participated in this research mentioned in this chapter: Dr. I. Fearon provided the primer sequence for P2X2 subunit (357bp, listed in Table 1.1); Dr. M. Zhang provided the voltage-clamp recordings shown in Figure 1.1 and confocal data shown in Figure 1.8 panels D-F were provided by Cathy Vollmer, who also performed all dissections and cell preparations. Many thanks to all participants involved in this publication. (N.B. all data used were printed with permission).

CHAPTER 1

EXPRESSION OF P2X RECEPTOR SUBUNITS IN RAT CAROTID BODY CHEMOAFFERENT NEURONS

SUMMARY

Hypoxic chemotransmission in the rat carotid body (CB) is mediated in part by ATP acting on suramin-sensitive P2X purinoceptors. Here we use RT-PCR, cloning, and sequencing techniques to show P2X2 and P2X3 receptor expression in petrosal neurons, some of which develop functional chemosensory units with CB receptor clusters in co-culture. Confocal immunofluorescence indicated co-localization of P2X2 and P2X3 protein in many petrosal neurons and CB afferent terminals *in situ*. Thus ATP and P2X2/P2X3 purinoceptors play important roles in carotid body chemotransmission.

INTRODUCTION

Recent work in this laboratory demonstrated a role for ATP as a co-transmitter during hypoxic signaling in the rat carotid body, a peripheral chemosensory organ (Zhang *et al.*, 2000). This organ helps maintain blood homeostasis via the control of ventilation following changes in partial pressure of blood gases (Po_2 and Pco_2) and pH (Gonzalez *et al.*, 1994). With the aid of a co-culture model, clusters of carotid body chemoreceptors

(glomus or type I cells) developed functional synaptic connections with dissociated neurons from the petrosal ganglion (Zhang *et al.*, 2000), which supplies the main chemoafferent innervation to the organ. With this model of a chemosensory unit, it was shown that a hypoxic stimulus was transduced at the level of the type I cells, and that the information was transmitted to nearby petrosal neurons via co-release of ATP and ACh (Zhang *et al.* 2000). The purinergic receptors mediating the ATP component of the response were proposed to consist of P2X2/P2X3 heteromultimers (Zhang *et al.*, 2000). This hypothesis was based largely on the observation that physiologically identified, hypoxia-responsive neurons in co-culture showed slow desensitization kinetics following ATP application, and are activated by α,β-methylene ATP (α,β-metATP; see Figure 1.1). In addition, immunoreactive P2X2 subunits were localized to petrosal chemoafferent neurons and carotid body nerve endings *in situ* (Zhang *et al*, 2000).

In the present study, reverse transcriptase polymerase chain reaction (RT-PCR), where mRNA expressed in the cells is converted to cDNA, was used to identify and validate the presence of the P2X2 and P2X3 receptor subunits in petrosal neurons. PCR, carried out with specific primers for the P2X subunits, was used to amplify the cDNA obtained from a population of isolated petrosal neurons. In addition, cloning and sequencing techniques were used to confirm the identity of the RT-PCR products. The vector provided by the TOPO TA Cloning Kit for Sequencing (Invitrogen) was utilized to transform competent *E. coli* (TOPO One–Shot cells; Figure 1.2). The PCR fragment inserts in these sub-cloned plasmids were then sequenced.

Figure 1.1 The P2X purinergic receptor channels differ among themselves with respect to the rates of desensitization during prolonged agonist stimulation. A, B and **C** represent voltage-clamp recordings of ionic currents from different petrosal neurons (PN) in co-culture; the bar above the trace represents the duration of ATP application to the PN. These recordings are characteristic of the known responses for homomeric P2X2 (A), homomeric P2X3 (B) and heteromeric P2X2/P2X3 (C) receptors. All recordings were carried out under voltage clamp at a holding potential of -60mV. Data provided by Min Zhang; printed with his permission.

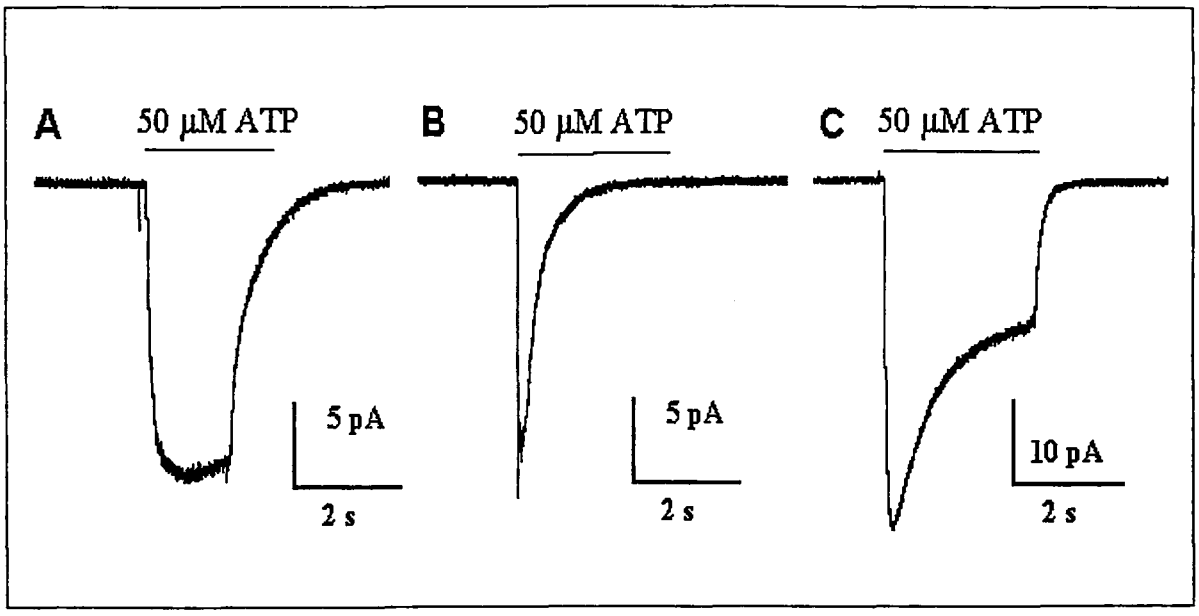
A
50 µM ATP
5 pA
2 s
B
50 µM ATP
5 pA
2 s
C
50 µM ATP
10 pA
2 s

Figure 1.2 Map of pCR 4-TOPO vector (Invitrogen) used to sub-clone the P2X subunits. The map shows the features of pCR 4-TOPO and the sequences surrounding the TOPO cloning site, as indicated by the circled area. The two arrows point to restriction sites for ***EcoR1***. Restriction endonucleases (RE) are site-specific endodeoxyribonucleases that cause cleavage of both strands of DNA at points within or near the specific site recognized by the enzyme and are important tools in genetic engineering (Lehninger et al., 1993). Restriction sites are palindromic sequences with two-fold axis of symmetry. These are regions that are recognized by RE, which cut double stranded DNA. The cuts can have 5' or 3' extensions or can be blunt ended. These ends are essential when a sequence of DNA from another organism has to be inserted into the plasmid. RE digest and mapping are used to determine whether or not the inserted PCR fragment is the correct one (Watson et al., 1997). In the present experiments the *EcoR1* RE was used to cleave the *EcoR1* sites in the pCR 4-TOPO vector.

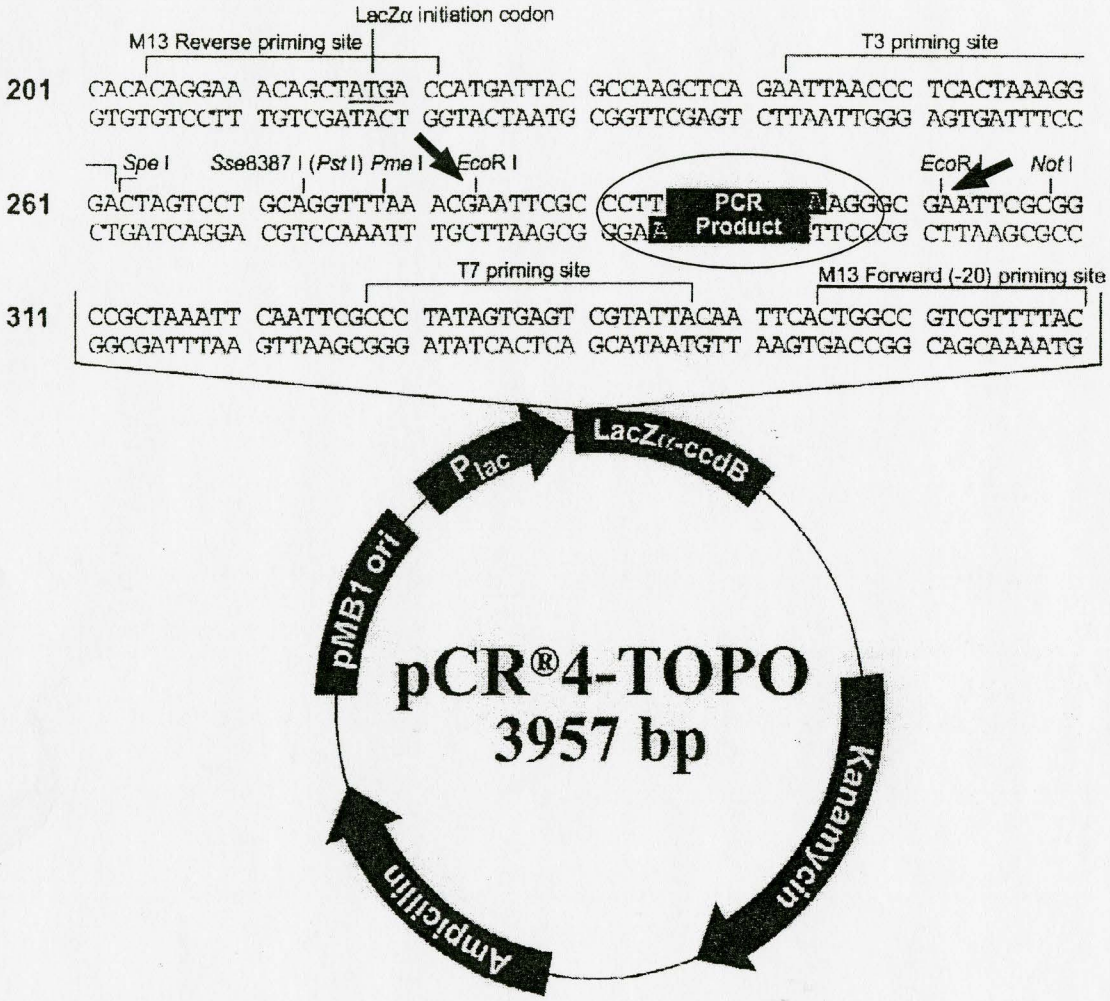
LacZα initiation codon
M13 Reverse priming site
T3 priming site
201
CACACAGGAA ACAGCTATGA CCATGATTAC GCCAAGCTCA GAATTAACCC TCACTAAAGG
GTGTGTCCTT TGTCGATACT GGTACTAATG CGGTTCGAGT CTTAATTGGG AGTGATTTCC
Spe I
Sse8387 I (Pst I)
Pme I
EcoR I
EcoR I
Not I
261
GACTAGTCCT GCAGGTTTAA ACGAATTCGC CCTT
PCR Product
AAGGGC GAATTCGCGG
CTGATCAGGA CGTCCAAATT TGCTTAAGCG GGAA
TTCCCG CTTAAGCGCC
T7 priming site
M13 Forward (-20) priming site
311
CCGCTAAATT CAATTCGCCC TATAGTGAGT CGTATTACAA TTCACTGGCC GTCGTTTTAC
GGCGATTTAA GTTAAGCGGG ATATCACTCA GCATAATGTT AAGTGACCGG CAGCAAAATG
P lac
LacZ(α-ccdB
pMB1 ori
pCR®4-TOPO
3957 bp
Kanamycin
Ampicillin

Double label immunofluorescence techniques were used to study the expression of P2X2 and P2X3 subunits at the protein level in petrosal neurons, which were identified with anti-neurofilament and anti-tyrosine hydroxylase antibodies.

Experiments performed in Chapter 1 introduce the molecular techniques used to characterize the P2X subunits and provide the basis for experiments in the following chapters.

MATERIALS AND METHODS

Isolation of petrosal neurons:

The carotid bifurcation, with attached nodose and petrosal complex, was excised after rat pups (Wistar; Charles River, Quebec) were first rendered unconscious by a blow to the back of the head (produced by rapid deceleration) and killed immediately by decapitation. All procedures for animal handling and tissue removal were carried out according to the guidelines of the Canadian Council on Animal Care (CCAC). Since in the rat, chemoafferent neurons are located in the distal one-third to one-half of the petrosal ganglion (Katz & Black, 1986; Finely, Polak & Katz, 1992), we isolated this region by pulling on the glossopharyngeal (IXth) nerve, which joins the ganglion at the distal end. Following separation from the IXth nerve, the excised ganglia were exposed to a 0.1% trypsin –0.1 % collagenase enzymatic solution (Gibco BRL Life Technologies, Burlington, ON, Canada) for 1 hr at 37°C and then mechanically dissociated with forceps. The dispersed cell solution was collected and triturated in growth medium containing:

F-12 nutrient medium (Gibco) supplemented with 10% (v/v) fetal bovine serum (Gibco), 80 U-1 insulin (Sigma Chemical Co., St. Louis, MO), 0.6% (w/v) glucose, 2mM glutamine and 1% penicillin-streptomycin (Gibco).

Confocal Immunofluorescence:

Cryostat sections of the carotid bifurcation and separate cultures of carotid body type 1 and petrosal neurons from 2- to 3 week-old rats were processed for immunofluorescence (Zhang *et al.*, 2000). For petrosal cultures, the cell suspension was plated onto a thin layer of Matrigel (Collaborative Research, Bedford, MA, USA) that was previously applied to the central wells of modified tissue-culture dishes. All cultures were grown at 37°C in a humidified atmosphere of 95% air-5% CO_2. Rat pups (2-3 weeks old) were first anesthetized by intraperitoneal administration of Somnotol (65 mg/kg), before perfusion via the aorta with phosphate-buffered saline (PBS) followed by PBS containing 4% paraformaldehyde. The carotid bifurcations were excised bilaterally and immersed in 4% paraformaldehyde for 1 hr at room temperature. Following incubation overnight in 20% sucrose at 4°C, sections (thickness, ~18 μm) were cut in a cryostat and collected on glass slides coated with 2% silane (Sigma Chemical Co., St. Louis, MO). After air drying onto glass slides, the sections were washed (3 x 5 min each) in PBS before exposure to a blocking solution containing 2% bovine serum albumin (BSA) in PBS (BSA/PBS) for ~45 min at room temperature, followed by overnight incubation at 4°C in a cocktail of the primary antisera. The primary antibodies were: (i) anti-neurofilament (NF; 1:500 dilution, a monoclonal antibody against NF 68kDa (Boehringer

Mannheim, Montreal), (ii) anti-tyrosine hydroxylase (TH; 1:1000 dilution), a polyclonal antibody against TH (Boehringer Mannheim) (iii) anti-P2X2 (1:800 dilution), a rabbit polyclonal antibody raised against a highly purified peptide corresponding to amino acid residues 457-472 of the rat P2X2 receptor (Alomone Laboratories, Jerusalem, Israel), (iv) anti-P2X3 (1:500 dilution), a guinea pig polyclonal antiserum raised against amino acid residues 383-397 of the rat P2X3 receptor (Neuromics, Minneapolis, MN, USA), and (vi) anti-P2X3 (1:60 dilution), a rabbit polyclonal antiserum raised against amino acid residues 383-397 of the rat P2X3 receptor (Oncogene Research Products, MA, USA). The secondary antibodies (Jackson Immunoresearch Laboratories, West Grove, PA) consisted of Cy3-conjugated goat anti-rabbit IgG (1:500 dilution), FITC-conjugated goat anti-mouse IgG (1:100 dilution), FITC-conjugated goat anti-guinea pig IgG (1:20 dilution) and Texas Red-conjugated goat anti-mouse IgG (1:50 dilution). The secondary antibodies used for visualizing the markers were as follows: i) NF - FITC-conjugated goat anti-mouse IgG or Texas Red conjugated goat anti-mouse IgG; ii) TH - Cy3-conjugated goat anti-rabbit IgG; iii) P2X2 - Cy3-conjugated goat anti-rabbit IgG and iv) P2X3 - FITC-conjugated goat anti-guinea pig IgG. Secondary antibodies were diluted in PBS containing 1% BSA, 10% normal goat serum and 0.3% Triton X-100. Samples were covered with Vectashield Mounting Medium (Vector Laboratories, Burlington, ON) before viewing under a BIORAD Microradiance 2000 Confocal Microscope, equipped with argon (2 lines, 488 and 514 nm) and helium/neon (543 nm). Lasersharp software was used for image acquisition. Digitized images of positive immunofluorescence were taken at 1 μm step intervals following excitation of the two fluorochromes. In control

experiments pre-incubation of the primary P2X2 and P2X3 antisera for 1 hr with excess of each of their respective blocking peptides resulted in complete abolition of staining.

Reverse transcriptase polymerase chain reaction (RT-PCR):

Total RNA was obtained from between 50-150 mechanically isolated neurons following combined enzymatic and mechanical dissociation of rat petrosal ganglia as previously described (Nurse and Zhang 1999; Zhang *et al.*, 2000). Postnatal rat pups 9-13 days old were killed by a blow to the head followed by excision of the carotid bifurcations and dissection of the petrosal ganglia. After dissociation of the tissue, isolation of individual neurons was carried out under a dissecting microscope with the aid of a glass microelectrode (tip diameter ~40-60 μm; Flaming/Brown Micropipette Puller, Model P-97; Sutter Instruments Co.), to which suction was applied via an electrode holder and attached polyethylene tubing. The isolated neurons were pooled and total RNA extracted using the Qiagen RNeasy kit (Qiagen Inc, Mississauga, ON, Canada) according to the manufacturer's instructions. To remove contaminating genomic DNA, isolated RNA was treated with RNase-free DNase (Qiagen, Mississauga, ON, Canada) or treated with 0.1 U/μl RQ1 DNase (Promega Corporation, Madison, WI, USA) for 30 minutes at 37 °C prior to the Reverse Transcription reaction.

RNA was reverse transcribed using Superscript II reverse transcriptase (Gibco BRL Life Technologies, Burlington, ON, Canada). The RT mixture consisted of the following (mM unless stated): 50 Tris-HCl, 75 KCl, 3 $MgCl_2$, 0.025 μg/μl oligo $(dT)_{12\text{-}18}$, 20 DTT, 0.5 each dNTP, 2 U/μl RNaseOut ribonuclease inhibitor (Gibco BRL) and 10 U/μl

reverse transcriptase. The reaction mixture had a total volume of 20 µl. Reactions were run at 42 °C for 60 min then at 70 °C for 15 min in a GeneAmp PCR System 9700 thermal cycler (Perkin-Elmer, Norwalk, CT, USA). Reaction products were stored at 4 °C prior to running the PCR reaction. Control reactions were performed where RT was omitted from the reaction mix.

Following reverse transcription, DNA was amplified in a single round of PCR. The PCR reaction consisted of the following (mM unless stated): 20 Tris-HCl, 50 KCl, 1.5 $MgCl_2$, 0.2 each dNTP, 0.2 µM each upstream and downstream primers, 5 µl DNA template and 2.5 U/µl Platinum Taq polymerase (Gibco BRL). Total reaction volume was 25 µl with DNase-free water. Gene-specific primers were designed using the Jellyfish software (Biowire.com, Mountain View, CA, USA) and synthesized by The Central Facility of the Institute for Molecular Biology and Biotechnology (MOBIX), McMaster University, Hamilton, Ontario. See Table 1.1 for a list of primers used in this study. The PCR was held at 94 °C for 2 min and cycled 35 times. Each cycle consisted of 94 °C for 30 s (denaturation), 55 °C (P2X3 and ß-actin) or 52 °C (P2X2) for 30 s (annealing) and 72 °C for 1 min (extension). This was followed by a 10 min final extension at 72 °C. PCR products were visualized on an ethidium bromide-stained 2 % agarose gel under UV illumination. The 100 bp DNA ladder, used as markers (M), was obtained from Gibco BRL.

Table 1.1 List of primer sequences used in this study.

The table lists the primer sequences for P2X2 and P2X3 receptor subunits used for RT-PCR, cloning and quantitative (LightCycler) PCR. The P2X2 (156 bp) and P2X3 (219 bp) primer sets were designed for quantitative PCR, while the other primer sets were used for RT-PCR and cloning. The internal control primer sequence for β-actin is also listed.

Table 1.1: List of Primer Sequences used in this study

Target	Forward (F) or Reverse (R)	Primer Sequence (5' to 3')	The region spanned in the Gene	Target Sequence Length (bp)	GenBank Accession Number
P2X2	(F)	GAT AAA CGG CAC TAC CA	924 - 1080	156	U14414
	(R)	CCA GTC ACA CAG GAA GGA			
P2X2	(F)	GAA TCA GAG TGC AAC CCC AA	826 - 1183	357	U14414
	(R)	TCA CAG GCC ATC TAC TTG AG			
P2X2	(F)	TCC ATC ATC ACC AAA GTC AA	231- 620	392	U14414
	(R)	TTG GGG TAG TGG ATG CTG TT			
P2X3	(F)	AAC CTC ACC GAC AAG GAC AT	751 - 970	219	X91167
	(R)	CAT CCA GCC GAG TGA AGG AA			
P2X3	(F)	TTG AGG GTA GGG GAG GTG GT	817 - 1143	326	X91167
	(R)	GCT GAT AAT GGT GGG GAT GA			
β -Actin	(F)	AAG ATC CTG ACC GAG CGT GG	571 - 897	327	NM_031144
	(R)	CAG CAG TGT GTT GGC ATA GAG G			

Cloning and sequencing of P2X2 and P2X3 PCR products:

The QIAquick Gel Extraction Kit (QIAGEN Inc., Missisauga, ON) was used to extract PCR fragments from the agarose gel according to the manufacturer's instructions. The extracted DNA band was eluted with sterile RNase/DNase free water. The putative P2X DNA fragments were ligated into a pCR 4-TOPO vector (Invitrogen Corp., Carlsbad, CA) and transformed into the competent TOPO 10 cells provided by the TOPO-TA cloning kit for sequencing. The transformed cells were plated onto LB/Ampicillin plates and incubated overnight at 37°C. Isolated colonies were picked from the plates and grown in 5 ml of LB/Amp media overnight on a 37°C shaker. Mini prep alkaline lysis protocol (Sambrook *et al.*, 1989) and an isopropanol precipitation reaction was used to extract DNA from 1 ml of cultured cells. The plasmid DNA from several colonies was analyzed by restriction enzyme digest (1 hr at 37°C) with *EcoR1* (Gibco BRL), and the bands were separated on a 1.2% agarose gel. Positive colonies containing the correct insert size were cultured in 500 ml of LB/Ampicillin and the plasmid DNA was purified by a maxi prep alkaline lysis protocol (Sambrook *et al.*, 1989) followed by equilibrium centrifugation in a CsCl-ethidium bromide gradient. The DNA sample was then sequenced (MOBIX, McMaster University) using an ABI Prism automated sequencer (with T7 polymerase). The sequencing results were analyzed by BLAST 2, NIH computer software for identification of gene sequences and by using Vector NTI Software (Informax Inc, USA). The sequences were matched to the *Rattus norvegicus* P2X2 receptor mRNA (Genebank accession # U14414) and P2X3 receptor mRNA (Genebank accession # X91167).

RESULTS

RT-PCR Identification of P2X mRNA in Isolated Petrosal Neurons

The RT-PCR technique was employed in order to establish whether or not petrosal neurons expressed mRNA encoding both the P2X2 and P2X3 subunits. In each experimental series, a relatively pure neuronal population was obtained by isolating 50-150 individual neurons as described in the Methods. RT-PCR with specific primers for P2X2 and P2X3 (listed in Table 1.1), gave bands of 392 bp (Figure 1.3 A) and 326 bp (Figure 1.3 B), respectively. β-actin mRNA is expressed at moderately abundant levels in most cell types and encodes an ubiquitous cytoskeletal protein. It was one of the first RNAs to be used as an internal control (Bustin *et al.*, 2001). β-Actin was used as an internal control in these experiments, producing a band of 327 bp (Figure 1.3 B). To confirm that the RNA samples were devoid of contaminating genomic DNA, negative control RT-PCR reactions were carried out by omitting the reverse transcriptase enzyme (Figure 1.3 B). The primers for P2X2 span the first transmembrane domain, whereas the P2X3 primers span the second transmembrane domain. Figure 1.4 A and B illustrate primer-alignments of all primer sets used for P2X2 and P2X3 respectively. New primers for P2X2 were designed primarily for single-cell PCR experiments carried out in this laboratory on functional petrosal neurons by Drs. I. Fearon and M. Zhang. This set of primers produced a PCR fragment of 357 bp (Figure 1.3 B; Table 1.1). The RT-PCR reactions were carried out on samples isolated from five separate preparations of P9-P13 petrosal neurons, and in each case, results similar to those displayed in Figure. 1.3 A and B were obtained.

Figure 1.3 Detection of mRNA for P2X2, P2X3 and β-actin in isolated petrosal neurons. A. RT-PCR was carried out on groups of isolated petrosal neurons using gene-specific primers for P2X2. Expected product sizes are (in bp): P2X2 392. In the marker lane (M) the top band is a 500 bp fragment. In negative control reactions (without RT) no PCR products were observed. The 2 % agarose gel was stained with ethidium bromide and viewed under UV illumination. **B.** RT-PCR was carried out on groups of isolated petrosal neurons using gene-specific primers for P2X2 and P2X3 receptors, and β-actin. Expected product sizes are (in bp): P2X2 (357), P2X3 (326), β-actin (327). The marker lane (M) shows bands at 100 bp increments with the 600 bp fragment at increased intensity. The negative control lanes (–) are reactions without RT enzyme; no PCR products were observed in these lanes. The 2 % agarose gel was stained with ethidium bromide and viewed under UV illumination.

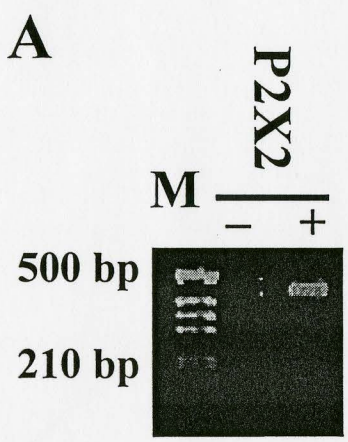
A
P2X2
M
–
+
500 bp
210 bp

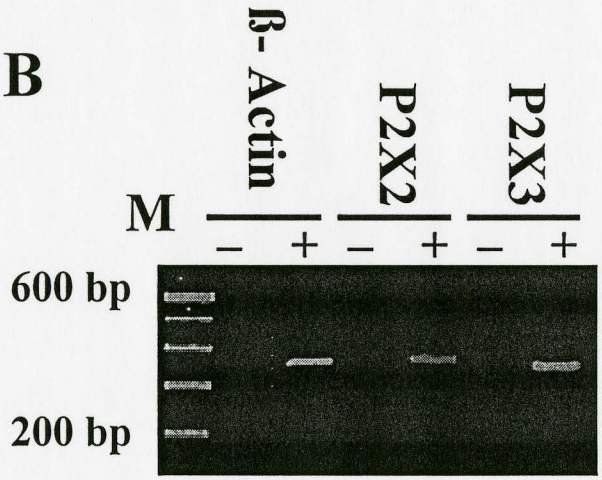
B
ß- Actin
P2X2
P2X3
M
–
+
–
+
–
+
600 bp
200 bp

Figure 1.4 PCR fragment alignments for both P2X2 and P2X3 subunit with specific primers. (**A**) Diagram of P2X2 (Accession # U14414) cDNA (1831 bp), indicating the coding sequence of the P2X2 gene (large orange arrow). The pink arrows are PCR fragments used for RT-PCR and cloning; the 357 bp fragment was designed for single cell RT-PCR and the 156 bp PCR fragment (yellow arrow) is the primer set designed for the LightCycler system (quantitative RT-PCR). The 357 bp and 156 bp fragments have overlapping sequences and span the second transmembrane domain, while the 392 bp fragment spans the first transmembrane domain. (**B**) Diagram of the P2X3 (Accession # X91167) cDNA (1762 bp), indicating the coding sequence of the P2X3 gene (large orange arrow). The pink arrow is a PCR fragment used for RT-PCR and cloning, the 326 bp fragment. The 219 bp PCR fragment (yellow arrow) is the primer set designed for the LightCycler system (quantitative RT-PCR). Both the 326 bp and 219 bp fragments have overlapping sequences and span the second transmembrane domain. ***N.B.*** all PCR fragments span the coding region of the gene. All primer sequences are listed in Table 1.1.

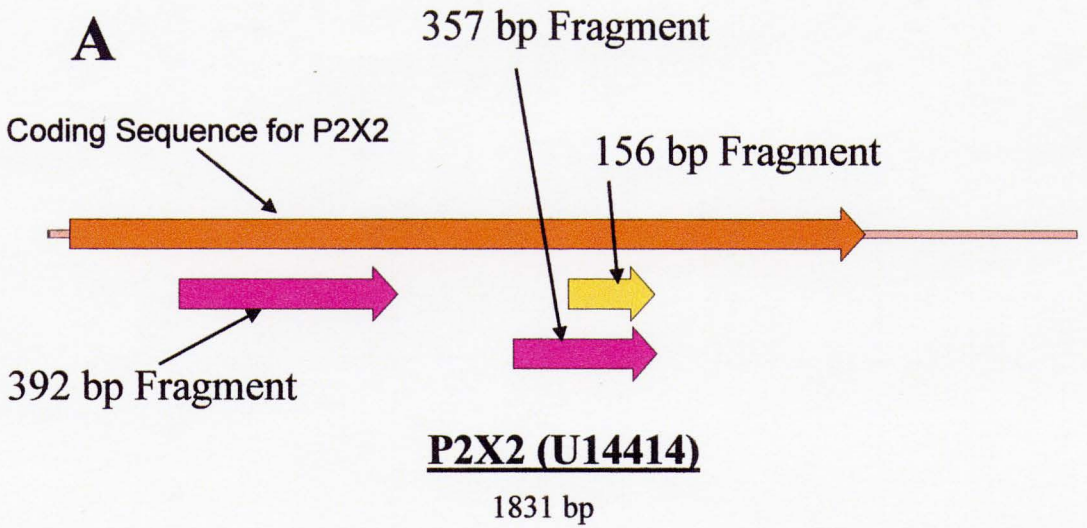
A
357 bp Fragment
Coding Sequence for P2X2
156 bp Fragment
392 bp Fragment
P2X2 (U14414)
1831 bp

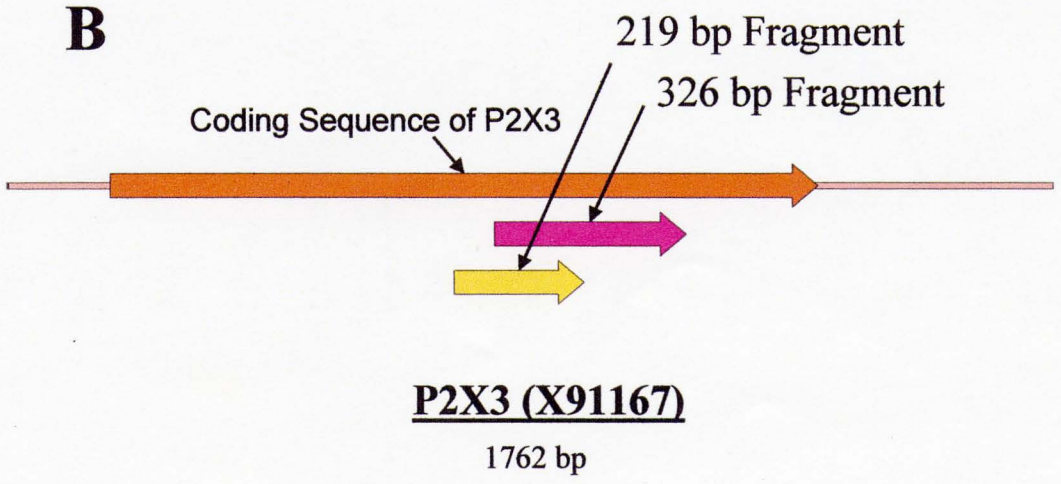
B
219 bp Fragment
326 bp Fragment
Coding Sequence of P2X3
P2X3 (X91167)
1762 bp

Cloning and sequencing of P2X2 and P2X3 PCR products

The putative P2X2 and P2X3 target sequences amplified by RT-PCR were then extracted from agarose gels, ligated into the pCR 4-TOPO vector, and subsequently sequenced as described in the Methods. BLAST analysis of the sequence data confirmed that the putative P2X2 (392 bp) (n = 5), P2X2 (357 bp) (n = 2), and P2X3 (326 bp) (n =5) PCR products were 100% identical at the nucleotide level to the known P2X2 (Genebank accession #U14144) and P2X3 (Genebank accession #X91167) target sequences (see Figure 1.5). The P2X2 (156 bp) PCR product amplified by the LightCycler (LC) was also cloned and sequenced and the product was 100% identical at the nucleotide level to the known P2X2 receptor sequence (n =2). However, P2X3 (219bp) primer designed for the LC spans the same region as the P2X3 (326bp) primers designed for RT-PCR (See Figure 1.4 B and 1.5 B), but to date it has not been cloned or sequenced.

Localization of P2X2 and P2X3 Subunits in tissue sections and isolated petrosal neurons by Confocal Immunofluorescence

Cryostat sections of the carotid bifurcation and separate cultures of carotid body type 1 and petrosal neurons from 9 to 15 day-old rats were processed for immunofluorescence. The majority of neurons that innervate CB type I cells express tyrosine hydroxylase (TH) immunoreactivity, a cytoplasmic marker for CB chemoafferent petrosal neurons (Katz and Black 1986; Finely *et al.*, 1992). Figures 1.6 (A-C) are immunofluorescence photomicrographs of cultured petrosal neurons that stain positively for both P2X3 and TH (Note: co-localization of P2X2 and TH immunostaining

Figure 1.5 Sequence alignments for both P2X2 and P2X3 cloned subunits from petrosal neurons. (A) Diagram of the P2X2 (Accession # U14414) cDNA (1831 bp), indicating the mRNA sequence in the rat (large red arrow). The black arrows are cloned and sequenced fragments observed from isolated PNs; all three fragments were identical at the sequence and amino acid level to the published sequence. (B) Diagram of the P2X3 (Accession # X91167) cDNA (1831 bp), indicating the mRNA sequence in the rat (large red arrow). The black arrows are cloned and sequenced fragments observed from isolated PNs; the 326 bp fragment was identical at the sequence and amino acid level to the published sequence. All primers used for the RT-PCR are listed in Table 1.1.

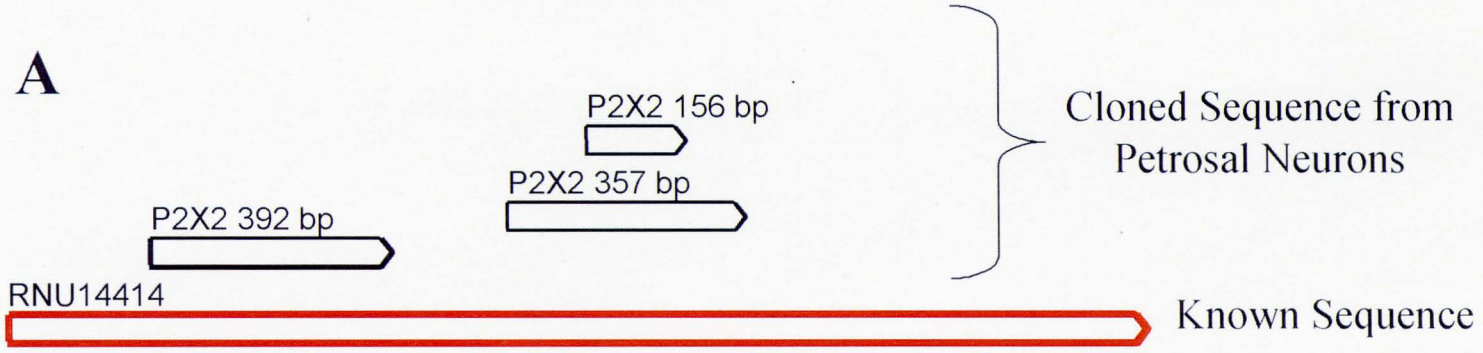
A
P2X2 156 bp
P2X2 357 bp
P2X2 392 bp
Cloned Sequence from
Petrosal Neurons
RNU14414
Known Sequence

P2X2


B
P2X3 326 bp
Cloned Sequence from
Petrosal Neurons
RNX91167
Known Sequence

P2X3

Figure 1.6 Petrosal Neuron in culture immunostained for TH and P2X3 subunit.

A-C represent the same petrosal neurons [P-13] after 3 days in culture; **(A)** phase contrast photomicrograph; **B.** PN immunostained with P2X3 antibody and visualized with a FITC-conjugated secondary antibody; **C.** PN immunostained with tyrosine hydroxylase (TH) antibody and visualized with a CY3-conjugated secondary antibody. The *arrow* points to a petrosal neuron positive for both TH and P2X3. Calibration bar (A, lower left) represents 40 μm.

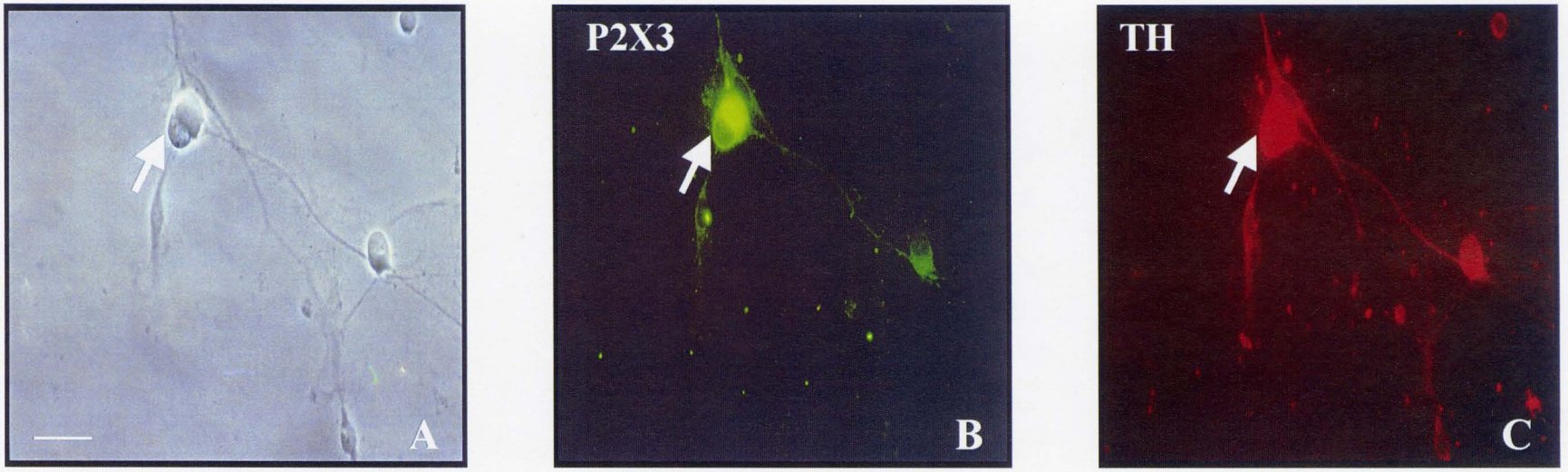
A
P2X3
B
TH
C

in PNs has previously been shown by Zhang *et al.*, 2000). In the present study approximately 42% of P2X3 positive petrosal neurons *in vitro* also stain positively for TH (n = 2).

Antibody against the neuronal marker, neurofilament (NF; 68kDa protein) was also used to identify petrosal neurons. Figures 1.7 (A-F) are immunofluorescence photomicrographs of petrosal neurons stained for both a P2X subunit and NF. All P2X2/P2X3 positive petrosal neurons also stained positively for NF.

The observation that the P2X2 and P2X3 mRNA were expressed in petrosal chemoafferent neurons, and that functional P2X receptor channels mediated hypoxic chemotransmission in co-culture (Zhang *et al.*, 2000; Figure 1.3), led us to investigate the localization of the corresponding proteins *in situ*. P2X2 and P2X3 subunits were localized using double-label immunofluorescence and confocal microscopy on tissue sections of 12-15 day-old rat petrosal ganglia and carotid bodies (CB). Many neurons in the petrosal ganglia were strongly positive for both P2X2 and P2X3 subunits (Fig. 1.8 A-C). Examination of several immunostained sections (n = 8) revealed that though the majority of neurons were positive for both subunits (>60 %), a significant fraction (15-20 %) was positive for only one or the other subunit. Since the petrosal ganglion contains neurons that project to targets other than the CB, it was of interest to investigate whether both subunits were expressed in CB afferent terminals *in situ*. Importantly, nerve terminals, found in association with CB chemoreceptor lobules, were positive for both P2X2 and P2X3 immunoreactivity (Figure 1.8 D-F, data provided by Cathy Vollmer). For these experiments, 3 sections from each of 4 different CBs were immunostained, and

Figure 1.7 Petrosal Neurons in culture immunostained with NF and P2X2/P2X3.

A-C represent the same microscopic field of petrosal neurons [P-16] after 3 days in culture immunostained with NF and P2X2 antibodies. **A.** phase contrast photomicrograph; **B.** PN immunostained with antibody against the 68kDa neurofilament protein and visualized with a FITC-conjugated secondary antibody; **C.** PN immunostained with P2X2 antibody and visualized with a CY3-conjugated secondary antibody. The *arrow* points to a petrosal neuron positive for both NF and P2X2. **D-F** represent the same microscopic field of petrosal neurons [P-16] after 3 days in culture immunostained with NF and P2X3 antibodies. **D.** a phase contrast photomicrograph; **E.** PN immunostained with antibody against the 68kDa neurofilament protein and visualized with a FITC-conjugated secondary antibody; **F.** PN immunostained with P2X3 antibody and visualized with a CY3-conjugated secondary antibody. The *arrow* points to a petrosal neuron that is NF positive and P2X3 negative. The *arrowhead* points to a petrosal neuron positive for both NF and P2X3. Calibration bar represents 40 μm in A-C, and 20 μm in D-F.

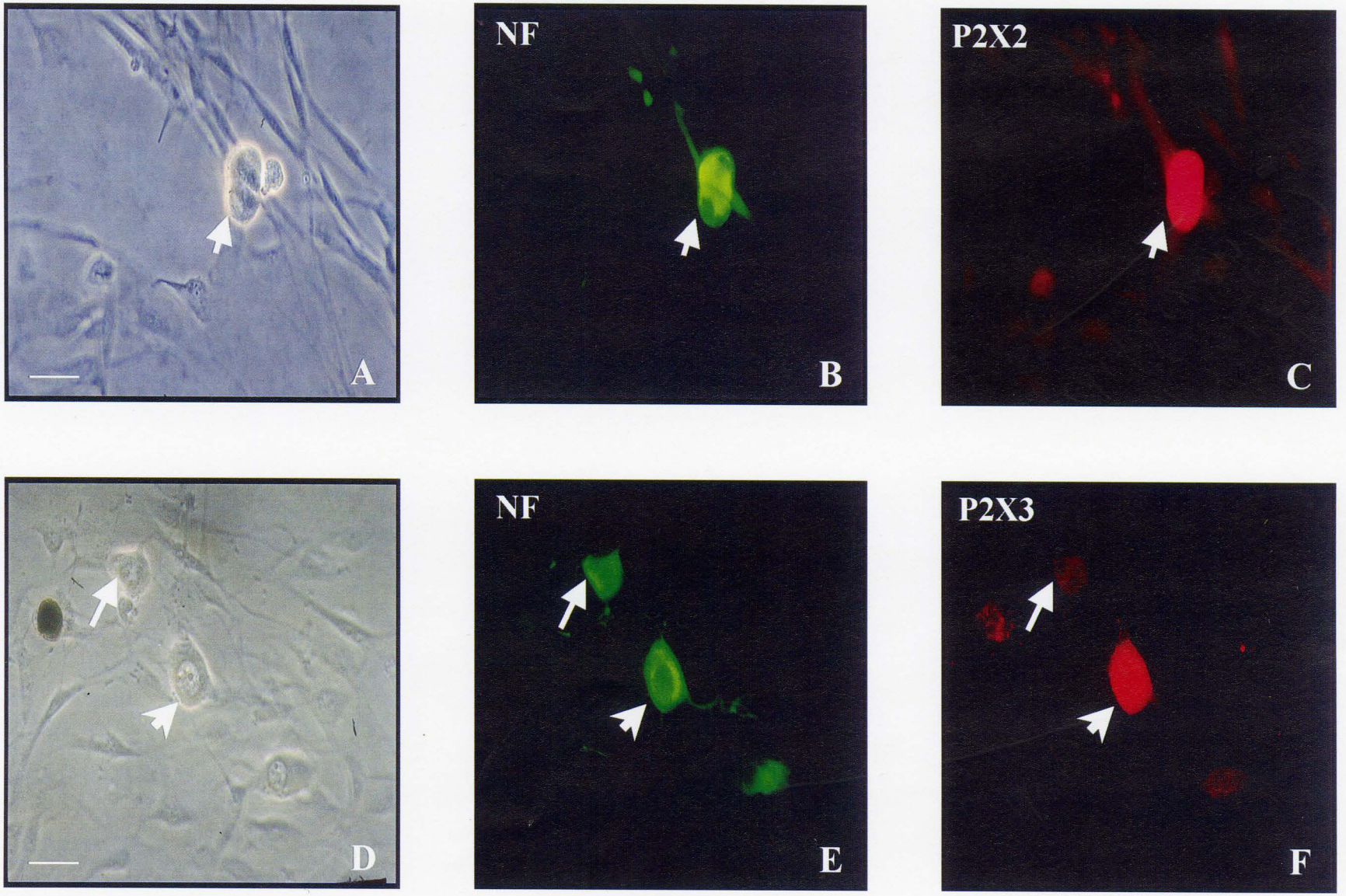
A
NF
B
P2X2
C
D
NF
E
P2X3
F

Figure 1.8 Expression of P2X2 and P2X3 subunits in tissue sections of petrosal ganglia and carotid body as revealed by Confocal Immunofluorescence.

A-C Represent the same tissue section from the petrosal ganglion of a 15 day-old rat after immunostaining with P2X2 and P2X3 antibodies. Localization of P2X2 (**A**) and P2X3 (**B**) subunits is revealed by Cy3 and FITC fluorescence respectively; dual exposure in (**C**) shows overlap of P2X2 and P2X3 staining. **D-F** Represent the same section from the carotid body of a 14 day-old rat after similar immunostaining with P2X2 and P2X3 antibodies as in **A-C**. Note complete overlap of P2X2 and P2X3 immunostaining in nerve terminals, which are apposed to lobules of chemoreceptor cells. Calibration bar represents 40 μm in A-C, and 50 μm in C-E. (N.B. photomicrographs shown in panel **D-F** provided by Cathy Vollmer, printed with her permission.)

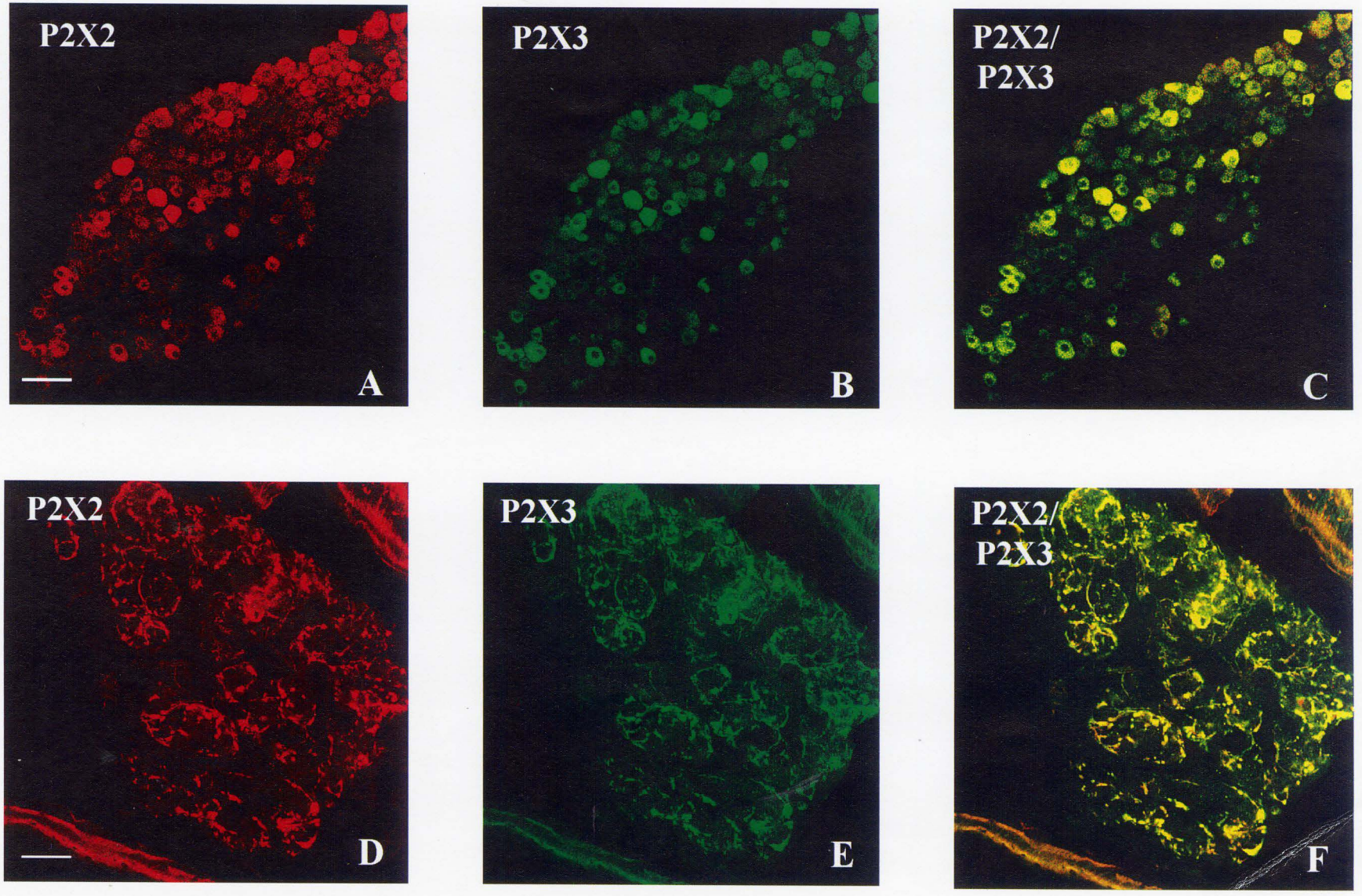
P2X2
A
P2X3
B
P2X2/
P2X3
C
P2X2
D
P2X3
E
P2X2/
P2X3
F

in all cases there was complete overlap of P2X2 and P2X3 immunofluorescence. This was also the case during routine examination of serial confocal sections, at 1 μm steps, through the ~18 μm thick tissue section. Thus, isolated petrosal neurons express P2X2 and P2X3 mRNA and protein subunits.

DISCUSSION

Co-released ACh and ATP, acting on postsynaptic P2X2 and P2X3 receptors plays a major role in rat carotid body PO_2 chemotransmission (Zhang *et al.*, 2000). Homomeric P2X3 and P2X2 receptors, as well as heteromeric P2X2/P2X3 receptors mediate a major component of ATP-mediated responses in other systems (Lewis *et al.*, 1995; Collo *et al.*, 1996).

The P2X proteins are receptor subunits in which separate subunits are assembled to form an ion channel. Therefore, for a P2X2 homomeric receptor only P2X2 subunits form the functional receptor. However, the P2X2/P2X3 heteromeric receptor has a combination of both P2X2 and P2X3 subunits, but the stoichiometry is still unknown (Raleivc and Burnstock, 1998). It has been proposed that the number of subunits per receptor could be as few as three or four subunits or as many as six (Kim *et al.*, 1997). The P2X proteins consist of 379 to 472 amino acids and have two conserved transmembrane domains with most of the protein occurring extracellularly as an intervening hydrophilic loop. The extracellular loop has conserved disulfide bridges and contains the binding site for ATP (Raleivc and Burnstock, 1998; Ennion *et al.*, 2000;

Jaing *et al.*, 2000) and sites for antagonists and modulators (Buell *et al.*, 1996). The second transmembrane domain (TM2) lines the pore and the assembly of the P2X receptor subunits is dependent upon motifs in this transmembrane domain (Torres *et al.*, 1999).

In this laboratory the pharmacological properties of ATP receptors on isolated petrosal neurons were similar to the known pharmacology of P2X2/P2X3 heteromeric receptors, i.e. they were (i) activated by αβmetATP, and (ii) showed little or no desensitization (Zhang *et al.*, 2000). The activation of P2X receptors by ATP leads to opening of cation channels that are quite permeable to Ca^{2+} (Koshimizu *et al.*, 1999). Co-expression of P2X3 with P2X2 in heterologous expression systems yields ATP-activated currents that were similar to those in sensory neurons (Figure 1.1). This was accounted for by hetero-polymerization of the P2X2 and P2X3 subunits co-expressed in HEK293 (human embryonic kidney) cells, and initially cloned from the dorsal root ganglion (DRG; Lewis *et al.*, 1995). The present study provides the first demonstration that carotid body chemoafferent neurons express mRNA for both P2X2 and P2X3 purinoceptor subunits. These experiments utilized RT-PCR, cloning and sequencing techniques on populations of freshly isolated petrosal neurons (Figure 1.3 and 1.5). This expression pattern is consistent with the idea that P2X2/P2X3 heteromultimeric receptors are the functional receptors, activated by ATP released as a co-transmitter from the chemoreceptor type I cells. This release of ATP occurs along with other excitatory neurotransmitters (e.g. ACh), which help mediate postsynaptic excitation of sensory afferent terminals during carotid body chemoexcitation by natural stimuli, e.g. hypoxia.

Binding of released ATP to P2X receptors is associated with a rise in $[Ca^{2+}]_i$, which is mediated by Ca^{2+} influx through these channels, as well as by depolarization of cells and activation of voltage-gated Ca^{2+} channels (Ralevic and Burnstock, 1998). Depending on the relative levels of P2X subunit co-expression, the operational profile of the resultant P2X receptors can change from one phenotype to another (Liu *et al.*, 2001). For example, in voltage-clamp recordings from *Xenopus* oocytes, when a constant amount of P2X3 mRNA was transfected with increasing amounts of P2X2 mRNA, the expressed P2X receptor changed from a P2X3-like receptor to a P2X2-like receptor (Liu *et al.*, 2001).

Khakh *et al.* (1999) have shown that there is an increase in pore diameter, which is dependent on previous exposure of homomeric P2X2 and heteromeric P2X2/P2X3 receptors to ATP. This ability of the P2X ion-channels to change their ionic selectively has profound implications in the central and peripheral purinergic synapses (Khakh *et al.*, 1999). In the CB chemoafferent pathway, these properties may regulate sensory impulse traffic that ultimately affect ventilatory reflexes. For example, when the sensory discharge increases, ventilation also increases and the opposite occurs when the discharge is reduced (Eyzaguirre and Zapapta, 1984).

As with other physiological stimuli, a hypoxic stimulus / response can be categorized as either acute or chronic. Acute response occurs over a time scale of seconds to minutes and involves the post-translational modification of proteins or other macromolecules, e.g. phosphorylation of receptors. Conversely, chronic responses occur over minutes to hours and involve changes in gene expression (Semenza, 1999). Possible

changes in gene expression of the two P2X subunits in petrosal neurons were examined in the developmental study discussed in Chapter 2. The expression profile of these receptors was also examined in CB type I cells under various conditions and is discussed in Chapter 3 of this thesis.

Moreover, P2X2 and P2X3 proteins co-localized in CB chemoafferent neurons and afferent nerve terminals apposed to chemoreceptor lobules *in situ* (Figure 1.8), as demonstrated by serial confocal immunofluorescence. While these data alone do not exclude the possibility that homomeric P2X2 and P2X3 receptors may function in the same chemosensory neuron, the native receptors on identified functional neurons showed a slowly desensitizing response to α,β–methylene ATP (Buell *et al.*, 1996), a fact not readily explained by independent association of the two subunits into homomeric receptor complexes (Lewis *et al.*, 1995; Radford *et al.*, 1997). The immunofluorescence study also showed that TH-positive chemoafferent neurons immunostained for NF as well as the P2X2 and P2X3 subunits (Figure 1.6 and 1.7). These data provide strong evidence that the P2X2/P2X3 positive neurons are present in the chemoafferent petrosal ganglia and are consistent with the notion that ATP is an excitatory co-transmitter in the CB chemotransduction pathway.

CHAPTER 2

COMPARISON OF P2X PURINOCEPTOR SUBUNIT EXPRESSION IN PETROSAL AND NODOSE NEURONS DURING DEVELOPMENT USING QUANTITATIVE RT-PCR

SUMMARY

Petrosal and nodose neurons share a similar developmental origin (i.e. the ectodermal placodes) and GDNF is a required survival factor for both the neuronal groups. In this study, the profiles of P2X receptor subunit expression in the petrosal and nodose neurons were found to differ from each other. The petrosal neurons showed an slight increase in the expression of P2X2 and P2X3 mRNA by P-21, whereas in nodose neurons the corresponding expression levels peaked by P-9, but fell significantly by P-21. However, in both cases the expression levels for the P2X2 mRNA were higher than those of P2X3 mRNA and the expression profile for both the P2X subunits develop along a parallel time course.

INTRODUCTION

The sequence of events leading to an increase in CB chemoreceptor nerve activity during hypoxia is currently unsettled, but secretion of excitatory neurotransmitters from chemoreceptor type I cells appears to play an important role (Fidone *et al.*, 1982; Gonzalez *et al.*, 1994; Zhang *et al.*, 2000; Prabhakar, 2000). Several putative excitatory

neurotransmitters have been proposed including, ACh, adenosine, serotonin, DA, substance P, NO (Gonzalez *et al.*, 1994) and ATP (Zhang *et al.*, 2000). The evidence for DA as an excitatory neurotransmitter in this system is not favored, at least in the rat CB (Hertzberg *et al.*, 1990; Donnelly, 2000), and there also is evidence against a role for adenosine as an excitatory neurotransmitter (Gauda *et al.*, 2000). Recent evidence from this laboratory favours the idea that co-released ATP and ACh from type I cells is the major mechanism mediating hypoxic chemoexcitation in the rat carotid body (Zhang *et al.*, 2000). Indeed, as discussed in Chapter 1 of this thesis, purinergic P2X2 and P2X3 subunits are expressed in postsynaptic CB chemoafferent neurons, consistent with ATP acting as a co-transmitter. The chemoreceptors in the CB are active and responsive in the fetus (Hertzberg *et al.*, 1990), but undergo a significant increase in their responsiveness to hypoxia in the postnatal period (Donnelly, 2000). However, several days to weeks after birth, normal adult chemoreceptor activity is detected, indicating that a significant developmental increase in activity has occurred during this early postnatal period (Marchal *et al.*, 1992; Carroll *et al.*, 1993). It is conceivable that ATP and P2X receptor development might play an important role in resetting of chemoreceptor sensitivity in the first three weeks of development. Since the CB sensitivity to hypoxia undergoes postnatal maturation (Hertzberg *et al.*, 1990), it was of interest to investigate whether or not this is paralleled by developmental changes in P2X receptor expression in petrosal ganglion. For reasons discussed below the nodose ganglion provided a useful control for these studies.

Brain-derived neurotrophic factor (BDNF) a member of the neurotrophin family, has been suggested to be necessary for the survival of peripheral sensory neurons and central nervous system (CNS) neurons (Liu *et al.*, 1995; Brady *et al.*, 1999). In BDNF (-/-) knockout mice, in which the BDNF gene is disrupted, there is a 55-65% reduction in neuronal number within the nodose and petrosal ganglia (Erickson *et al.*, 2000). Glial-cell line derived neurotrophic factor (GDNF) is a 20 kDa glycosylated polypeptide that has distant, but significant, homology to members of the TGF beta superfamily (Brady *et al.*, 1999). GDNF promotes survival of dopamine-containing neurons in the central nervous system (Erickson *et al.*, 1996) and is involved in the development and survival of neurons in the nodose-petrosal complex (Erickson *et al.*, 2000). Moreover, both factors are required during the same period of development, between embryonic day (E) 15.5 and E17.5. These findings demonstrate the petrosal ganglia requires both BDNF and GDNF, while nodose ganglia requires only GDNF (Buchaman and Davies, 1993Erickson *et al.*, 2000). Another study examined the role of BDNF using transgenic mice that overexpress BDNF in epithelial target tissues. These BDNF transgenic mice showed an increase in innervation density and showed a selective 38% increase in surviving neurons in the nodose-petrosal complex (LeMaster *et al.*, 1999). The survival of both petrosal and nodose ganglia is dependent on GDNF. Therefore, nodose neurons, which innervate targets other than the CB and also express both P2X2 and P2X3 subunits (Vulchanova *et al.*, 1997), provide a good control for the study of potential target influences on receptor expression in petrosal neurons.

The aim of this study was to examine possible developmental changes in expression of the P2X2 and P2X3 mRNA in the chemoafferent petrosal neurons. Two primary reasons for this study were: i) to relate these findings to a possible role of excitatory P2X receptors in the development of hypoxic chemosensitivity in the CB, and ii) to correlate the data with those previously obtained on the development of dopamine D-2 receptors (DA D2-R), which are thought to play an inhibitory role in CB chemotransmission.

MATERIALS AND METHODS

Isolation of petrosal and nodose cells and RNA:

The procedures used for the isolation of nodose / petrosal complex were similar to those described in Chapter 1. Total RNA was obtained from 150 mechanically isolated neurons following combined enzymatic and mechanical dissociation of separated rat petrosal and nodose ganglia (see Chapter 1). RNA was extracted at the following postnatal stages: newborn to three-week-old rat pups (embryonic day-21 or P-0, P-1, P-6, P-9, and P-21). Three different samples (n = 3) of 150 isolated neurons were obtained for the following days: E-21, P-1, P-6, P-9 and P-21.

Reverse transcriptase polymerase chain reaction (RT-PCR)

Total RNA was obtained from 150 mechanically isolated petrosal or nodose neurons (see Materials and Methods Chapter 1). RT-PCR was performed as described in Chapter 1, followed by agarose gel electrophoresis to view the amplified products. A

standard PCR was carried out using 3-5 µl of cDNA as a control to confirm that the mRNA was converted to cDNA for the quantitative PCR analysis. The remaining 15-17 µl of cDNA was saved for the quantitative PCR analysis (Figure 2.1).

Quantitative RT-PCR using LightCycler

LightCycler (LC) system monitors real-time quantitative PCR. The LightCycler - Fast Start DNA Master SYBR Green 1 (Roche Diagnostics, Basel, Switzerland) kit was used. The kit required the addition of: 3-4 mM of $MgCl_2$, 2µl of template and primers for a 20µl reaction mixture. First, DNase treated RNA was reverse transcribed into cDNA (see details above in the RT-PCR section) and 2µl of the RT reaction was used for a LightCycler PCR reaction. The LightCycler recorded the fluorescence emitted by the reaction mixture and the data were analyzed using the LightCycler software 3.2.

The LC PCR was held at 94 °C for 10 min and cycled 35-45 times. New primers were designed for P2X2 (156 bp) and P2X3 (219 bp), since a smaller amplicon size increases the efficiency of the PCR in the LightCycler (Bustin *et al.*, 2000; see Table 1.1). Each PCR cycle consisted of 94 °C for 15 s (denaturation), 53 °C (P2X3), 60°C (ß-actin) or 54 °C (P2X2) for 5s (annealing) and 72 °C for 12, 17, 9 s (extension), respectively. This was followed by a 2 min final extension at 72 °C. The Melting Curve Analysis was carried out in three steps: the reaction was heated to 95°C and then cooled for 15s to 55-65 °C and then slowly heated to 95 °C at the rate of 0.1°C/ s. The LC-PCR products were separated on a 2 % agarose gel and viewed under UV illumination.

Figure 2.1 Overall Experimental Method for the Quantitative RT-PCR using LightCycler System – Flowchart. RNA was extracted from 150 isolated neurons of which 8µl of the DNase-treated RNA was reverse transcribed in a 20µl reaction. 2µl per LightCycler reaction was used and a control was performed with 5µl of cDNA. All RT-PCR products were separated on a 2% agarose gel and viewed under UV illumination.

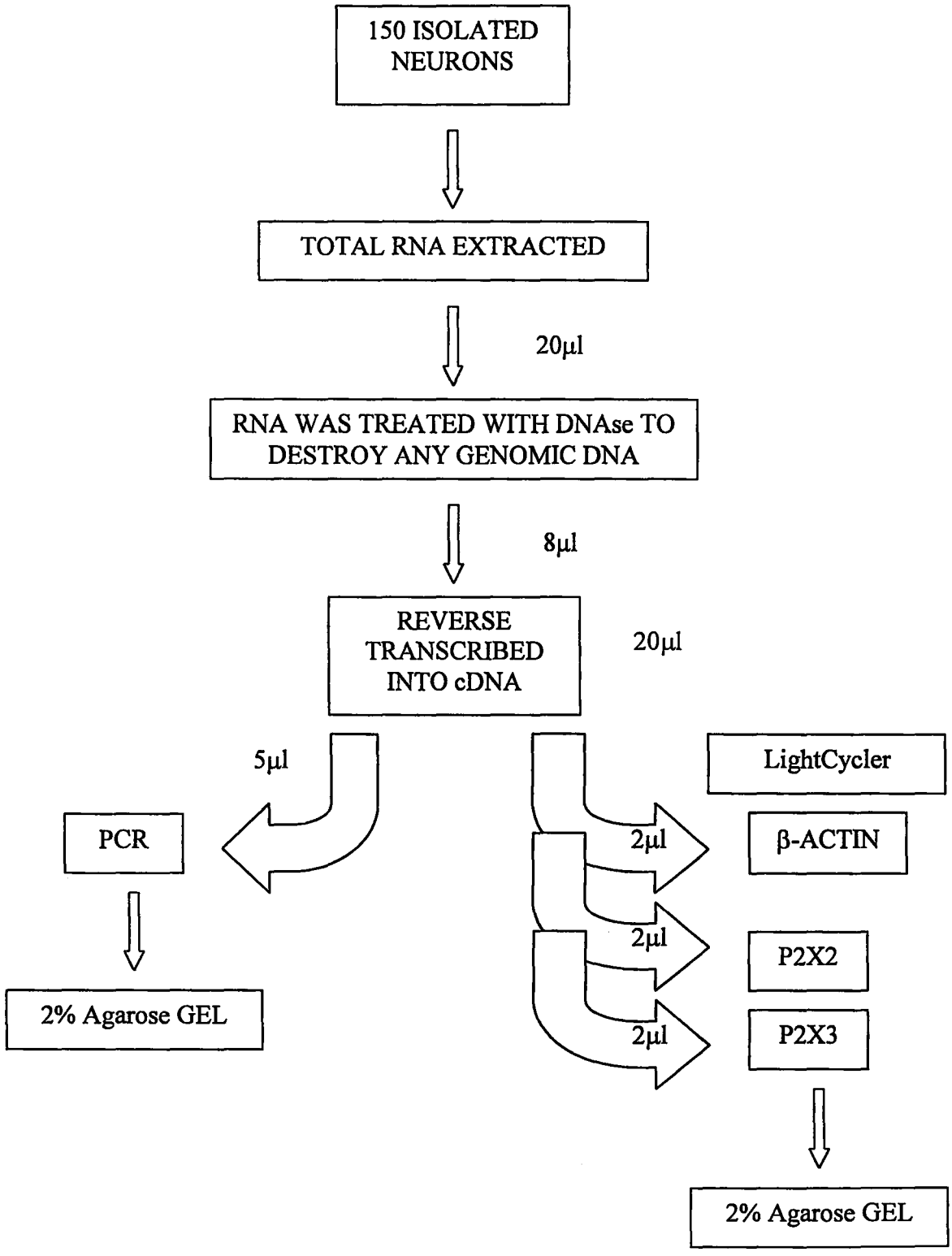
150 ISOLATED NEURONS
TOTAL RNA EXTRACTED
20µl
RNA WAS TREATED WITH DNAse TO DESTROY ANY GENOMIC DNA
8µl
REVERSE TRANSCRIBED INTO cDNA
20µl
5µl
PCR
2% Agarose GEL
LightCycler
2µl
β-ACTIN
2µl
P2X2
2µl
P2X3
2% Agarose GEL

Confocal Immunofluorescence

Cryostat sections of the carotid bifurcation included the nodose / petrosal complex (see Chapter 1 for more details). The primary antibodies were: (i) anti-P2X2 (1:800 dilution), a rabbit polyclonal antibody raised against a highly purified peptide corresponding to amino acid residues 457-472 of the rat P2X2 receptor (Alomone Laboratories, Jerusalem, Israel), and (ii) anti-P2X3 (1:500 dilution), a guinea pig polyclonal antiserum raised against amino acid residues 383-397 of the rat P2X3 receptor (Neuromics, Minneapolis, MN, USA). The secondary antibodies (Jackson Immunoresearch Laboratories, West Grove, PA) consisted of Cy3-conjugated goat anti-rabbit IgG (1:500 dilution), and FITC-conjugated goat anti-guinea pig IgG (1:20 dilution), respectively. Cultured cells were immunostained and viewed as described in Chapter 1.

RESULTS

Developmental changes in expression of P2X subunits in the Petrosal and Nodose ganglia

Quantitative RT-PCR was employed to study the developmental pattern of expression of P2X2 and P2X3 mRNA in petrosal and nodose neurons at E-21/P-0, P-1, P-6, P-9 and P-21 (n = 3). mRNA from these cells was first extracted and reverse transcribed into cDNA. This cDNA was then used in a LightCycler reaction to determine the amount of message in each cell population. After the final PCR cycle, a melting

curve analysis was performed, where the products were denatured at 95°C, annealed at 55°C or 65°C and slowly heated to 95°C. During this slow heating process fluorescence was measured at 0.1°C increments. The data recorded were then plotted against the temperature (panel ***A*** in Figures 2.2, 2.3 and 2.4). The fluorescence (F1) of the SYBR Green I dye bound to the double stranded amplicon dropped sharply as the fragment was denatured. The melting peaks were visualized by taking the first negative derivative (-dF / dT) and plotting this against the temperature (panel ***B*** i.e. Figures 2.2, 2.3 and 2.4). The peaks for β-actin, P2X2 and P2X3 occurred at 89, 86.5 and 88.5 °C, respectively (Figure 2.2-4). The curve labeled "Water- no template" is a negative control reaction in which no template (cDNA) was added; this reaction was performed to measure the background level of SYBR Green I fluorescence. This also is a good control to distinguish the primer dimer peak from the product peak, as exemplified in panel ***B*** Figure 2.3, where the negative control peak occurs at 79°C and no product is seen at the melting temperature (86.5°C). Similar trends are also seen in Figure 2.2 and 2.4. (N.B: as an additional control all samples were checked with a standard RT-PCR to ensure that reverse transcription of mRNA to cDNA was successful; see Figure 2.1).

The LightCycler software calculates the area under each curve; this value can then be normalized against an internal control, such as β-actin. Figures 2.5 and 2.6 are normalized curves plotted against time (days) for the petrosal and nodose neurons, respectively. The data were normalized by dividing the area under the curve for either P2X2 or P2X3 products by that of β-actin. The expression level of β-actin mRNA was relatively constant over the first three weeks of postnatal development. As indicated by

Figure 2.2 Melting Curve Analysis for ß -actin

A. Real-time PCR (LightCycler) readout from the MCA program. Each line represents a sample as listed on the left hand side, i.e. sample #1 = control without template cDNA, samples #2-10 are cDNA from petrosal or nodose neurons at various stages of development. The curve dips at 90°C. ***B***. The first negative derivative (fluorescence / temperature) provides an easy view of the melting temperature specific for the ß -actin amplicon. The *arrow* points to the ß -actin and primer dimer peak at 89 °C and 85°C, respectively.

A

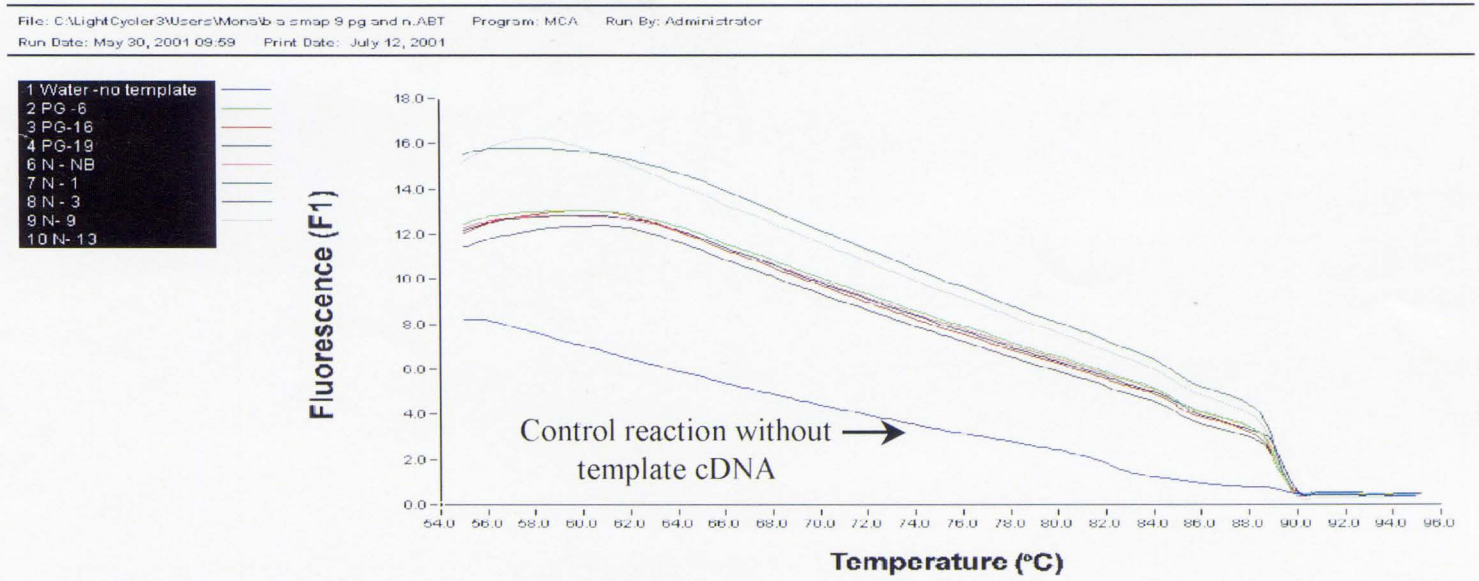
File: C:\LightCycler3\Users\Mona\b-a smap 9 pg and n.ABT Program: MCA Run By: Administrator
Run Date: May 30, 2001 09:59 Print Date: July 12, 2001
1 Water -no template
2 PG -6
3 PG-16
4 PG-19
6 N - NB
7 N - 1
8 N - 3
9 N- 9
10 N- 13
Fluorescence (F1)
Control reaction without template cDNA
Temperature (°C)

B

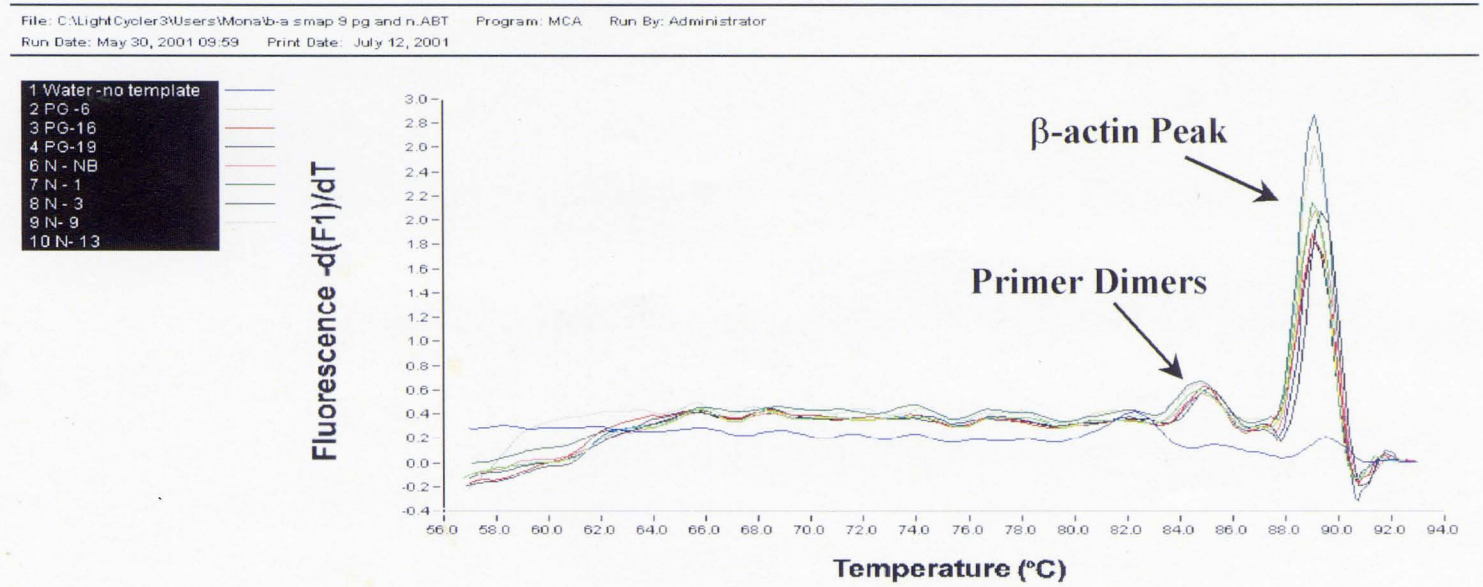
File: C:\LightCycler3\Users\Mona\b-a smap 9 pg and n.ABT Program: MCA Run By: Administrator
Run Date: May 30, 2001 09:59 Print Date: July 12, 2001
1 Water -no template
2 PG -6
3 PG-16
4 PG-19
6 N - NB
7 N - 1
8 N - 3
9 N- 9
10 N- 13
Fluorescence -d(F1)/dT
β-actin Peak
Primer Dimers
Temperature (°C)

Figure 2.3 Melting Curve Analysis for P2X2 receptor subunit

A. Real-time PCR (LightCycler) readout from the MCA program. Each line represents a sample as listed on the left hand side, i.e. sample #1 = control without template cDNA, samples #2-5 are cDNA from petrosal neurons at P-0, 1, 9 and 13. The curve dips at 87.5°C. ***B***. The first negative derivative (fluorescence / temperature) provides an easy view of the melting temperature specific for the P2X2 amplicon. The *arrow* points to the P2X2 and primer dimer peak at 86.5 °C and 79°C, respectively.

A

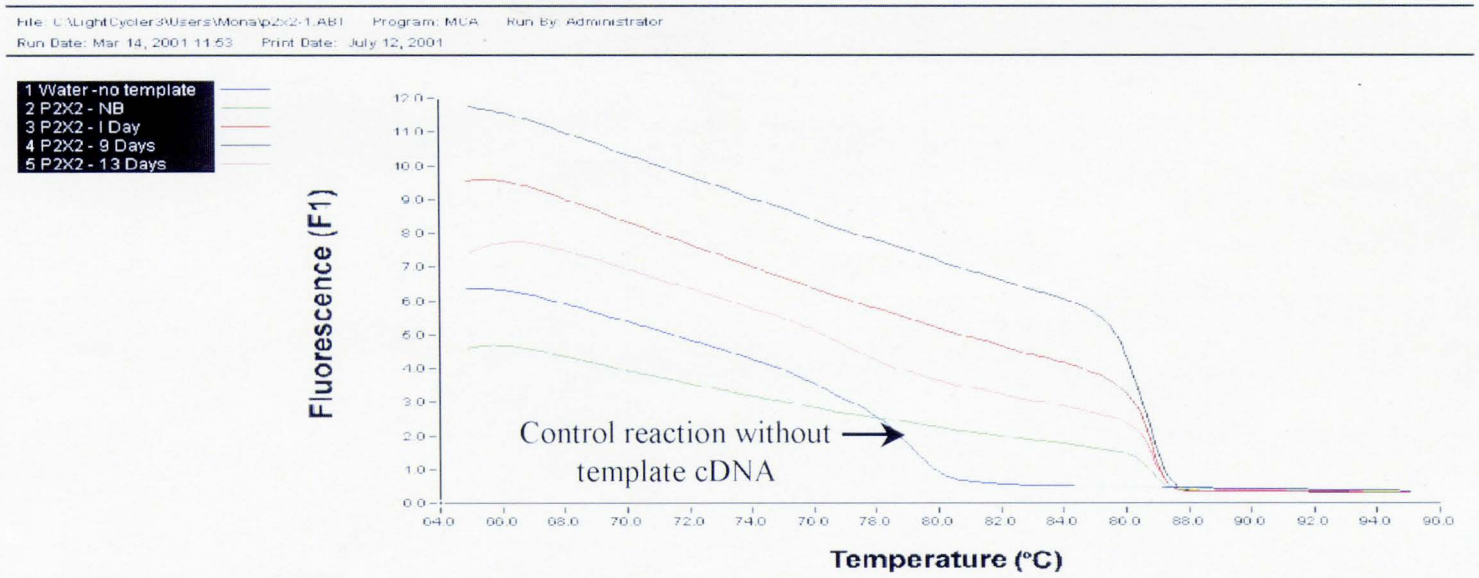
File: C:\LightCycler3\Users\Mona\p2x2-1.ABI Program: MCA Run By: Administrator
Run Date: Mar 14, 2001 11:53 Print Date: July 12, 2001
1 Water -no template
2 P2X2 - NB
3 P2X2 - I Day
4 P2X2 - 9 Days
5 P2X2 - 13 Days
Fluorescence (F1)
Control reaction without template cDNA
Temperature (°C)

B

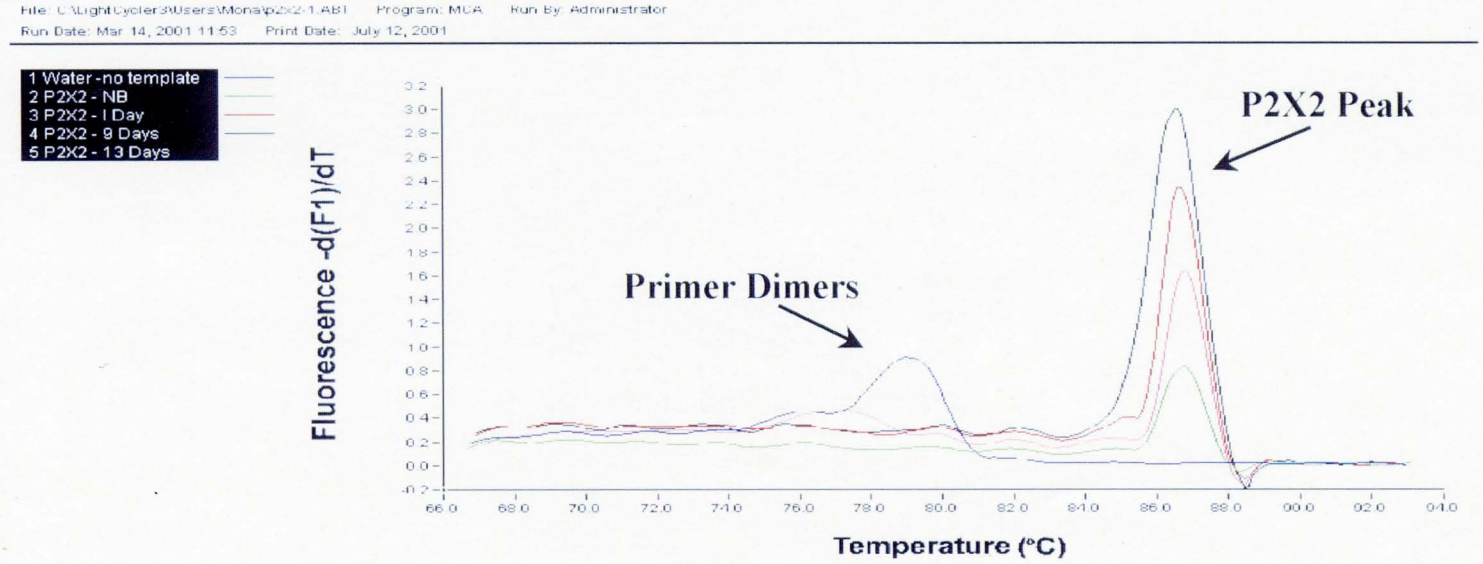
File: C:\LightCycler3\Users\Mona\p2x2-1.ABI Program: MCA Run By: Administrator
Run Date: Mar 14, 2001 11:53 Print Date: July 12, 2001
1 Water -no template
2 P2X2 - NB
3 P2X2 - I Day
4 P2X2 - 9 Days
5 P2X2 - 13 Days
Fluorescence -d(F1)/dT
P2X2 Peak
Primer Dimers
Temperature (°C)

Figure 2.4 Melting Curve Analysis for P2X3 receptor subunit

A. Real-time PCR (LightCycler) readout from the MCA program. Each line represents a sample as listed on the left hand side, i.e. sample #1 = control without template cDNA, samples #2-6 are cDNA from petrosal neurons at P-0, 1, 3, 9 and 13. The curve dips at 89°C. ***B***. The first negative derivative (fluorescence / temperature) provides an easy view of the melting temperature specific for the P2X3 amplicon. The *arrow* points to the P2X3 and primer dimer peak at 88.5 °C and 78°C, respectively.

A

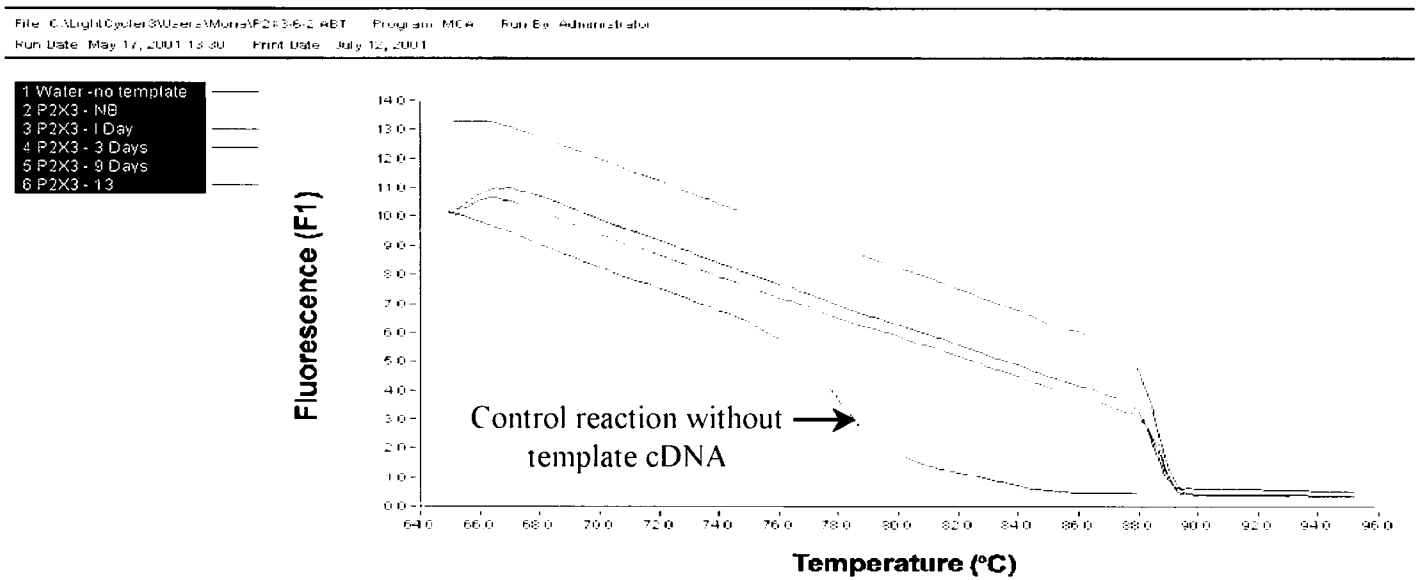
1 Water -no template
2 P2X3 - NB
3 P2X3 - 1 Day
4 P2X3 - 3 Days
5 P2X3 - 9 Days
6 P2X3 - 13
Fluorescence (F1)
Control reaction without template cDNA
Temperature (°C)

B

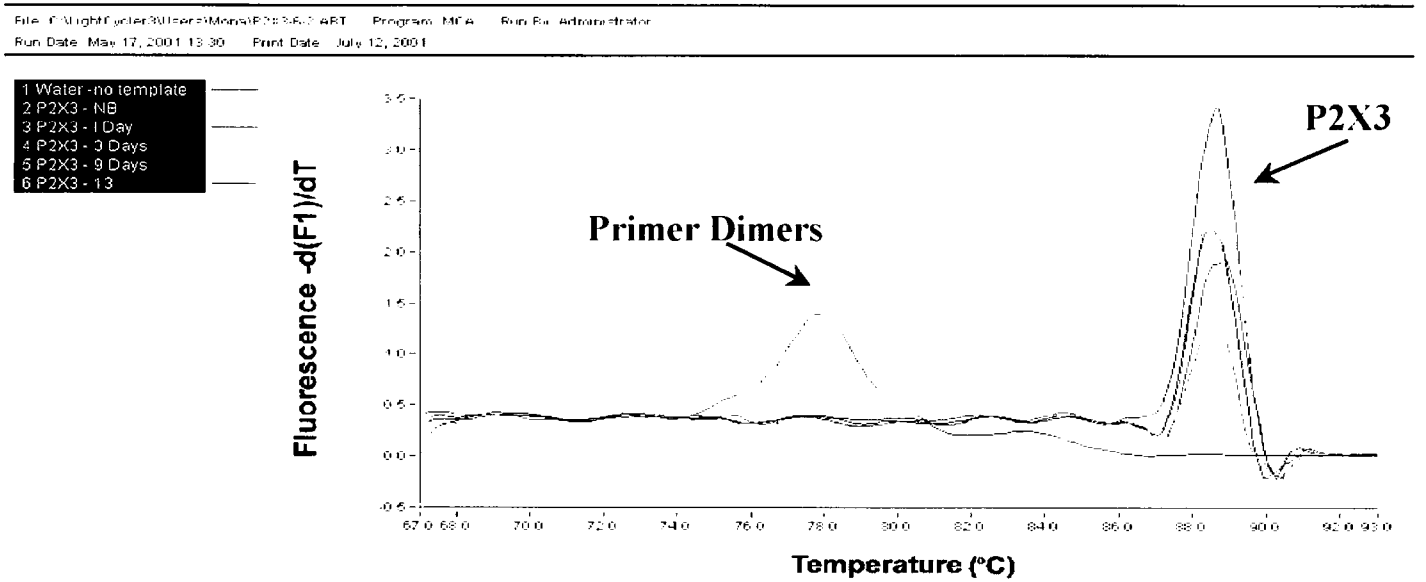
1 Water -no template
2 P2X3 - NB
3 P2X3 - 1 Day
4 P2X3 - 3 Days
5 P2X3 - 9 Days
6 P2X3 - 13
Fluorescence -d(F1)/dT
Primer Dimers
P2X3
Temperature (°C)

Figure 2.5 Quantitative analysis of P2X2 and P2X3 mRNA expression in isolated petrosal neurons during postnatal development.

A. Data were normalized and expressed as a ratio by dividing the area under the melting curve for either P2X2 or P2X3 products by that of β-actin. RNA extracted from isolated petrosal neurons at embryonic day (E)–21, postnatal (P)– 1, 6, 9 and 21 was amplified and measured using the LightCycler system with specific primers for P2X2 (□) and P2X3 (●; n = 3, in both cases). The error bars represent the standard error of the mean (S.E.M.). ***B***. The plot compares the ratio of P2X2 : P2X3 (i.e. P2X2 divided by P2X3; n = 3) versus developmental age. The error bars represent the standard error of the mean (S.E.M.).

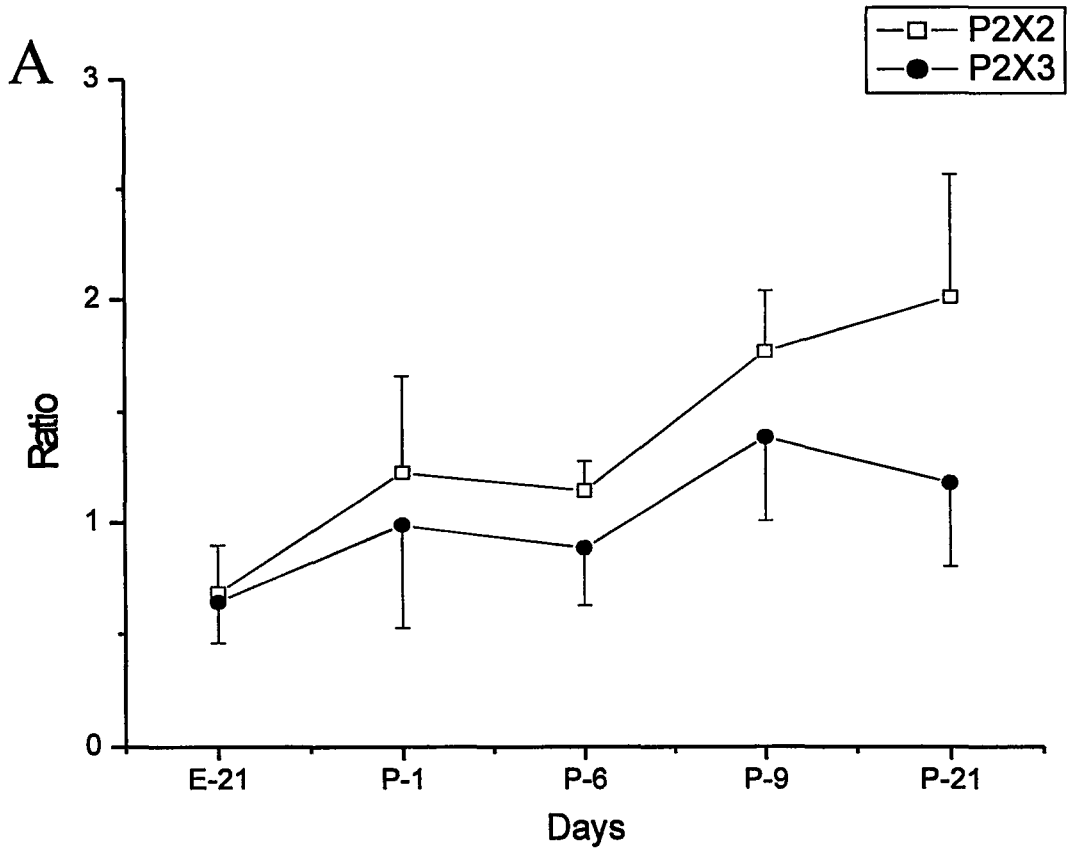
A
P2X2
P2X3
Ratio
3
2
1
0
E-21
P-1
P-6
P-9
P-21
Days

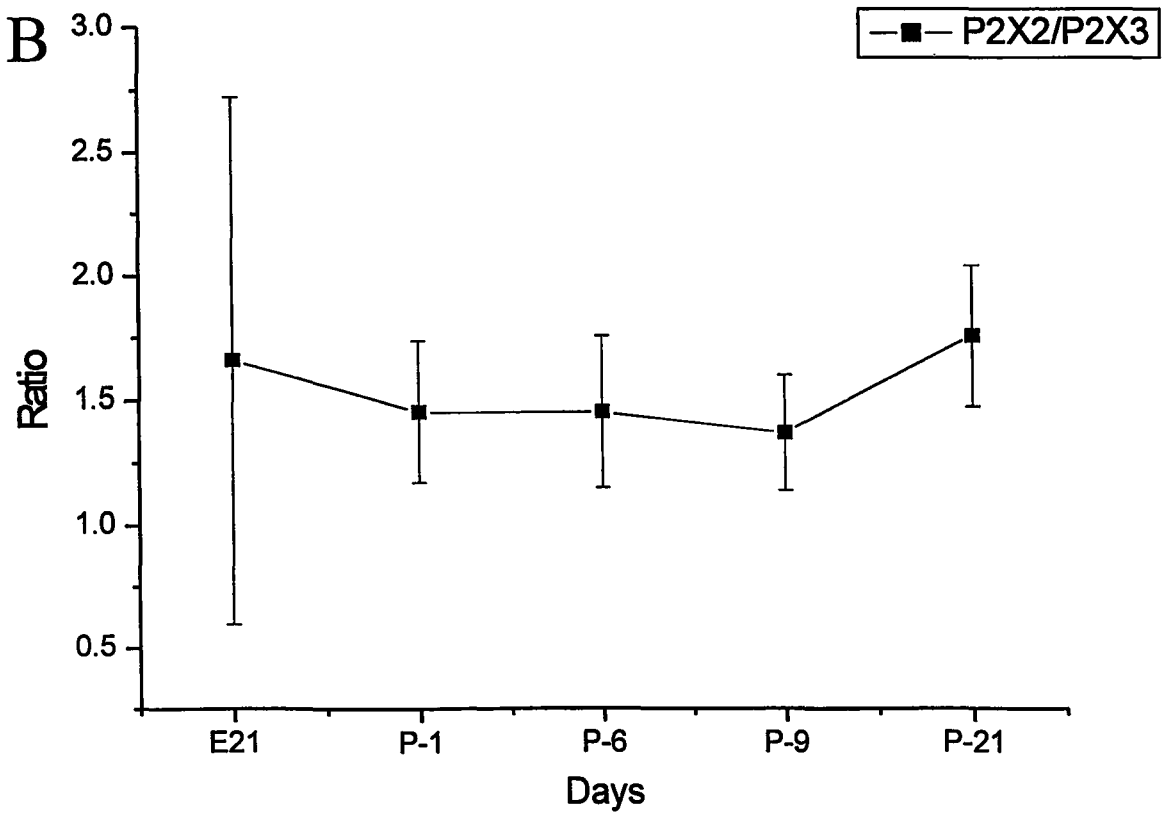
B
P2X2/P2X3
Ratio
3.0
2.5
2.0
1.5
1.0
0.5
E21
P-1
P-6
P-9
P-21
Days

Figure 2.6 Quantitative analysis of the P2X2 and P2X3 mRNA expression in isolated nodose neurons during postnatal development.

A. Data were normalized and expressed as a ratio by dividing the area under the curve for either P2X2 or P2X3 products by that of β-actin. RNA extracted from isolated nodose neurons at postnatal (P)-0, 1, 6, 9 and 21 was amplified and measured using the LightCycler system with specific primers for P2X2 (□) and P2X3 (●; n = 3, in both cases). There is a significant increase in expression of both P2X2 and P2X3 at P-9 relative to mRNA levels at P 0 – 6 and P-21. The error bars represent the standard error of the mean (S.E.M.), *$P<0.01$ and **$P < 0.05$ in one-way ANOVA. (N.B. Asterisks (*) indicated above the P2X2 curve belong to the P2X2 data, whereas the asterisks (**) indicated below the P2X3 curve represents the P2X3 data; *, ** are significant values when compared to P-9). ***B***. The plot compares the ratio of P2X2 : P2X3 (i.e. P2X2 divided by P2X3, n = 3) versus developmental age. The error bars represent the standard error of the mean (S.E.M.).

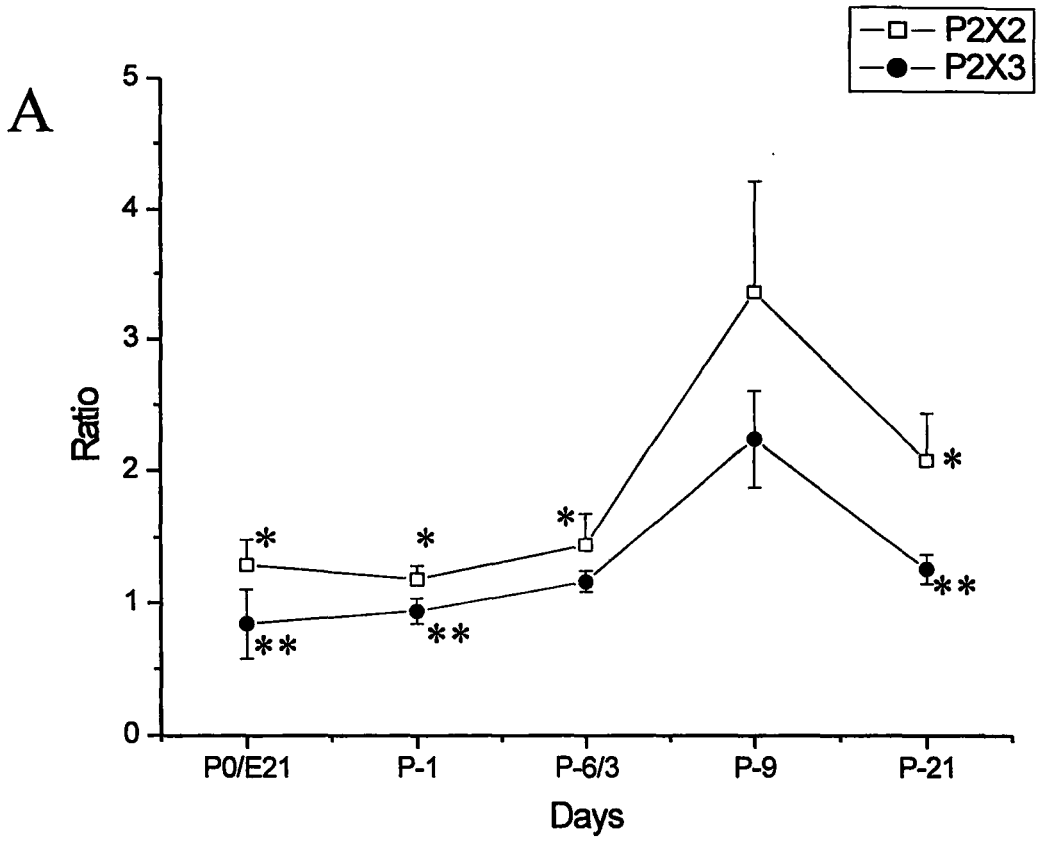
A
P2X2
P2X3
Ratio
0
1
2
3
4
5
P0/E21
P-1
P-6/3
P-9
P-21
Days
*
**

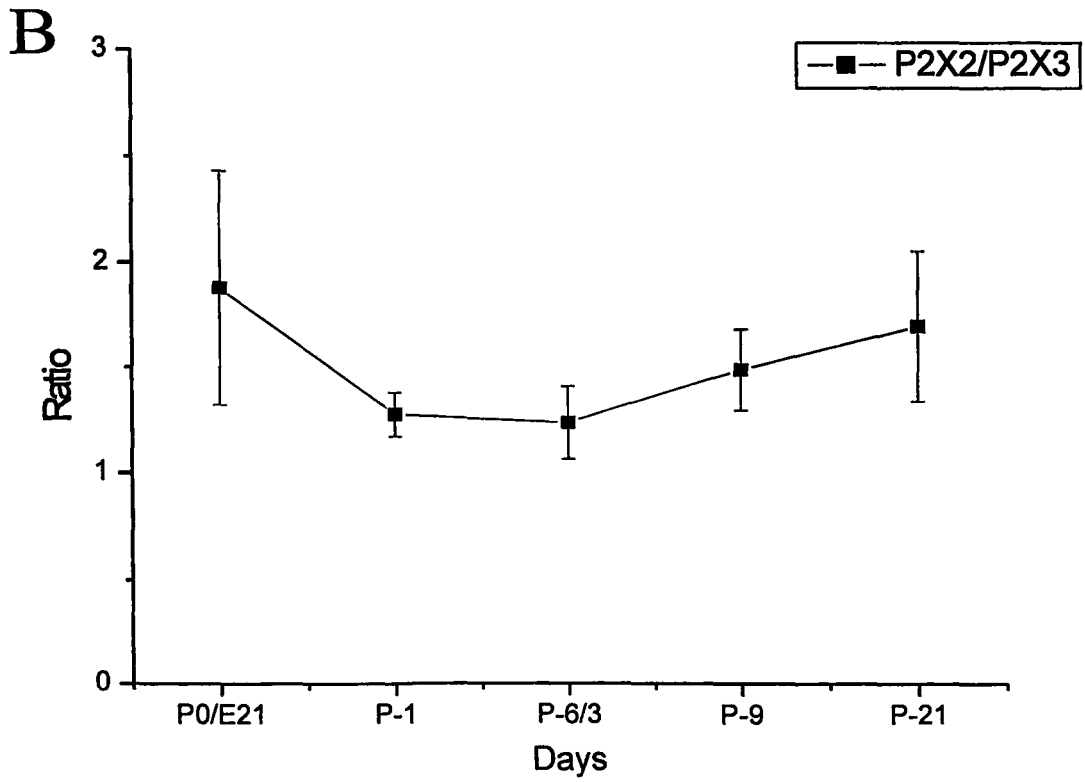
B
P2X2/P2X3
Ratio
0
1
2
3
P0/E21
P-1
P-6/3
P-9
P-21
Days

Figures 2.5 and 2.6 the P2X2:β-actin ratio was always higher than the P2X3:β-actin ratio. Thus, there is more P2X2 mRNA expressed than P2X3 mRNA, the significance of which will be discussed later. There was a slight increase in the expression levels of both P2X2 and P2X3 in the petrosal neurons between E-21 to P-21 (Fig. 2.5, **A**). In Figure 2.5 ***B***, P2X2 mRNA levels were divided by the corresponding ones for P2X3 and plotted against time (days). This allowed the ratio P2X2/P2X3 mRNA levels to be studied during the first 3 weeks of postnatal development. These data revealed the ratio of P2X2:P2X3 mRNA expression remained relatively constant over this time period (Figure 2.5 ***B***).

In contrast, there was a significant increase in the expression levels of both P2X2 and P2X3 in the nodose neurons (Fig. 2.6, **A**; *P < 0.05 and ** P <0.01 one-way ANOVA) by P-9, followed by a decrease by P-21. In Figure 2.6 ***B***, P2X2 mRNA levels were divided by the corresponding ones for P2X3 and plotted against time (days). This allowed the ratio P2X2/P2X3 mRNA levels to be studied during the first 3 weeks of postnatal development. These data revealed that, as was the case for petrosal neurons, the ratio of P2X2:P2X3 mRNA expression remained relatively constant over this time period for nodose neurons (Figure 2.6 ***B***). Figure 2.7 is a gel photomicrograph of products obtained from LightCycler PCR after staining with ethidium bromide; panels ***A*** and ***B*** in Figure 2.7 were obtained from petrosal and nodose samples respectively.

Figure 2.7 Detection of mRNA for P2X2, P2X3 and β-actin in isolated petrosal and nodose neurons at developmental ages E-21, P-1, P-6, P-9 and P-21.A. LightCycler quantitative RT-PCR was carried out on groups of isolated **petrosal** neurons at embryonic day (E)–21, postnatal (P)–1, 6, 9 and 21 using gene-specific primers for P2X2, P2X3 and β-actin. Expected product sizes are (in bp): P2X2 (156), P2X3 (219) and β-actin (327). The marker lane (M) shows bands at 100 bp increments with the 600 bp fragment at increased intensity. In negative control reactions (C) without template or cDNA, no PCR products were observed. The 2 % agarose gel was stained with ethidium bromide and viewed under UV illumination. **B.** LightCycler quantitative RT-PCR was carried out on groups of isolated **nodose** neurons at embryonic day (E)–21, postnatal (P)–1, 6, 9 and 21 using gene-specific primers for P2X2, P2X3 and β-actin. Expected product sizes are (in bp): P2X2 (156), P2X3 (219) and β-actin (327). The marker lane (M) shows bands at 100 bp increments with the 600 bp fragment at increased intensity. In negative control reactions (C) without template or cDNA, no PCR products were observed. The 2 % agarose gel was stained with ethidium bromide and viewed under UV illumination.

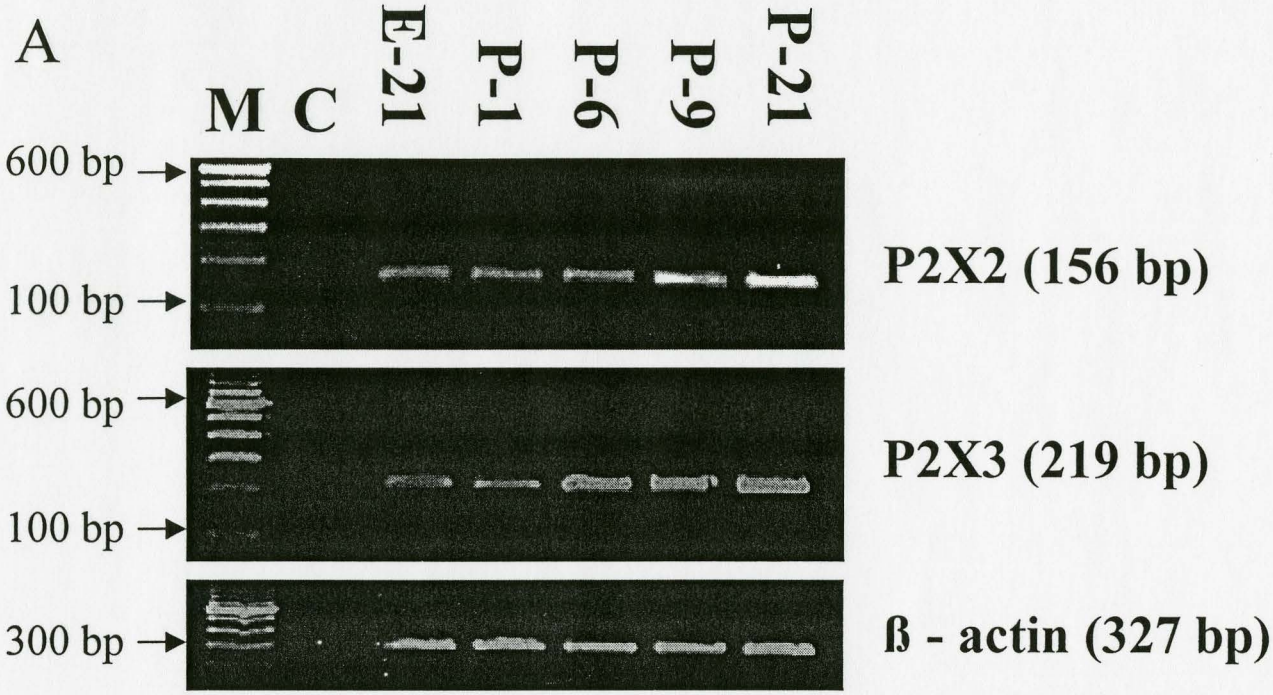
A
M C
E-21
P-1
P-6
P-9
P-21
600 bp
100 bp
600 bp
100 bp
300 bp
P2X2 (156 bp)
P2X3 (219 bp)
ß - actin (327 bp)

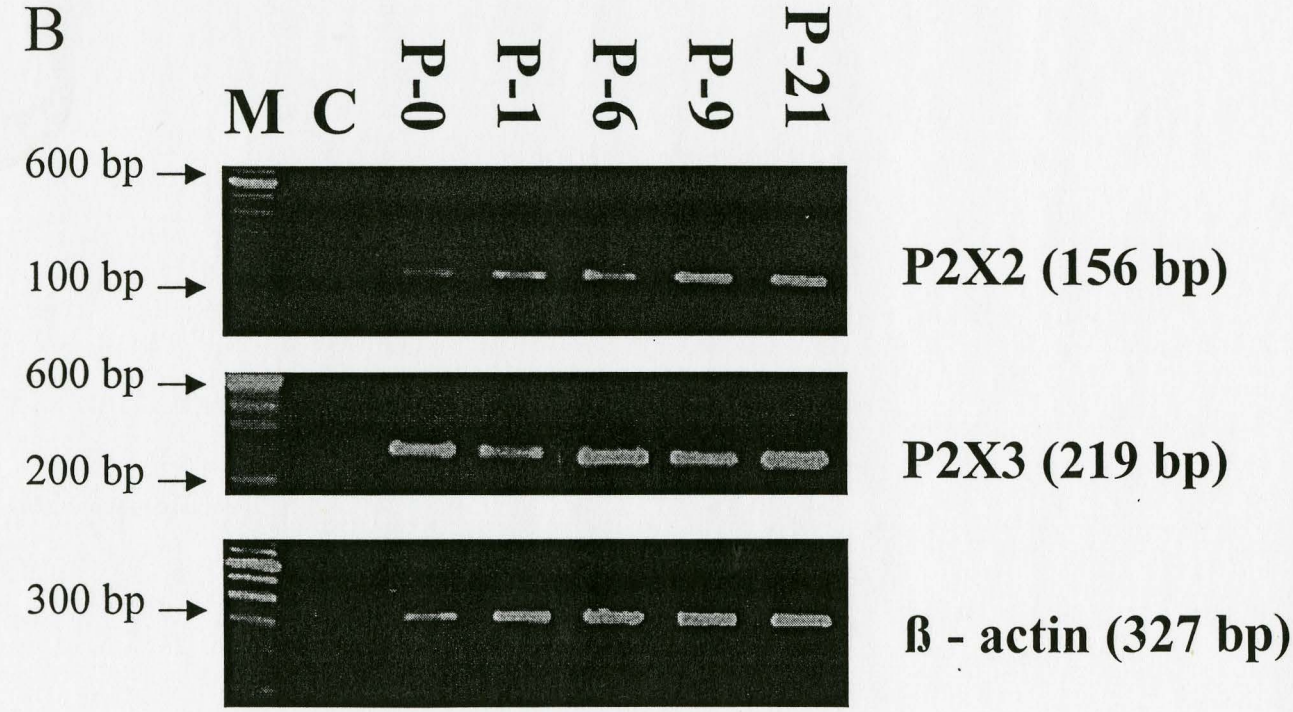
B
M C
P-0
P-1
P-6
P-9
P-21
600 bp
100 bp
600 bp
200 bp
300 bp
P2X2 (156 bp)
P2X3 (219 bp)
ß - actin (327 bp)

Localization of P2X2 and P2X3 Subunits in isolated Nodose neurons by Confocal Immunofluorescence

The observations that both P2X2 and P2X3 mRNA were expressed in nodose neurons (Figure 2.7), led us to investigate the localization of the corresponding proteins *in situ*. P2X2 and P2X3 subunits were localized using double-label immunofluorescence and confocal microscopy on tissue sections of 12-15 day-old rat nodose ganglia. Most of the neurons in the nodose ganglia were strongly positive for both P2X2 and P2X3 subunits (Fig. 2.8 A-C).

Comparison of developmental profile of dopamine content in the carotid body with mRNA levels of P2X subunits in isolated petrosal neurons

Hertzberg *et al.* (1990) studied developmental changes in dopamine content in the rat CB using high performance liquid chromatography (HPLC). For comparison, the data from that study are superimposed on those from the present one on P2X2/P2X3 mRNA expression (Figure 2.9). Although the two parameters being compared are not related, it is likely that they both determine the overall sensitivity of the CB chemoafferent pathway via excitatory vs. inhibitory contributions.

The DA content increased dramatically by P-1 (N.B. * indicates a significant difference relative to fetal values $P < 0.05$), while the mRNA levels for both P2X2 and P2X3 remain fairly constant until P-9, when a slight increase can be detected.

Figure 2.8 Expression of P2X2 and P2X3 subunits in tissue sections of nodose ganglia as revealed by Confocal Immunofluorescence.

A-C represents the same tissue section from the nodose ganglion of a 9 day-old rat after immunostaining with antibodies against P2X2 and P2X3 receptors. Localization of P2X2 (**A**) and P2X3 (**B**) subunits is revealed by Cy3 and FITC fluorescence respectively; dual exposure in (**C**) shows overlap of P2X2 and P2X3 staining. Calibration bar represents 20 μm in all panels.

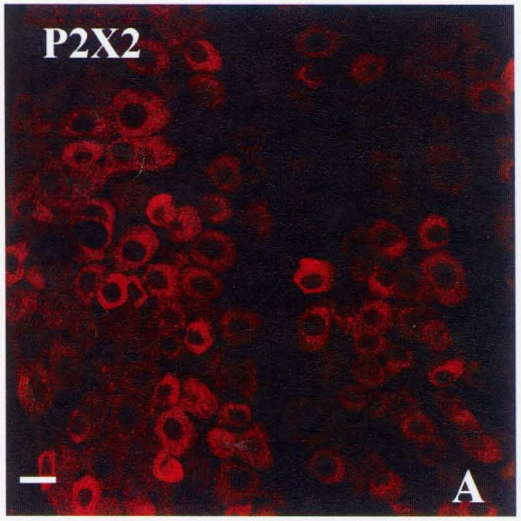
P2X2
A

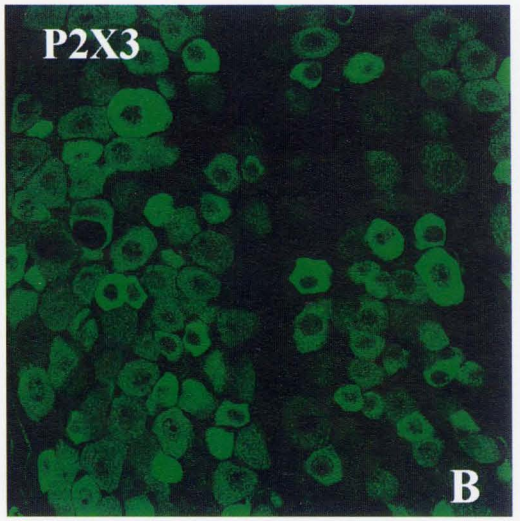
P2X3
B

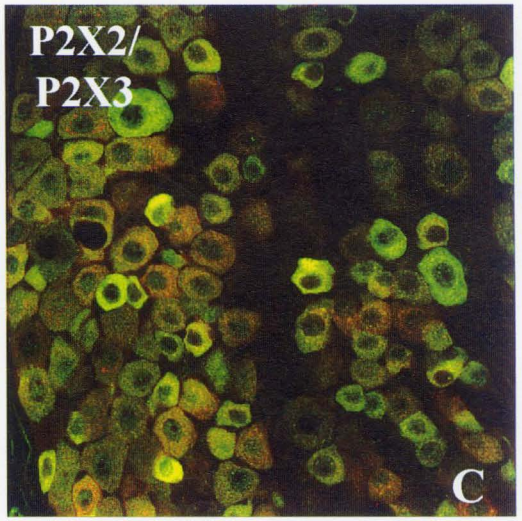
P2X2/
P2X3
C

Figure 2.9 Comparison of developmental profile of dopamine content in the carotid body with mRNA levels of P2X subunits in isolated petrosal neurons.

A. A comparison of the dopamine (DA) content from a pair of carotid bodies to the expression of P2X2 subunits in the petrosal ganglia. The left-hand y-axis represents the DA content (pmol per pair of CB; n = 5; □) and the right-hand y-axis represents the ratio of P2X2:ß-actin from 150 isolated petrosal neurons (n = 3; ●). The DA curve is adapted from Hertzberg, T. *et al.* (1990). The error bar represents the standard error of the mean (S.E.M.), *P<0.05. Panel ***B*** as in **A** except that it compares the DA content in the CB to the mRNA P2X3:ß-actin ratio in the PG.

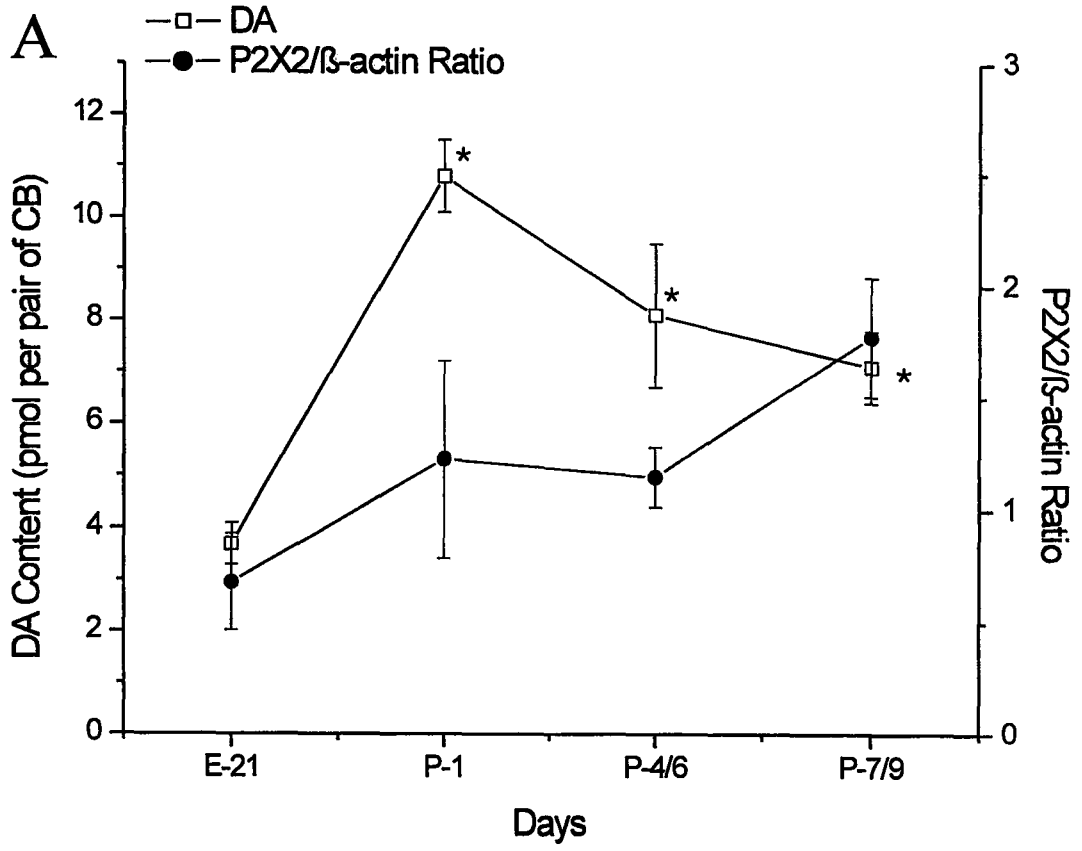
A
DA
P2X2/ß-actin Ratio
DA Content (pmol per pair of CB)
P2X2/ß-actin Ratio
0
2
4
6
8
10
12
0
1
2
3
*
*
*
E-21
P-1
P-4/6
P-7/9
Days

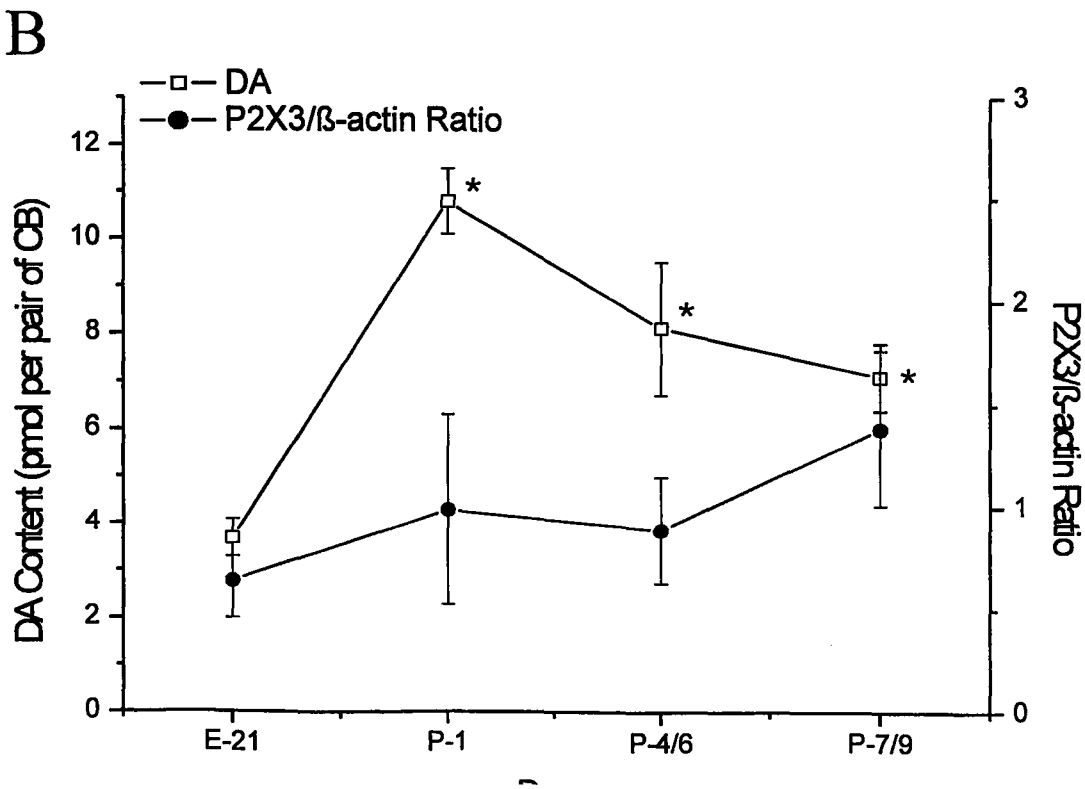
B
DA
P2X3/ß-actin Ratio
DA Content (pmol per pair of CB)
P2X3/ß-actin Ratio
0
2
4
6
8
10
12
0
1
2
3
*
*
*
E-21
P-1
P-4/6
P-7/9

DISCUSSION

Many cellular decisions concerning survival, growth and differentiation are reflected in altered patterns of gene expression, and the ability to quantitate transcription levels for specific genes is central to research into gene function (Zamorano *et al.*, 1996). There are several benefits to using real-time quantitative PCR, such as, being able to monitor the amplification of the PCR products simultaneously, in real-time and on-line. Reproducibility is made easier since the air is evenly circulated to distribute the temperature uniformly within the thermo-cycler to ensure identical PCR conditions. The LightCycler system is very sensitive and can measure low levels of mRNA (cDNA) from small sample sizes (e.g. 150 neurons in this study) which otherwise could not be detected. Further, the accurate identification of amplified PCR products with the aid of the melting curve analysis (Figures 2.2-2.4) is an added bonus. Due to these benefits of the LightCycler system it has been possible to study the expression profiles of P2X2 and P2X3 receptor mRNA in both rat petrosal and nodose ganglia in this study.

The nodose ganglion was used as a control, since it also expresses both P2X2 and P2X3 receptor subunits and has a similar development origin as the petrosal ganglion, but innervates different peripheral targets (Erickson *et al.*, 2000). Quantitative analysis was performed on E-21, P-1, P-6, P-9 and P-21 petrosal and nodose samples (See Figure 2.5 and 2.6, respectively). Comparison of these data reveals an overall increase in the expression of P2X2 and P2X3 by P-9, followed by a drastic decrease by P-21 in the NG. The expression level for β-actin remains fairly constant in both cases. Thus, although, the survival of nodose and petrosal neurons require the same growth factor i.e. GDNF,

during late fetal development (Erickson *et al.*, 2000), the pattern of expression of two P2X subunits is different between the two ganglia. The significance of the peak in P2X2 and P2X3 mRNA expression observed at postnatal day 9 in the nodose neurons is presently unknown.

However, it appears that expression levels of both P2X2 and P2X3 mRNA develop in a parallel fashion, though there seems to be proportionally more P2X2 mRNA expression relative to P2X3 mRNA (Figure 2.5 *A* and 2.6 *A*). Since the carotid body is a major target for the petrosal ganglion, and P2X2/P2X3 heteromultimers appear to be the functional receptors in the CB chemoafferent pathway, this parallel P2X2/P2X3 expression pattern in the PG may simply reflect the molecular basis for assembling heteromeric proteins. This is also consistent with immunocytochemical data showing the majority of petrosal neurons co-express P2X2 and P2X3 proteins. Moreover, single cell RT-PCR studies in this laboratory have recently shown that identified petrosal neurons, which responded to hypoxia express both P2X2 and P2X3 mRNA (Prasad et al., 2001; in press). These data however do not rule out the possible presence of homomeric P2X2 and homomeric P2X3 receptors in a subpopulation of these neurons.

Developmental studies have been carried out examining dopamine and dopamine D2 receptors (Hertzberg *et al.*, 1990; Gauda *et al.*, 1996; Donnelly, 2000), but no conclusive role for dopamine has been established. In 1998, Bairam *et al.* proposed that the dual effects of DA on carotid sinus nerve discharge rate (CSND) might be due to the activation of both D2 and D1 receptors. The CSND is dependent on DA levels, i.e. low doses of DA elicit an inhibitory response while at high doses DA has an excitatory

response. This dose dependence is due to the affinity of dopamine to DA D2-R being higher than that for the D1-receptors. A similar mechanism has been studied in the central nervous system in the striatum (Smialowski *et al.*, 1987). Further studies by Huey *et al.* (2000) have proposed that changes in DA (2)-R mRNA in the arterial chemoreflex pathway and corresponding changes at the protein and signaling levels may contribute to the time-dependent changes in ventilation observed with chronic hypoxia.

Tyrosine Hydroxylase (TH) is the rate-limiting enzyme in the biosynthetic pathway of catecholamines, which includes dopamine, noradrenaline and adrenalin, and is essential for mouse fetal development (Zhou *et al.*, 1995). In the carotid body, the level of tyrosine hydroxylase messenger RNA expression is greatest at birth, and significantly decreases by 48 h postnatal age and remains decreased at P-21 (Gauda *et al.*, 1996). Alternatively, Hertzberg *et al.* (1990) reported that DA content (measured by HPLC) decreased in the rat CB by P-7 (Figure 2.9). However, D2-dopamine receptor mRNA levels expressed in CB type I cells increased progressively during postnatal development (Gauda *et al.*, 2000).

In the present study, the mRNA levels for the P2X2 and P2X3 subunits in the petrosal neurons are increased by P-21 and show a trend, where the levels might progressively increase as the pathway matures. There seems to be a push and pull mechanism in the developmental regulation of the chemotransduction pathway (after the first week of postnatal development). Accordingly, ATP and ACh might induce an excitatory response whereas, DA induces an inhibitory one (see Figure 2.9 the DA curve falls at P-7 and the P2X2 and P2X3 curve climbs at P-9).

Gauda *et al.* (1997) have shown that mRNA for both the excitatory A_{2a}-adenosine receptor, and the inhibitory D (2)-dopamine receptor, is developmentally regulated in type I cells in the carotid body, and this contributes to the maturation of hypoxic chemosensitivity. However, the presence of A_1-adenosine receptor mRNA in cell bodies of the petrosal ganglion suggests that adenosine might also have an inhibitory role in hypoxic chemotransmission (Gauda *et al.*, 2000). Activation of presynaptic A_1-receptors by endogenous adenosine inhibits acetylcholine release in the guinea-pig ileum (Lee *et al.*, 2001). To further explain this model there is evidence that adenosine is produced during hypoxia in CB (Chen *et al.*, 1997) and studies have shown that A_{2a} adenosine receptors are expressed in type I cells and that activation of A_{2a} receptors modulates Ca^{2+} accumulation during hypoxia (Kobayashi *et al.*, 2000).

However, adenosine is not released like other classical neurotransmitters but is produced when extracellular ATP is degraded by ecto-ATPase on the cell membranes. Earlier histochemical studies located ATPase in the cell membranes of type I cells, sustentacular cells and nerve fibers (Cunha and Ribeiro, 2000). ATP released by the type I cell into the synapse can act on postsynaptic P2X receptors (i.e. inducing an excitatory response), or degraded by membrane-bound and/or free ATPase yielding adenosine, which can act via the A_1 receptors and stimulate an inhibitory response. This model conforms to the proposed 'push and pull' hypothesis. Both adenosine and dopamine have an overall inhibitory role in the chemotransduction pathway, while ATP and ACh have an excitatory role.

During the first few days of postnatal development, following the increase in Po_2 at birth, the chemoreceptors are silenced (Hertzberg *et al.*, 1990). There is a dramatic increase in DA content in the CB (i.e. inhibition of carotid sinus discharge) during the first 24 h , followed by the dramatic drop in DA content after P-1 and a steady increase of excitatory P2X receptors in the first week (Figure 2.9). Subsequently, the DA D2-Rs are highly expressed and the levels of P2X receptors seem to rise in the chemosensory pathway as the animal adapts to its new environment (i.e. higher Po2).

In conclusion, the chemotransduction pathway is complex and involves several players. The mechanisms by which the chemotransduction pathway is regulated, especially in response to varying environmental Po_2, requires further work. This study provides a glimpse as to the role of ATP and P2X receptors in this complex pathway.

CHAPTER 3

UP-REGULATION OF PURINERGIC RECEPTORS IN TYPE I CELLS BY CHRONIC HYPOXIA

SUMMARY

In cryostat sections, P2X2 and P2X3 subunits were not detected in type I cells of the rat carotid body (P-13) by confocal immunofluorescence. Developmental studies have indicated that expression levels of various autoreceptors on carotid body type I cells (e.g. dopamine D2-receptors, A2a and A2b adenosine receptors) change during the first week of postnatal life, as the animal breathes normoxic air. In the present study, the possibility that oxygen tension might regulate P2X receptor expression in rat type I cells was examined. RT-PCR was employed to compare expression levels of P2X subunits in isolated type I cells grown under different O_2 tensions. Compared to normoxic (20% O_2) control, a two-fold increase in expression of P2X2 mRNA was observed in type I cell clusters grown under chronic hypoxia (6% O_2 for 11-14 days). Immunofluorescence studies also indicated an up-regulation in P2X2 and P2X3 protein expression in type I cells grown under chronic hypoxia. The P2X receptor subunits expressed in the type I cells are proposed to stimulate neurotransmitter release via a positive feedback pathway.

INTRODUCTION

The carotid body (CB) behaves like a chemo-, thermo-, osmo- and flow receptor, but the nerve fibers (pathways) conveying the different types of information are the same. Consequently a single chemosensory fiber will change its discharge frequency when simulated by chemical, thermal and osmotic stimuli (Eyzaguirre and Zapapta, 1984). The O_2-sensitive glomus or type I cells are ovoid, with large nuclei and abundant mitochondria (Eyzaguirre and Zapapta, 1984), and secrete several neurotransmitters that regulate the carotid sinus discharge (Gonzalez *et al.* 1994, Zhang *et al.*, 2000).

Acute hypoxia (i.e. an environment where the Po_2 levels are low over a time scale of seconds to minutes) causes a rapid increase in carotid sinus nerve activity, providing afferent signals to the brainstem. In contrast, the effects of chronic hypoxia (i.e. an environment where the Po_2 levels are low over a time scale of hours to days) involve changes in gene expression (Semenza *et al.*, 1999). Exposure of CB type I cells to chronic hypoxia (6% O2) for 9-14 days increases their size (3-4 x control) (Mills and Nurse, 1993) and excitability (Stea *et al.*, 1992). Furthermore, cyclic AMP (cyclic adenosine monophosphate) has been identified as a possible intracellular mediator of at least some of the effects induced by chronic hypoxia (Nurse, 1995). Studies performed by Offord *et al.* (1989) on rat skeletal muscle cells demonstrated that elevation of intracellular cAMP mimics the effects of chronic hypoxia. Further, acute hypoxia is known to increase the cAMP levels in the carotid body (Wang *et al.*, 1991; Monteiro *et al.*, 1996).

In cryostat sections, the P2X2 and P2X3 subunits were not detected in somas of rat carotid body type I cells (P-13) by confocal immunofluorescence (Figure 1.8). However, other developmental studies have indicated that expression levels of various autoreceptors (e.g. dopamine D2-receptors, A_{2a} and A_{2b} adenosine receptors) on type I cells change during the first week of postnatal life, as the animal breathes normoxic air. We therefore wondered whether O_2 tension might regulate P2X receptor expression in type I cells. First, RT-PCR was employed to compare expression levels of P2X mRNA in the CB of newborn (P-0) to P-9 rat pups. Second, we also wanted to determine whether or not chronic hypoxia affected the expression profiles of P2X2 and P2X3 mRNA. In these experiments RNA extracted from isolated type I cell clusters grown under chronic hypoxia was measured using the LightCycler system.

Immunofluorescence studies were carried out on cultured type I cells grown in medium containing excess of dibutyryl cyclic AMP (a permeable analog of cAMP) or selective inhibitor of cAMP-dependent protein kinase (PKA blocker – KT5720) under normoxic and chronically hypoxic conditions, respectively. These experiments were carried out to test for the possible involvement of cAMP-dependent pathway in mediating the effects of chronic hypoxia.

MATERIALS AND METHODS

Isolation of type 1 cells and RNA

The procedures used for the isolation of type I cells were similar to those described in Chapter 1. Primary cultures of dissociated rat carotid bodies were prepared from postnatal P-0 and P-9 pups. The cultures were incubated at 37° C in a humidified atmosphere of 95% air: 5% CO_2 for 2- 3 days before exposing them to one of the following treatments for an addition 10-14 days: i) control normoxic environment (20% O_2 / 75% N_2 / 5% CO_2); ii) a hypoxic environment (6% O_2 / 89% N_2 / 5% CO_2); iii) a normoxic environment with permeable cAMP analog, dibutyryl cyclic AMP, also known as, N6,O2'-dibutyryladenosine 3',5'-cyclic monophosphate (1 mM; Sigma Chemical Co., St. Louis, MO) present in the growth medium; and iv) a hypoxic environment with KT5720 (100nM; Alomone Laboratories, Jerusalem, Israel) a selective PKA blocker, in the growth medium. Total RNA was obtained from 10-35 isolated type I clusters consisting typically of 15-20 type I cells. After 10-14 days of Nox or CHox, clusters were removed from dish by mechanical suction (n = 4).

Reverse transcriptase polymerase chain reaction (RT-PCR)

Total RNA was obtained from 10-35 type 1 clusters that were mechanically isolated (refer to Chapter 1 for more details on cell isolation using suction and a micropipette). RT-PCR was performed as described in Chapter 1, followed by agarose gel electrophoresis to view the amplified products. A standard PCR was carried out using 3-5 µl of cDNA as a control, to confirm that the mRNA was converted to cDNA for the

Quantitative PCR analysis. The remaining 15-17 µl of RT reaction was saved for the quantitative PCR analysis.

Quantitative RT-PCR using LightCycler

The LightCycler (Roche Molecular Biochemicals) was used to perform quantitative PCR (refer to Chapter 2 for more details). The cDNA from the RT reaction was used for the LC reactions. P2X2 (156 bp) and P2X3 (219 bp) primers were used in these reactions (refer to Table 1.1). The LC-PCR products were separated on a 2 % agarose gel and viewed under UV illumination.

Confocal Immunofluorescence

Cultures of carotid body type 1 from postnatal (P-0 and P-9) rats were processed for immunofluorescence (see Chapter 1 for more details). The cultures were incubated at 37°C in a humidified atmosphere of 95% air: 5% CO_2 for 2- 3 days before exposing them to one of the treatments listed above. The primary antibodies used were: (i) anti-P2X2 (1:800 dilution), a rabbit polyclonal antibody raised against a highly purified peptide corresponding to amino acid residues 457-472 of the rat P2X2 receptor (Alomone Laboratories, Jerusalem, Israel), and (ii) anti-P2X3 (1:500 dilution), a guinea pig polyclonal antiserum raised against amino acid residues 383-397 of the rat P2X3 receptor (Neuromics, Minneapolis, MN, USA). The secondary antibodies (Jackson Immunoresearch Laboratories, West Grove, PA) consisted of Cy3-conjugated goat anti-rabbit IgG (1:500 dilution), and FITC-conjugated goat anti-guinea pig IgG (1:20

dilution), respectively. Cultured cells were immunostained and viewed as described in Chapter 1.

RESULTS

Detection of P2X2 and P2X3 mRNA in isolated CB type I cells by RT-PCR

In this study we tested for the expression of P2X2 and P2X3 autoreceptors on rat CB type I cells *in situ*. Immunostaining of P-13 CB sections (Figure 1.8) for both P2X2 and P2X3 receptor subunits gave negative results. To test whether or not P2X mRNA was expressed in the intact organ, RT-PCR was carried out on a pair of whole carotid bodies isolated from P-9 rats. Interestingly, both P2X2 and P2X3 mRNA were detected (Figure 3.1). The intact CB, which is a highly vascularized organ, contains a variety of other cell types which could contribute to P2X2 and P2X3 mRNA signal. Therefore, a relatively pure population of type I cell clusters (P-9) were mechanically isolated from 2-3 day old CB cultures. Though these clusters are enriched for type I cells the presence of contaminating type II (glial) cells could not be excluded. RT-PCR was then carried out on these isolated type I cell clusters. Faint bands for P2X2 and P2X3 mRNA were detected by PCR for cultured (type I) samples obtained from P9, P0 and embryonic E-21 carotid bodies (Figure 3.1).

Figure 3.1 Detection of mRNA for P2X2, P2X3 and β-actin in isolated CB type I cells.

RT-PCR was carried out on RNA isolated from whole carotid body (P-9), and cultured type I clusters from E-21, P-0 and P-9 pups using gene-specific primers for P2X2 and P2X3 receptors, and β-actin. The P2X3 band in the P-0 lane is very faint (and might not be visible in this photomicrograph). Expected product sizes are (in bp): P2X2 (156), P2X3 (219), β-actin (327). The marker lane (M) shows bands at 100 bp increments with the 600 bp fragment at the top (indicated by *arrows*). The negative control lanes (-) are reactions without RT enzyme; no PCR products were observed in these lanes. The 2 % agarose gel was stained with ethidium bromide and viewed under UV illumination.

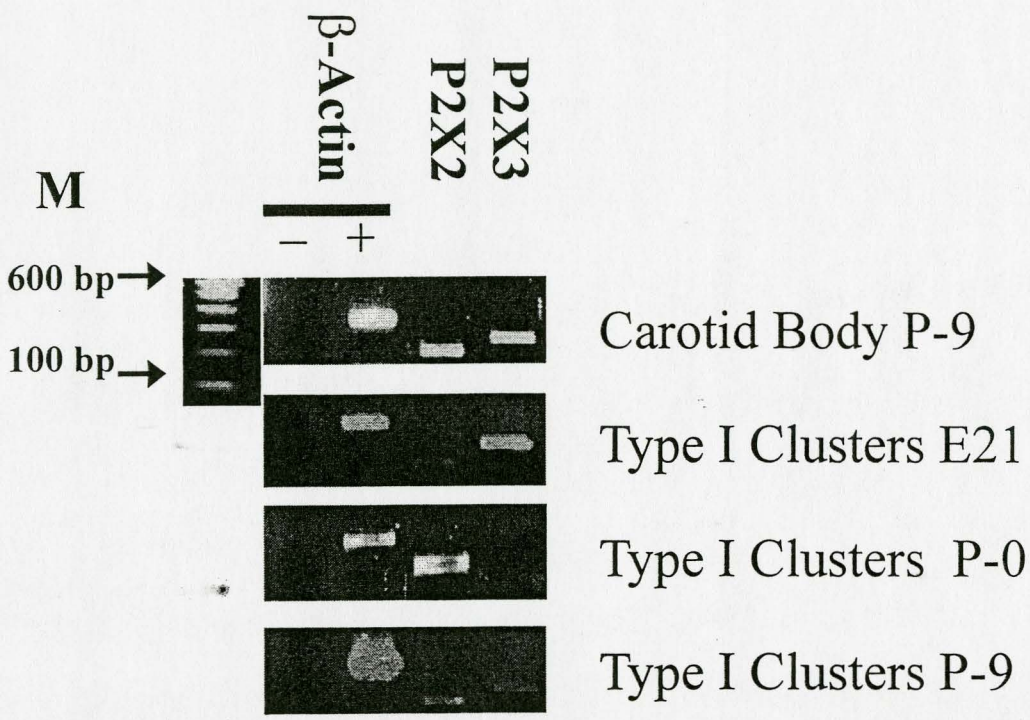
M
600 bp
100 bp
β-Actin
P2X3
P2X2
–
+
Carotid Body P-9
Type I Clusters E21
Type I Clusters P-0
Type I Clusters P-9

Detection and quantitative analysis of P2X2 and P2X3 mRNA in isolated CB type I cells grown under chronically hypoxic conditions

Quantitative RT-PCR was employed to measure possible changes in expression levels of both P2X2 and P2X3 mRNA in cultured type I cells grown under chronic hypoxia (6% O_2 / 89% N_2 / 5% CO_2) for 11- 14 days. Figures 3.2 and 3.3 represent data acquired from the LightCycler system for the P2X mRNA. Figure 3.3 shows a 200% increase in expression level of P2X2 mRNA in chronically hypoxic (CHox) type I clusters compared to normoxic (Nox) controls. (N.B. * indicates expression has significantly increased, but the P value calculated by the Mann-Whitney test is "not quiet significant", i.e. P is slightly greater than 0.05 relative to basal, Nox P2X2/β-actin ratio). A slight increase in expression level of P2X3 mRNA in chronically hypoxic (CHox) type I clusters compared to normoxic (Nox) controls was observed (Figure 3.3). A gel photomicrograph for type I cell clusters incubated in normoxic and hypoxic environments is shown in Figure 3.2. Most interestingly, an increase in expression of P2X2 and P2X3 subunits at the protein level was observed in cultured type I cells by confocal immunofluorescence, after 14 days in chronic hypoxia (Figure 3.4).

Expression of P2X2 and P2X3 subunits in isolated type I cell clusters cultured with dibutyryl cAMP and PKA blocker as revealed by Confocal Immunofluorescence

We hypothesized that the effects of chronic hypoxia on P2X receptor expression in type I cells was mediated via a cAMP-dependent PKA pathway. To test this, confocal immunofluorescence studies were carried out on Nox cultures incubated with 1mM

Figure 3.2 Detection of mRNA for P2X2, P2X3 and β-actin in isolated type 1 cell clusters cultured in chronic hypoxia.

A. LightCycler quantitative RT-PCR was carried out on groups of isolated type I clusters for **P–0** pups. Cultures incubated at 37° C in a humidified atmosphere of 95% air: 5% CO_2 for 2- 3 days before exposure to one of the following treatments for an addition 10-14 days: 1) control normoxic environment (20% O_2 / 75% N_2 / 5% CO_2); *or* 2) a hypoxic environment (6% O_2 / 89% N_2 / 5% CO_2). Total RNA was obtained from 10-35 isolated type 1 clusters and PCR was performed using gene-specific primers for P2X2, P2X3 and β-actin. Expected product sizes are (in bp): P2X2 156, P2X3 219, and β-actin 327. The marker lane (M) shows bands at 100 bp increments with the 600 bp fragment at increased intensity. In negative control reactions (without RT) no PCR products were observed (not shown). The 2 % agarose gel was stained with ethidium bromide and viewed under UV illumination. Same experiment repeated in panel ***B.*** but with type I clusters isolated from **P-9** rat pups.

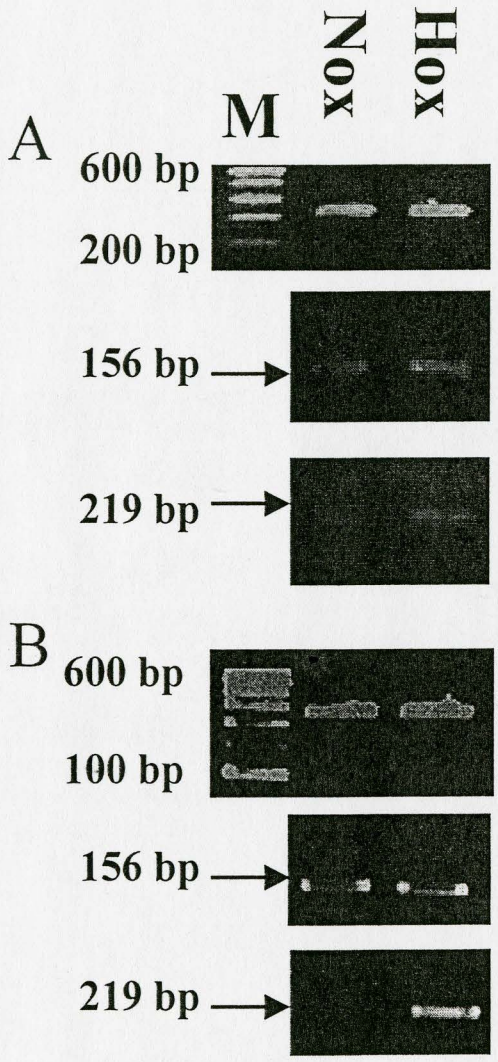
A
M
NOX
HOX
600 bp
200 bp
156 bp
219 bp
Type I cell Clusters P-0
ß -Actin
P2X2
P2X3
B
600 bp
100 bp
156 bp
219 bp
Type I cell Clusters P-9
ß-Actin
P2X2
P2X3

Figure 3.3 Quantitative analysis of P2X2 and P2X3 mRNA in isolated type I cell clusters grown in chronic hypoxia.

A. LightCycler quantitative RT-PCR was carried out on groups of isolated type I clusters, that were incubated at 37° C in a humidified atmosphere of 95% air: 5% CO_2 for 2- 3 days before exposure to one of the following treatments for an addition 10-14 days: 1) control normoxic environment (20% O_2 / 75% N_2 / 5% CO_2); *or* 2) a hypoxic environment (6% O_2 / 89% N_2 / 5% CO_2). Total RNA was obtained from 10-35 isolated type 1 clusters and PCR was performed using gene-specific primers for P2X2, P2X3 and β-actin (n = 4). Histogram shows the effect of chronic hypoxia on the expression levels of P2X2 and P2X3 relative to β-actin. Error bars represent the standard error of the mean (S.E.M.); * indicates expression has increased by 200% relative to basal Nox P2X2/β-actin ratio). Open and hatched bars represent P2X3/β-actin and P2X2/β-actin expression ratio, respectively.

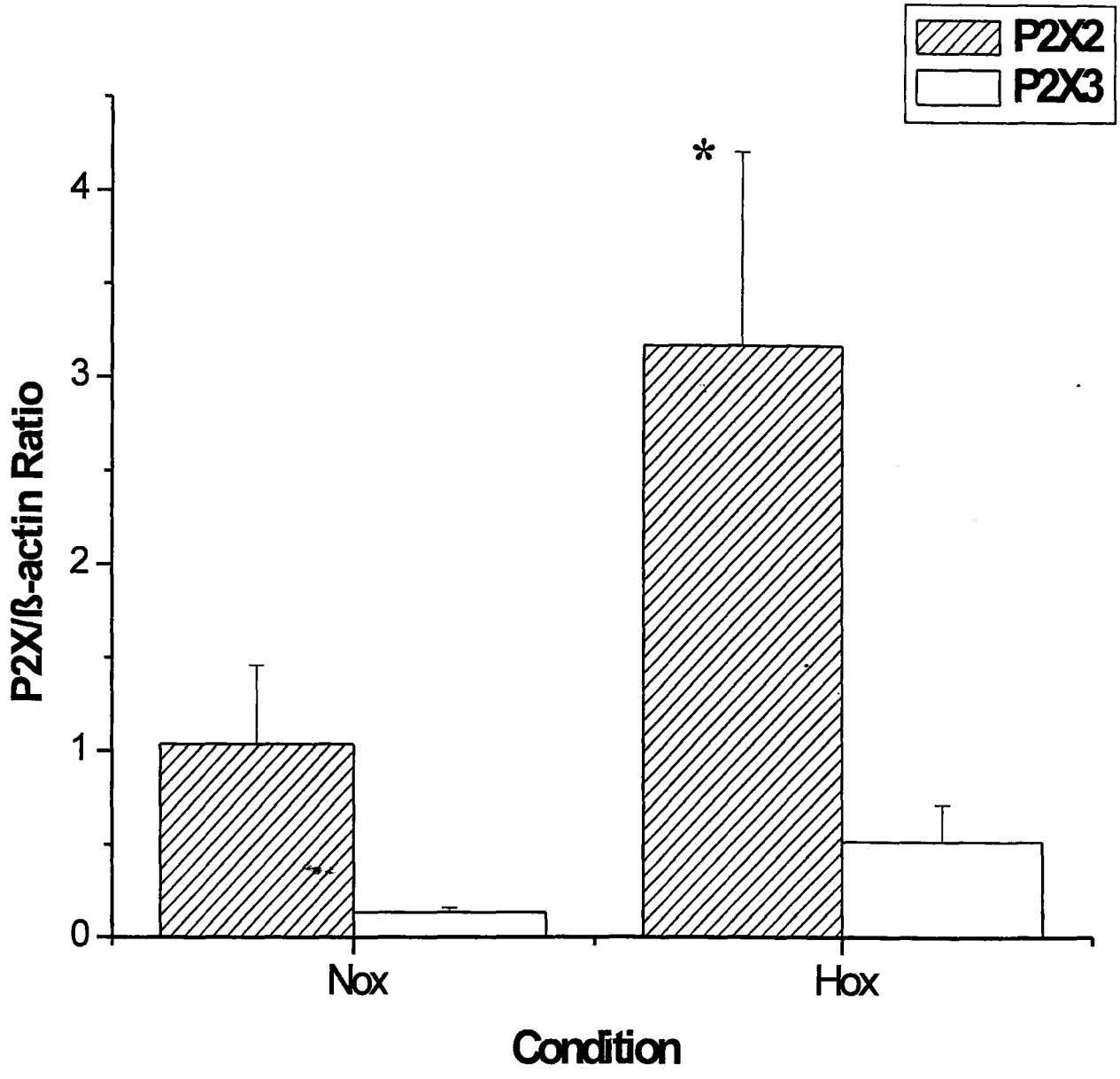
P2X2
P2X3
*
4
3
2
1
0
P2X/ß-actin Ratio
Nox
Hox
Condition

Figure 3.4 Expression of P2X2 and P2X3 subunits in isolated type I cell clusters cultured in chronic hypoxia as revealed by Confocal Immunofluorescence.

A-C represents the same type I cluster of a 9 day-old rat after immunostaining with antibodies against P2X2 and P2X3 receptors. Isolated type I clusters were incubated at 37° C in a humidified atmosphere of 95% air: 5% CO_2 for 2-3 days before exposing them for an additional 10-14 days to a control normoxic environment (20% O_2 / 75% N_2 / 5% CO_2); localization of P2X2 (**A**) and P2X3 (**B**) subunits is revealed by Cy3 and FITC fluorescence respectively; dual exposure in (**C**) shows overlap of P2X2 and P2X3 staining. In panels **D-F** isolated type I clusters, that were incubated at 37° C in a humidified atmosphere of 95% air: 5% CO_2 for 2- 3 days before exposing them to an additional 10-14 days to a hypoxic environment (6% O_2 / 89% N_2 / 5% CO_2). **D-F** represent the same microscopic field of a type I cluster from a 9 day-old rat after similar immunostaining with P2X2 and P2X3 antibodies as in **A-C**. Calibration bar represents 40 μm in A-F

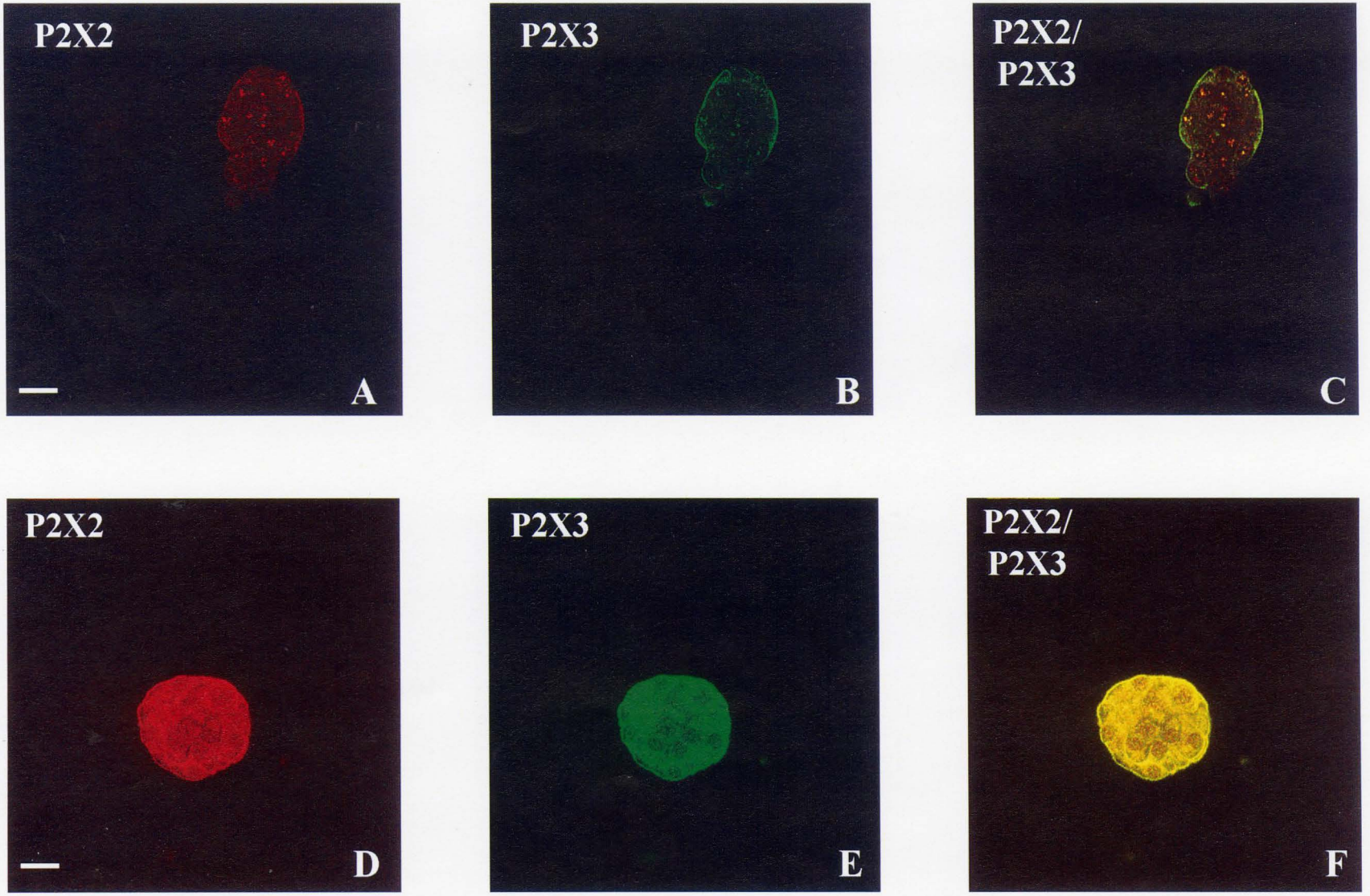
P2X2
A
P2X3
B
P2X2/
P2X3
C
P2X2
D
P2X3
E
P2X2/
P2X3
F

dibutyryl cyclic AMP (a permeable cAMP analog) for 14 days (Figure 3.5***A***, n = 4), and in CHox cultures incubated with the PKA blocker KT5720 for 14 days (Figure 3.5***B***; n=2). An slight increase in expression of P2X2 and P2X3 subunits at the protein level was observed in cultured type I cells grown under normoxic conditions with dibutyryl cAMP in the growth medium, when compared to Nox controls (Figure 3.5***A*** vs. Figure 3.4 ***A***). No change in expression of P2X2 and P2X3 subunits at the protein level was observed in cultured type I cells grown under chronically hypoxic conditions with PKA blocker (KT5720) in the growth medium, when compared to CHox controls (Figure 3.5***B*** vs. Figure 3.4 ***B***).

DISCUSSION

Carotid body (CB) type I cells release neurotransmitters onto afferent nerve terminals of the petrosal ganglia in the chemotransduction pathway involved in oxygen sensing (Gonzalez *et al.*, 1994). Presynaptic receptors for DA, ACh, 5-HT, and adenosine are expressed by these type I cells. The current study examined the hypothesis that presynaptic receptors on these cells are regulated by O_2 tension. In particular, strong evidence was obtained that expression of P2X (P2X2 and P2X3) ATP-receptor subunits in type I clusters from perinatal rat CB was indeed up regulated by chronic hypoxia (Figure 3.2 and Figure 3.3). In the peripheral nervous system ATP can act as a presynaptic modulator (Salgado *et al.*, 2000). Cunha *et al.* (2000) proposed that ATP can have biphasic presynaptic neuromodulatory effects: an inhibitory effect through the

Figure 3.5 Expression of P2X2 and P2X3 subunits in isolated type I cell clusters cultured with cAMP and PKA blocker as revealed by Confocal Immunofluorescence.

A-C represent the same type I cluster of a 9 day-old rat after immunostaining with antibodies against P2X2 and P2X3 receptors. Isolated type I clusters were incubated at 37° C in a humidified atmosphere of 95% air: 5% CO_2 for 2-3 days before exposing them for an additional 10-14 days to a normoxic environment with dibutyrl cyclic AMP (1 mM) present in the growth medium; localization of P2X2 (**A**) and P2X3 (**B**) subunits is revealed by Cy3 and FITC fluorescence respectively; dual exposure in (**C**) shows overlap of P2X2 and P2X3 staining. In panels **D-F** isolated type I clusters were incubated at 37° C in a humidified atmosphere of 95% air: 5% CO_2 for 2- 3 days before exposing them for an additional 10-14 days to a chronically hypoxic environment in the presence of KT5720 (100nM), a selective PKA blocker in the growth medium. **D-F** represent the same type I cluster from a 9 day-old rat after similar immunostaining with P2X2 and P2X3 antibodies as in **A-C**. Calibration bar represents 40 μm in A-F. (N.B. normoxic and hypoxic controls (i.e. without treatment) for this experiment are shown in Figure 3.4 A-C and Figure 3.4 D-F, respectively.)

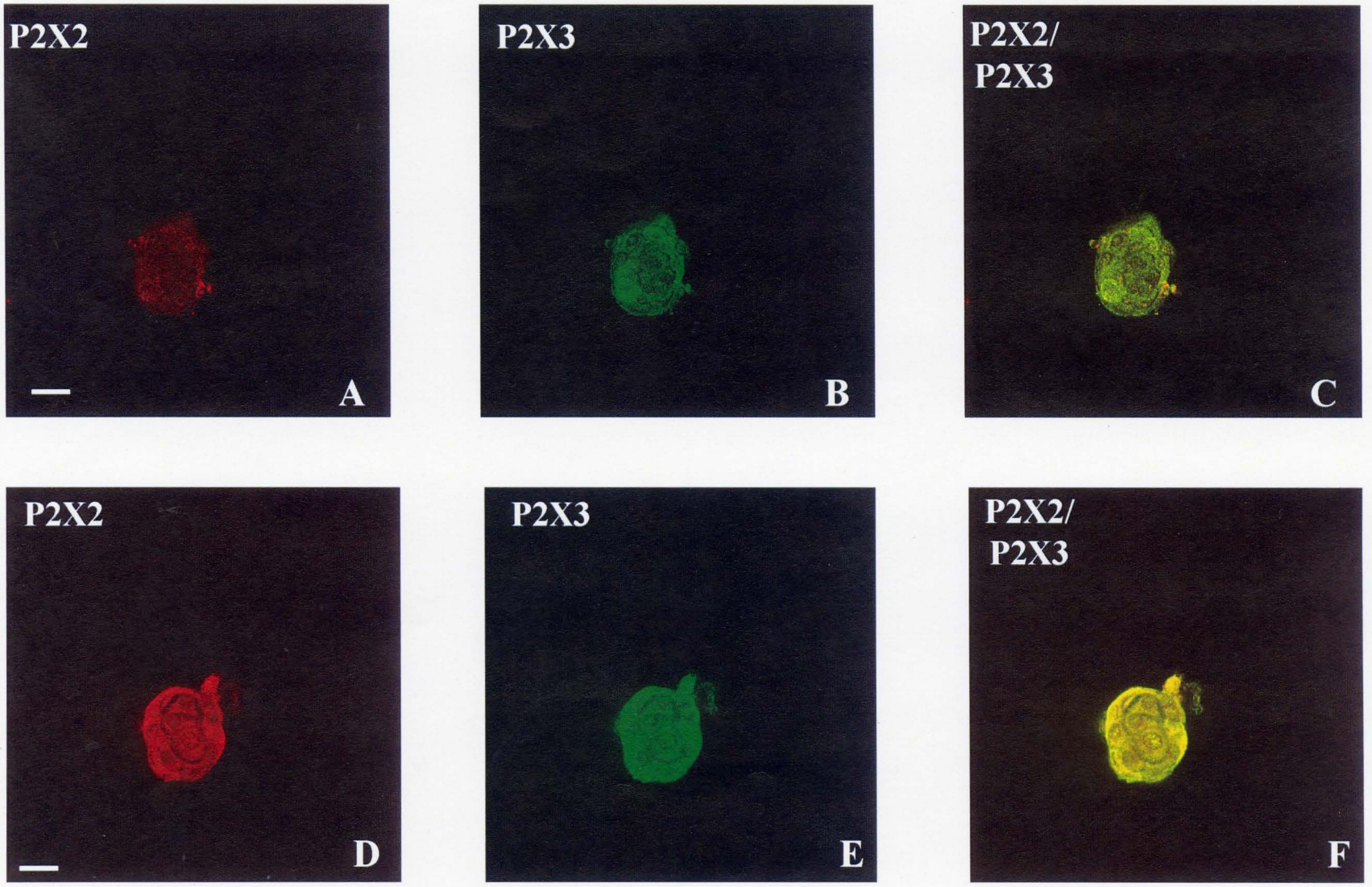
P2X2
A
P2X3
B
P2X2/
P2X3
C
P2X2
D
P2X3
E
P2X2/
P2X3
F

activation of P2Y receptors and facilitatory effect via activation of P2X receptors. The P2X receptor subunits expressed in the type I cells are proposed to have a positive effect on neurotransmitter release.

In mammals, ventilatory acclimatization to hypoxia is associated with an enhanced chemosensitivity of the O_2-sensing carotid body, resulting in an increased respiratory drive (Lahiri *et al.*, 2000). The increase in the carotid sinus discharge that occurs during acute hypoxia is in part due to the release of ATP and ACh from type I cells (Zhang *et al.* 2000). In the latter study, the effect of ATP, acting via P2X2/P2X3 heteromeric receptors, was presumed to be postsynaptic since these receptors were found on petrosal neurons and their terminals, but not type I cells. In the present study, quantitative RT-PCR was performed on type I cells incubated in chronic hypoxia for 11-14 days (Figure 3.2-3.4). Interestingly, there was a 2-fold increase in the expression level of P2X2 mRNA in type I cells exposed to chronic hypoxia (CHox) when compared to normoxic (Nox) controls (Figure 3.3). This increase is evident in gel photomicrographs where the band intensity for both P2X2 and P2X3 subunits is brighter for PCR products obtained from CHox samples when compared to Nox ones. The increase in P2X expression is also seen at the protein level, as demonstrated by confocal immunofluorescence (Figure 3.4). The up-regulation of the P2X receptor subunits during chronic hypoxia suggests that ATP may now act presynaptically (as well) and enhance neurotransmitter release from type I cells by a positive feedback process. This adaptation may in turn lead to an increase in carotid sinus nerve discharge and may contribute to enhanced chemosensitivity during ventilatory acclimatization to hypoxia (Stea *et al.*, 1995).

Stea *et al.* (1995) proposed that chronic hypoxia, acting in part through cAMP-dependent pathways, increases electrical excitability and calcium mobilization in type 1 cells. Since hypoxia is known to increase cAMP levels in type I cells (Wang *et al.*, 1991), we tested whether or not elevation of intracellular cAMP alone can increase the expression levels of P2X subunits in type I cells. Using immunofluorescence, a slight increase at the protein level was seen in cultured type I cells grown with the permeable cAMP analog, dibutyryl cyclic AMP (Figure 3.4, A-C). Thus, it is plausible that the effects of chronic hypoxia on expression of presynaptic P2X receptors in type I cells may be mediated via cAMP-dependent pathway. Other studies involving treatment with agents that elevate intracellular cAMP demonstrated that the effect of chronic hypoxia on GAP-43 expression in type I cells was mediated, at least in part, by a cAMP-dependent pathway (Jackson and Nurse, 1995).

Cyclic–AMP-dependent protein kinase (a-Kinase; PKA), which catalyzes the transfer of terminal phosphate groups from ATP to specific serine or theronine of selected proteins, in turn regulates activity and the functions of related target proteins. This signal cascade leads to the regulation of gene expression (Alberts *et al.*1994). By blocking the PKA signal-transduction pathway with selective blockers, it is possible to inhibit the regulation of gene expression. A derivative of K25a, a potent cell permeable, selective inhibitor of cAMP-dependent protein kinase (KT5720) was used in this study to block the PKA pathway in type I cells incubated in chronic hypoxia (Figure 3.5, panel D-E). No difference in immunofluorescence intensity was observed in CHox type I cells

incubated with the PKA blocker (Figure 3.4, A-C and Figure 3.5, D-E). However, it is not clear that this assay is sensitive enough to allow firm conclusions to be drawn.

In summary, it appears that the expression of both P2X2 and P2X3 receptor subunits is up regulated by chronic hypoxia. This up-regulation in the expression profiles of the P2X subunits in type I cells strongly suggests that ATP plays a presynaptic role in modulating neurotransmitter release from these cells during acclimatization to hypoxia. Electrophysiological studies are now required to test this idea at the functional level.

GENERAL CONCLUSION

Co-released ACh and ATP, acting on postsynaptic P2X2 and P2X3 receptors plays a major role in rat carotid body PO_2 chemotransmission (Zhang *et al.*, 2000). Homomeric P2X3 and P2X2 receptors, as well as heteromeric P2X2/P2X3 receptors mediate a major component of ATP-mediated responses in other systems (Lewis *et al.*, 1995; Collo *et al.*, 1996). The present study provides the first demonstration that carotid body chemoafferent neurons express mRNA for both P2X2 and P2X3 purinoceptor subunits. These experiments utilized RT-PCR, cloning and sequencing techniques on populations of freshly isolated petrosal neurons (Figure 1.3 and 1.5). This expression pattern is consistent with the idea that P2X2/P2X3 heteromultimeric receptors are the functional receptors, activated by ATP released as a co-transmitter from the chemoreceptor type I cells. This release of ATP occurs along with other excitatory neurotransmitters (e.g. ACh), which help mediate postsynaptic excitation of sensory afferent terminals during carotid body chemoexcitation by natural stimuli, e.g. hypoxia.

Moreover, P2X2 and P2X3 proteins co-localized in CB chemoafferent neurons (Figure 1.8), as demonstrated by serial confocal immunofluorescence. While these data alone do not exclude the possibility that homomeric P2X2 and P2X3 receptors may function in the same chemosensory neuron, the native receptors on identified functional neurons showed a slowly desensitizing response to α,β–methylene ATP (Buell *et al.*, 1996), a fact not readily explained by independent association of the two subunits into homomeric receptor complexes (Lewis *et al.*, 1995; Radford *et al.*, 1997).

However, it appears that expression levels of both P2X2 and P2X3 subunits develop in a parallel fashion, though there seems to be proportionally more P2X2 mRNA expression relative to P2X3 mRNA (Figure 2.5 *A* and 2.6 *A*). Since the carotid body is a major target for the petrosal ganglion, and P2X2/P2X3 heteromultimers appear to be the functional receptors in the CB chemoafferent pathway, this parallel P2X2/P2X3 expression pattern in the PG may simply reflect the molecular basis for assembling heteromeric proteins. This is also consistent with immunocytochemical data showing the majority of petrosal neurons co-express P2X2 and P2X3 proteins.

The mRNA levels for the P2X2 and P2X3 subunits in the PNs are increased by P-21 and show a trend, where the levels might progressively increase as the pathway matures. There seems to be a push and pull mechanism in the regulation of the chemotransduction pathway (after the first week of postnatal development). Both adenosine and dopamine have an overall inhibitory role in the chemotransduction pathway, while ATP and ACh have an excitatory role.

The current study examined the hypothesis that presynaptic receptors on type I cells are regulated by O_2 tension. In particular strong evidence was obtained that expression of P2X (P2X2 and P2X3) ATP-receptor subunits in type I clusters from perinatal rat CB was indeed up regulated by chronic hypoxia (Figure 3.2 and Figure 3.3). The P2X receptor subunits expressed in the type I cells are proposed to have a positive feedback effect on neurotransmitter release.

In the present study, quantitative RT-PCR was performed on type I cells incubated in chronic hypoxia for 11-14 days (Figure 3.2-3.4). Interestingly, there was a 2-fold

increase in the expression level of P2X2 mRNA in type I cells exposed to chronic hypoxia (CHox) when compared to normoxic (Nox) controls (Figure 3.3). The increase in P2X expression is also seen at the protein level, as demonstrated by confocal immunofluorescence (Figure 3.4). The up-regulation of the P2X receptor subunits during chronic hypoxia suggests that ATP may now act presynaptically (as well) and enhance neurotransmitter release from type I cells by a positive feedback process. This adaptation may in turn lead to an increase in carotid sinus nerve discharge and may contribute to enhanced chemosensitivity during ventilatory acclimatization to hypoxia (Stea *et al.*, 1995) (see Figure 1).

Immunofluorescence studies were carried out on cultured type I cells grown in medium containing dibutyryl cyclic AMP (a permeable analog of cAMP) or selective inhibitor of cAMP-dependent protein kinase (PKA blocker – KT5720) under normoxic and chronically hypoxic conditions, respectively (Figure 3.5, A-C and Figure 3.5, panel D-E). A slight increase in immunofluorescence intensity was observed in Nox type I cultures incubated with dibutyryl cAMP, but no difference in immunofluorescence intensity was observed in CHox cultures incubated with the selective PKA blocker. However, this assay may not be sensitive enough to draw firm conclusions.

In summary, these data provide strong evidence that the P2X2 and P2X3 mRNA and protein are expressed in the chemoafferent petrosal neurons. It also appears that the expression of both P2X2 and P2X3 receptor mRNA is up regulated by chronic hypoxia in type I cells, strongly suggesting that ATP plays a presynaptic role in modulating neurotransmitter release from these cells during acclimatization to hypoxia.

Figure 1. Schematic diagram of proposed schema for CB chemotransmission involving ATP, ACh, adenosine and DA. A decrease in Po_2 (i.e. hypoxia) (1) is sensed by CB type I cells which in turn (2) causes depolarization and an increase in intracellular Ca^{2+} leading to neurotransmitter release. ACh and ATP are co-released (3) from type I cells along with DA (4). ATP and ACh act via the P2X2/P2X3 heteromeric and nACh (6) receptors, respectively. Both ATP and ACh from rat CB type I cells bind receptors on postsynaptic chemoafferent petrosal neurons during hypoxic chemoexcitation and increase the carotid sinus discharge frequency leading to an increase in ventilation (7). Excess ATP in the synaptic cleft is degraded by ecto-ATPases (8) (either membrane bound or soluble) to adenosine, which can then act via the A1 receptors on the chemoafferent petrosal neurons sending an inhibitory signal (9). An inhibitory response is also elicited when DA binds postsynaptic D2 receptors (10). ACh (11) and ATP (12) also have presynaptic receptor's (P2X2/P2X3 and nACh) that have a positive effect on neurotransmitter release. Adenosine acting via the A2a receptors on type I cells modulates future release of ATP (13), whereas DA (via D2 receptors) inhibits neurotransmitter release (14). Both adenosine and dopamine have an overall inhibitory role in the chemotransduction pathway, while ATP and ACh have an excitatory role. ATP: adenosine triphosphate; ACh: Acetylcholine, DA dopamine; nACh: nicotinic acetylcholine receptor; P2X: purinergic receptors; PG: petrosal ganglion; CSN: carotid sinus nerve; CB: carotid body.

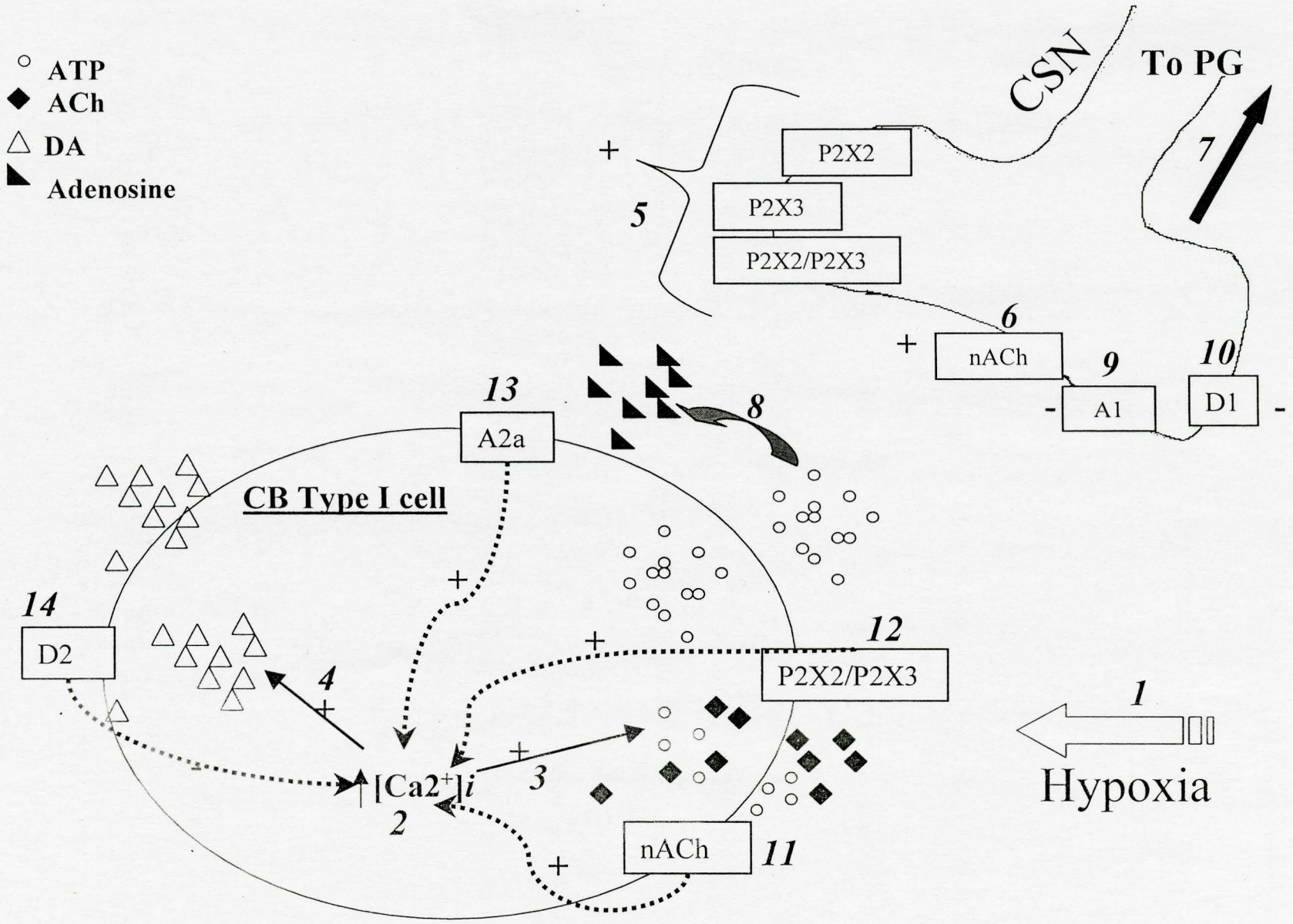
ATP
ACh
DA
Adenosine
CSN
To PG
7
+
5
P2X2
P2X3
P2X2/P2X3
6
+
nACh
9
10
-
A1
D1
-
13
A2a
8
CB Type I cell
14
D2
+
12
P2X2/P2X3
4
+
1
+
3
[Ca2+]i
2
Hypoxia
+
nACh
11

REFERENCES

ALBERTS, B., BRAY, D., LEWIS, J., ROBERTS, K. AND WATSON JD. (1994) In: Molecular Biology of The Cell. Garland Publishing, New York, NY.

BAIRAM, A, KHANDJIAN, EW. (1997). Expression of dopamine D2 receptor mRNA isoform in the carotid body of rat, cat and rabbit. *Brain Research* 760:287-289.

BAIRAM, A., FERENTTE, J., DAUPHIN, C., CARROLL, JL., KHANDJIAN, EW. (1998). Expression of dopamine D1-receptor mRNA in the carotid body of adult rabbits, cats and rats. *Neuroscience Research* 31:147-154.

BISCOE, TJ, DUCHEN MR, EISNER DA, O'NEILL SC, AND VALDEOLMILLOS M. (1989) Measurements of intracellular Ca^{2+} in dissociated type I cells of the rabbit carotid body. *Journal of Physiology (London)* 416:421-434.

BOYER, RF. (1993) In: Modern Experimental Biochemistry. Second Edition, Benjamin / Cummings, New York.

BRADY R, ZAIDI SI, MAYER C, KATZ DM. (1999). BDNF is a target-derived survival factor for arterial baroreceptor and chemoafferent primary sensory neurons. *Journal of Neuroscience* 19:2131-42.

BUCHMAN VL, DAVIES AM. (1993). Different neurotrophins are expressed and act in a developmental sequence to promote the survival of embryonic sensory neurons. *Development* 118:989-1001.

BUELL, G., COLLO, G. & RASSENDREN, F. (1996). P2X receptors: an emerging channel family. *European Journal of Neuroscience* 8:2221-2228.

BURNSTOCK G. (1972). Purinergic nerves. *Pharmacological Review* 24:509-581.

BURNSTOCK, G. (1997). The past, present and future of purine nucleotides as signalling molecules. *Neuropharmacology* 36:1127-1139.

BURNSTOCK, G. (2000) P2X receptors in sensory neurones. *British Journal of Anesthesiology* 84:476-88.

BURNSTOCK, G., WILLIAMS, M. (2000) P2 purinergic receptors: modulation of cell function and therapeutic potential. *The Journal of Pharmacology and Experimental Therapeutics* 295:862-869.

BUSTIN, SA. (2000). Absolute Quantification of mRNA using real-time reverse transcription polymerase chain reaction assays. *Journal of Molecular Endocrinology* 25:169-193.

CARROL JL, BAMFORD OW, AND FITZGERALD RS. (1993). Postnatal maturation of carotid chemoreceptor responses to O2 and CO2 in cat. *Journal of Applied Physiology* 75:2383-2391.

CHEN, J, DINGER B AND FIDONE SJ. (1997). cAMP production in rabbit carotid body: role of adenosine. *Journal of Applied Physiology* 82:1771–1775.

CHEN J, HE L, DINGER B, FIDONE S. (2000) Pharmacological effects of endothelin in rat carotid body. Activation of second messenger pathways and potentiation of chemoreceptor activity. *Advances in Experimental Medical Biology* 475:517-25.

COLLO, G., NORTH, R.A., KAWASHIMA, E., MERLO-PICH, E., NEIDHART, S., SURPRENANT, A. & BUELL, G. (1996). Cloning of P2X5 and P2X6 receptors and the distribution and properties of an extended family of ATP-gated ion channels. *Journal of Neuroscience* 16:2495-2507.

CUNHA, RA. AND RIBEIRO, JA. (2000). ATP as a presynaptic modulator. *Life Sciences* 68:119-137.

DIAZ-HERNANDEZ, M, GOMEZ-VILLAFUERTES, R, HERNANDO F, PINTOR, J AND MORAS-PORTUGAL MT. (2001). Presence of different ATP receptors in rat midbrain single synaptic terminals. Involvement of the P2X3 subunits. *Neuroscience Letters* 301:159-162.

DONNELLY DF AND DOYLE TP (1994). Developmental changes in hypoxia-induced catecholamine release from rat carotid body, in vitro. *Journal of Physiology* (London) 475:267-275.

DONNELLY DF. (1995) Does catecholamine secretion mediate the hypoxia-induced increase in nerve activity? *Biological Signals* 4:304-9.

DONNELLY, DF. (2000). Developmental aspects of oxygen sensing by the carotid body. *Journal of Applied Physiology* 88:2296-2301.

DUNN PM, ZHONG Y, BURNSTOCK G. (2001). P2X receptors in peripheral neurons. *Progressive Neurobiology* 65:107-34.

ENNION S, HAGAN S, EVANS RJ. (2000) The role of positively charged amino acids in ATP recognition by human P2X1 receptors. *Journal of Biological Chemistry* 275:29361-29367.

ERICKSON, JT., CONOVER, JC, BORDAY V. CAMPAGNAT J, BARBACID M, YANCOPPULOUS G. KATZ, DM. (1996). Mice lacking brain derived neurotrophic factor exhibit visceral sensory neuron losses distinct from mice lacking NT4 and display severe developmental deficit in control of breathing. *Journal of Neuroscience* 16:5361-5371.

ERICKSON, JT., TERESA, A., BROSENITSCH, AND KATZ, DM. (2000). Brain derived neurotrophic factor and glial cell line-derived neurotrophic factor are required simultaneously for survival of dopaminergic primary sensory neurons in vivo. *Journal of Neuroscience* 21:581-589.

EYZAGUIRRE, C. AND ZAPAPTA, P. (1984) Perspective in carotid body research. *Journal of Applied Physiology* 57:931-57.

FIDONE SC, GONZALEZ C, YOSHIZAKI, K. (1982). Effects of low O_2 on release of DA from rabbit carotid body in vitro. *Journal of Physiology* 333:93-110.

FIDIONE SJ AND GONZALEZ C (1986). The Respiratory System, Vol (2). In: Handbook of Physiology (sect 3), ed. Fishman, AP., pp. 247-312. *American Physiology Society.*

FINELY, JCW, POLAK, J AND KATZ, DM. (1992). Transmitter diversity in carotid body afferent neurons: dopaminergic and peptidergic phenotypes. *Neuroscience* 51:973-987.

GAUDA EB, BAMFORD O, GERFEN CR. (1996) Developmental expression of tyrosine hydroxylase, D2-dopamine receptor and substance P genes in the carotid body of the rat. *Neuroscience* 75:969-77.

GAUDA, EB., BAMFORD, O. AND GERFEN, CR. (1997). Developmental expression of tyrosine hydroxylase D2-dopamine receptors and substance P genes in the carotid body of the rat. *Neuroscience* 75:969-977.

GAUDA, EB., NORTHINGTON, FJ., LINDEN, J. AND ROSIN, DL. (2000). Differential expression of A2a, A1- adenosine and D2-dopamine receptor genes in rat peripheral arterial chemoreceptors during postnatal development. *Brain Research* 272:1-10.

GONZALEZ, C., ALMARAZ, L., OBESO, A., & RIGUAL, R. (1994). Carotid body chemoreceptors: from natural stimuli to sensory discharges. *Physiological Reviews* 74:829-898.

GRIFFITHS, JF., JEFFERY, H., MILLER, DT., SUZUKI, RC. (1996) In: An introduction to Genetic Analysis, ed. Lewontin and Gelbart WM. W. H. Freeman and Company, New York.

HERTZBERG, T., HELLSTROM, S., LAGERCRANTZ, H. AND PEQUIGNOT, JM. (1990). Development of the arterial chemoreflex and turnover of carotid body catecholamines in the newborn rat. *Journal of Physiology* 425:211-225.

HUEY KA, POWELL FL. (2000). Time-dependent changes in dopamine D(2)-receptor mRNA in the arterial chemoreflex pathway with chronic hypoxia. *Molecular Brain Research* 75:264-70

JACKSON A, NURSE C. (1995). Plasticity in cultured carotid body chemoreceptors: environmental modulation of GAP-43 and neurofilament. *Journal of Neurobiology* 26:485-96.

JACKSON, A. AND COLIN NURSE. (1997). Dopaminergic properties of cultured rat carotid body chemoreceptors grown in Normoxic and Hypoxic environments. *Journal of Neurochemistry* 69:645-654.

JIANG LH, RASSENDREN F, SURPRENANT A, NORTH RA. (2000). Identification of amino acid residues contributing to the ATP binding site of a P2X receptor. *Journal of Biological Chemistry* 275:34190-34196.

KATZ, DM., & BLACK, I. B. (1986). Expression and regulation of catecholaminergic traits in primary sensory neurons; relationship to target innervation in vitro. *Journal of Neuroscience* 6:983-989.

KHAKH, B.S., BAO, X.R., LABARCA, C. & LESTER, H.A. (1999). Neuronal P2X transmitter-gated cation channels change their ion selectivity in seconds. *Nature Neuroscience*, 2:322-30.

Khakh, BS. (2001) Molecular physiology of P2X receptors and ATP signalling at synapses. *Nature Review Neurosciences* 2:165-174.

KHAKH BS, BURNSTOCK G, KENNEDY C, KING BF, NORTH RA, SEGUELA P, VOIGT M, HUMPHREY PP. (2001). International union of pharmacology. XXIV. Current status of the nomenclature and properties of P2X receptors and their subunits. *Pharmacological Review* 53:107-18.

KIM M, YOO OJ, CHOE S. (1997). Molecular assembly of the extracellular domain of P2X2 an ATP-gated ion channels. *Biochemical Biophysical Research Communication* 240:618-622.

KING, B.F., TOWNSEND-NICHOLSON, A., WILDMAN, S.S., THOMAS, T., SPYER, K.M. & BURNSTOCK, G. (2000). Coexpression of rat P2X2 and P2X6 subunits in Xenopus Oocytes. *Journal of Neuroscience*, 20:4871-4677.

KOBAYASHI, S., CONFORTI, L. AND MILLHORN, DE. (2000). Gene expression and function of adenosine A_{2A} receptor in the rat carotid body. *American Journal of Physiology Lung Cell Molecular Physiology* 279:l273-L282.

KOSHIMIZU, T *(el al).* (1999). Contributions of C-terminal domain to the control of P2X receptor desensitization. *Journal of Biological Chemistry* 274:37651-37657.

KRAMER, M, F. AND COEN, DM.: Current Protocols on Molecular Biology (1999). sections: 15.1, 15.2, 15.3, 6.3-6.13, A.1- A. 2, B. 23, 1.25-1.28, B. 22, E. 10 –E.11, E.16, 1.42-1.46, 1.33-1.35.

LAHIRI, A., ROZANOV, C. AND CHERNIACK, NS. (2000). Alerted structure and function of the carotid body at high altitude and associated chemoreflexes. *High Altitude Medicine and Biology* 1:63-74.

LEE JJ, TALUBMOOK C, PARSONS ME. (2001) Activation of presynaptic A1-receptors by endogenous adenosine inhibits acetylcholine release in the guinea-pig ileum. *Journal of Autonomic Pharmacology* 21:29-38.

LEHNINGER, A. L., NELSON. D. AND COX, MM. (1993) In: Principles of Biochemistry, 2nd ed. Worth Publishers, New York.

LEMASTER AM, KRIMM RF, DAVIS BM, NOEL T, FORBES ME, JOHNSON JE, ALBERS KM. (1999). Overexpression of brain-derived neurotrophic factor enhances sensory innervation and selectively increases neuron number. *Journal of Neuroscience* 19:5919-31.

LEWIS, C., NELDHART, S., HOLY, C., NORTH, R.A., BUELL, G. & SURPRENANT, A. (1995). Coexpression of P2X2 and P2X3 receptor subunits can account for ATP-gated currents in sensory neurons. *Nature* 377:432-435.

LIU M, KING BF, DUNN PM, RONG W, TOWNSEND-NICHOLSON A, BURNSTOCK G. (2001). Coexpression of P2X(3) and P2X(2) receptor subunits in varying amounts generates heterogeneous populations of P2X receptors that evoke a spectrum of agonist responses comparable to that seen in sensory neurons. *The Journal of Pharmacology and Experimental Therapeutics* 296:1043-1050.

LIU, X., ERNFORS, P., WU, H., JAENISCH, R. (1995). Sensory but not motor neuron deficits in mice lacking NT4 and BDNF. *Nature* 375:238-241.

LOPEZ-BARNEO, J, LOPEZ-LOPEZ JR, URENA J, AND GONZALEZ C. (1988) Chemotransduction in the carotid body: K^+ current modulated by PO_2 in type I chemoreceptor cells. *Science* 241:580-582.

LUO X, ZHENG W, YAN M, LEE MG, MUALLEM S. (1999). Multiple functional P2X and P2Y receptors in the luminal and basolateral membranes of pancreatic duct cells. *American Journal of Physiology* 277:C205-C215.

MARCHAL F., BAIRAM A, HAOUZI P., CRANCE JP, DI GIULIO C, VERT P, AND LAHIRI S. (1992). Carotid chemoreceptor response to natural stimuli in newborn kitten. *Respiration Physiology* 87:183-193.

MCDONALD, DM. (1981). Peripheral chemoreceptors. Structure-function relationships of carotid bodies. In: Regulation of Breathing, edited by Hornbein, TF. New York: Dekker, pt 1, p.105-319.

MCDONDALD, DM. (1983). Morphology of the rat carotid sinus nerve. I. Course, connections, dimensions and ultrastructure. *Journal of Neurobiology* 12:345-372.

MILLS L, NURSE C. (1993). Chronic hypoxia in vitro increases volume of dissociated carotid body chemoreceptors. *Neuroreports* 4:619-22.

MONTERIRO, EC, VERA-CRUZ P MONTEIRO TC AND SILVA-E-SOUSA MA. (1996). Adenosine increase cAMP content of the rat carotid body in vitro. *Advance Experimental Medical Biology* 410:299-303.

NORTH, R.A. & BARNARD, E.A. (1997). Nucleotide receptors. *Current Opinions in Neurobiology* 7:346-357.

NORTH RA, SURPRENANT A. (2000). Pharmacology of cloned P2X receptors. *Annual Review Pharmacological Toxicology* 40:563-80.

NURSE CA. (1995). Carotid body adaptation to hypoxia: cellular and molecular mechanisms in vitro. *Biological Signals* 4:286-91.

NURSE, C.A. & ZHANG, M. (1999). Acetylcholine contributes to hypoxic chemotransmission in co-cultures of rat type 1 cells and petrosal neurons. *Respiration Physiology* 115:189-199.

OFFORD, J., CATTERALL, WA. (1989) Electrical activity, cAMP and cytosolic calcium regulate mRNA encoding sodium channels alpha subunits in rat muscle cells. *Neuron* 2:1447-1452.

PALMER, TM AND STIELES GL. (1994). The new biology of adenosine receptors. *Advance Enzymology. Related Area in Molecular Biology* 69:83-120.

PRABHAKAR NR, RUNOLD M, YAMAMOTO Y, LAGERCRANTZ H, VON EULER C. (1984). Effect of substance P antagonist on the hypoxia-induced carotid chemoreceptor activity. *Acta Physiol Scand* 121:301-3.

PRABHAKAR NR, KUMAR GK, CHANG CH, AGANI FH, HAXHIU MA. (1993). Nitric oxide in the sensory function of the carotid body. *Brain Research* 625:16-22.

PRABHAKAR, NR. (2000) Oxygen sensing by the carotid body chemoreceptors. *J Applied Physiology* 88:2287-95.

PRASAD, M., FEARON, I.M., ZHANG, M., LAING, M., VOLLMER C. AND NURSE, C.A. (2001) Expression of P2X2 and P2X3 purinoceptor subunits in carotid body chemoafferent neurons: Role in PO_2 and PCO_2 signaling. *Journal of Physiology (London)* (**currently in press**).

RASMUSSEN, R., MORRISON, T., HERRMANN, M., AND WITTWER, C. (1998) Quantitative PCR by continuous fluorescence monitoring of a double strand DNA specific binding dye. *Biochemica* 2.

RADFORD, K.M., VIRGINIO, C., SURPRENANT, A., NORTH, R.A. & KAWASHIMA, E. 1997). Baculovirus expression provides direct evidence for heteromeric assembly of P2X2 and P2X3 receptors. *Journal of Neuroscience* 17:6529-6533.

RALEIVC, V., AND BURNSTOCK, G. (1998). Receptors for purines and pyrimidines. *Pharmacological Reviews*. 50:413-92.

ROBINSON, TL. (1999). Molecular Markers of interstitial cells of CAJAL. *A Master of Science thesis.* McMaster University.

ROCHER, A., GONZALEZ C., ALMARAZ L. (1999). Adenosine inhibits L-type Ca^{2+} current and catecholamines release in rabbit carotid body chemoreceptor cells. *European Journal of Neuroscience* 99:673-681.

SALGADO AI, CUNHA RA, RIBEIRO JA. (2000). Facilitation by P(2) receptor activation of acetylcholine release from rat motor nerve terminals: interaction with presynaptic nicotinic receptors. *Brain Research* 877:245-50.

SAMBROOK, J., FRITSCH, E.F. & MANIATIS, T. (1989). In: Molecular Cloning: A laboratory Manual, second edition, Cold Spring Harbor, New York; Cold Spring Harbor Laboratory Press.

SEMENZA, GL. (1999). Perspectives on oxygen sensing. *Cell* 96:281-284.

SIMALOWSKI, A, BIJAK, M. (1987) Excitatory and inhibitory action of dopamine on hippocampal neurons in vitro. Involvement of D2 and D1 receptors. *Neuroscience* 23:95-101.

STEA, A, JACKSON A NURSE CA. (1992) Hypoxia and N6,O2'-dibutyryladenosine 3',5'-cyclic monophosphate, but not nerve growth factor, induce Na+ channels and hypertrophy in chromaffin-like arterial chemoreceptors. *Proceeding of the National Academy of Sciences U S A.* 89:9469-73.

STEA A, JACKSON A, MACINTYRE L, NURSE CA. (1995). Long-term modulation of inward currents in O2 chemoreceptors by chronic hypoxia and cyclic AMP in vitro. *Journal of Neuroscience* 15(3 Pt 2):2192-202.

SURPRENANT, A., BUELL, G.N. & NORTH R.A. (1995). P2X receptors bring new structure to ligand-gated ion channels. *Trends in Neuroscience* 18:224-229.

TORRES, G.E., EGAN, T.M. & VOIGT, M.M. (1999). Hetero-oligomeric assembly of P2X receptor subunits. *Journal of Biological Chemistry* 274: 6653-6659. (A)

TORRES, GE, TERRANCE M E AND VOIGT, MM. (1999). Identification of domain involved in ATP-gated ionotropic receptor subunit assembly. *The Journal of Biological Chemistry* 274:22359-22365. (B)

VIRGINIO C, NORTH RA, SURPRENANT A. (1998). Calcium permeability and block at homomeric and heteromeric P2X2 and P2X3 receptors, and P2X receptors in rat nodose neurons. *Journal of Physiology* 510:27-35.

VULCHANOVA, L., RIEDL, M.S., SHUSTER, S.J., BUELL, G., SURPRENANT, A., NORTH, R.A. & ELDE, R. (1997). Immunohistochemical study of the P2X2 and P2X3 receptor subunits in rat and monkey sensory neurons and their central terminals. *Neuropharmacology* 36:1229-1242.

WANG WJ, CHENG GF, YOSHIZAKI K, DINGER B AND FIDONE S (1991). The role of cAMP in chemoreception in the rabbit carotid body. *Brain Research* 540: 96-104.

WATSON, JD., GILMAN M., WITKOWSKI J. AND ZOLLER M. (1997). In: Recombinant DNA. Scientific American Books, W. H. Freeman and Company, New York.

WIERASZKO, A. GLODSMITH. G AND SEYFRIED TN. (1989). Stimulation-dependent release of adenosine triphosphate from hippocampal slices. *Brain Research* 485:244-250.

WITTWER CT, FILLMORE GC & HILLYARD DR. (1989). Automated polymerase chain reaction in capillary tubes with hot air. *Nucleic Acids Research* 17:4353-457.

ZAMORANO, PL., MAHESH VB., & BRANN DW. (1996). Quantitative RT-PCR for endocrine studies. *Neuroendocrinology* 63:397-497.

ZHANG M, NURSE CA. (2000) Does endogenous 5-HT mediate spontaneous rhythmic activity in chemoreceptor clusters of rat carotid body? *Brain Research* 872:199-203.

ZHANG, M., ZHONG, H., VOLLMER, C. & NURSE, C.A. (2000). Co-release of ATP and ACh mediate hypoxic signalling at rat carotid body chemoreceptors. *Journal of Physiology* 525:143-158.

ZHONG H, NURSE CA. (1997) Nicotinic acetylcholine sensitivity of rat petrosal sensory neurons in dissociated cell culture. *Brain Research* 766:153-61.

ZHONG, H., ZHANG, M. & NURSE, C.A. (1997). Synapse formation and hypoxic signalling in co-cultures of rat petrosal neurones and carotid body type 1 cells. *Journal of Physiology* 503:599-612.

ZHOU, Q., QUAIFE, CJ. PALMITER, RD. (1995). Target disruptions of the tyrosine hydroxylase gene reveals that catecholamines are required for mouse fetal development. *Nature* 347:640-643.

ZIMMERMANN, HERBERT. (1994). Signaling via ATP in the nervous system. *Trends in neuroscience* 17:420-426.

APPENDIX 1

EXPRESSION OF P2X SUBUNITS IN RAT ADRENAL MEDULLARY CHROMAFFIN CELLS

Unlike the carotid body which plays an important role in oxygen sensing throughout the lifespan of the organism (Gonzalez *et al.*, 1994), the chromaffin cells of the adrenal medulla play an important role during birth when the organism may encounter hypoxic stress. Adrenal medullary chromaffin cells (AMC) are exposed to ATP from two distinct sources: splanchnic nerve terminals where is it is co-released with ACh (Burnstock *et al.*, 1981) and from adjacent chromaffin cells. ATP is also found co-stored with catecholamines in the chromaffin cells at an ATP: catecholamine ratio of 1:4. Data presented by Hollins *et al.* (1997) reveal that expression of a P2X receptor functions as an auotreceptor capable of detecting vesicular release of ATP. There has been conflicting data on the expression of the P2X2 and P2X3 subunits in the AMC. Afework and Burnstock (2000) reported that no P2X immunoreactivity is seen in the adrenal gland of prenatal rats. However, they found that intrinsic adrenal neurons were positively stained for P2X2 and P2X3 receptors in postnatal day 17 rats (Afework and Burnstock, 1999). We propose that both P2X2 and P2X3 subunits are expressed in the AMC in the newborn period. We also tested this hypothesis on MAH cells, which are an immortal cell line derived for the sympathoadrenal precursor cells (i.e. a progenitor of adrenal chromaffin cells).

In order to establish the expression of the P2X subunits in rat adrenal chromaffin and MAH cells, RT-PCR and immunofluorescence techniques were used. Figure A.1

shows the expression pattern of P2X2 and P2X3 receptors in both these cells types. Figure A.2 is an immunofluorescence photomicrograph of the RAMCC (panel A-C) and MAH cells (panel D-F) immunostained with anti-P2X2 and anti-P2X3 antibodies. Table A.1 summarizes the expression profiles of various cell populations.

The distribution of P2X receptors subunits in the adrenal gland suggests a significant role for purine signaling in rat adrenal gland (Liu *et al.*, 1999). The occurrence of P2X receptors on presynaptic nerve fibers suggests that ATP might act as a pre-junctional modulator for the release of transmitters in the adrenal gland, in addition to their possible action as co-transmitter of the AMC's (Afework and Burnstock 1999).

Figure A.1 Detection of mRNA for P2X2, P2X3 and β-actin in rat AMC and MAH cells.

RT-PCR was carried out on isolated P-0 rat adrenal medullary chromaffin cells (RAMCC) and MAH cells using gene-specific primers for P2X2 and P2X3 receptors, and β-actin. Expected product sizes are (in bp): P2X2 (156), P2X3 (219), β-actin (327). The marker lane (M) shows bands at 100 bp increments with the 600 bp fragment at increased intensity. In negative control reactions without the RT enzyme (-), no PCR products were observed. The 2 % agarose gel was stained with ethidium bromide and viewed under UV illumination.

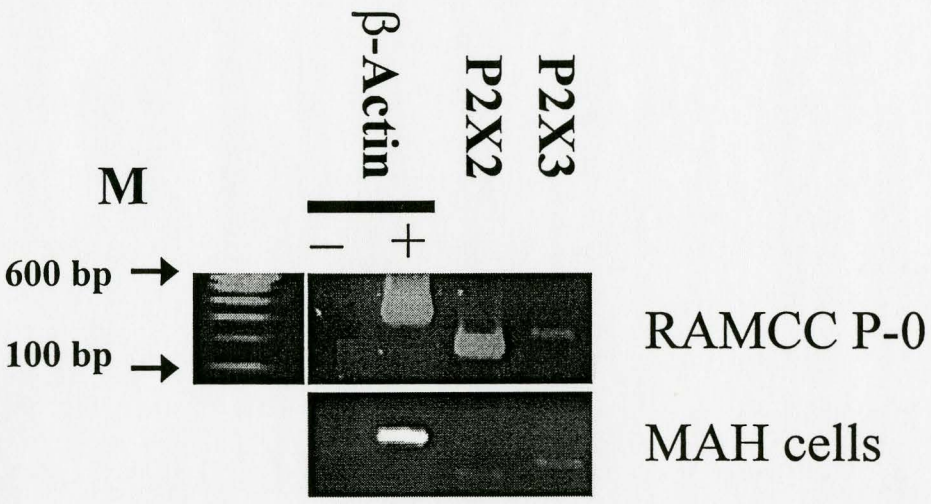
M
600 bp
100 bp
β-Actin
P2X2
P2X3
−
+
RAMCC P-0
MAH cells

Figure A.2 Expression of P2X2 and P2X3 subunits in cultured rat adrenal medullary chromaffin (AMC) and an immortalized AMC cell line (MAH cells) as revealed by Confocal Immunofluorescence.

A-C represent the same cultured rat AMC clusters from a P-0 pup, after immunostaining with antibodies against P2X2 and P2X3 receptor subunits. Localization of P2X2 (**A**) and P2X3 (**B**) subunits is revealed by Cy3 and FITC – conjugated secondary antibodies, respectively; dual exposure in (**C**) shows overlap of P2X2 and P2X3 staining. **D-F** represent the same microscopic field of MAH cells, after similar immunostaining with P2X2 and P2X3 antibodies as in **A-C**. Calibration bar represents 40 μm in A-C, and 20 μm in C-F.

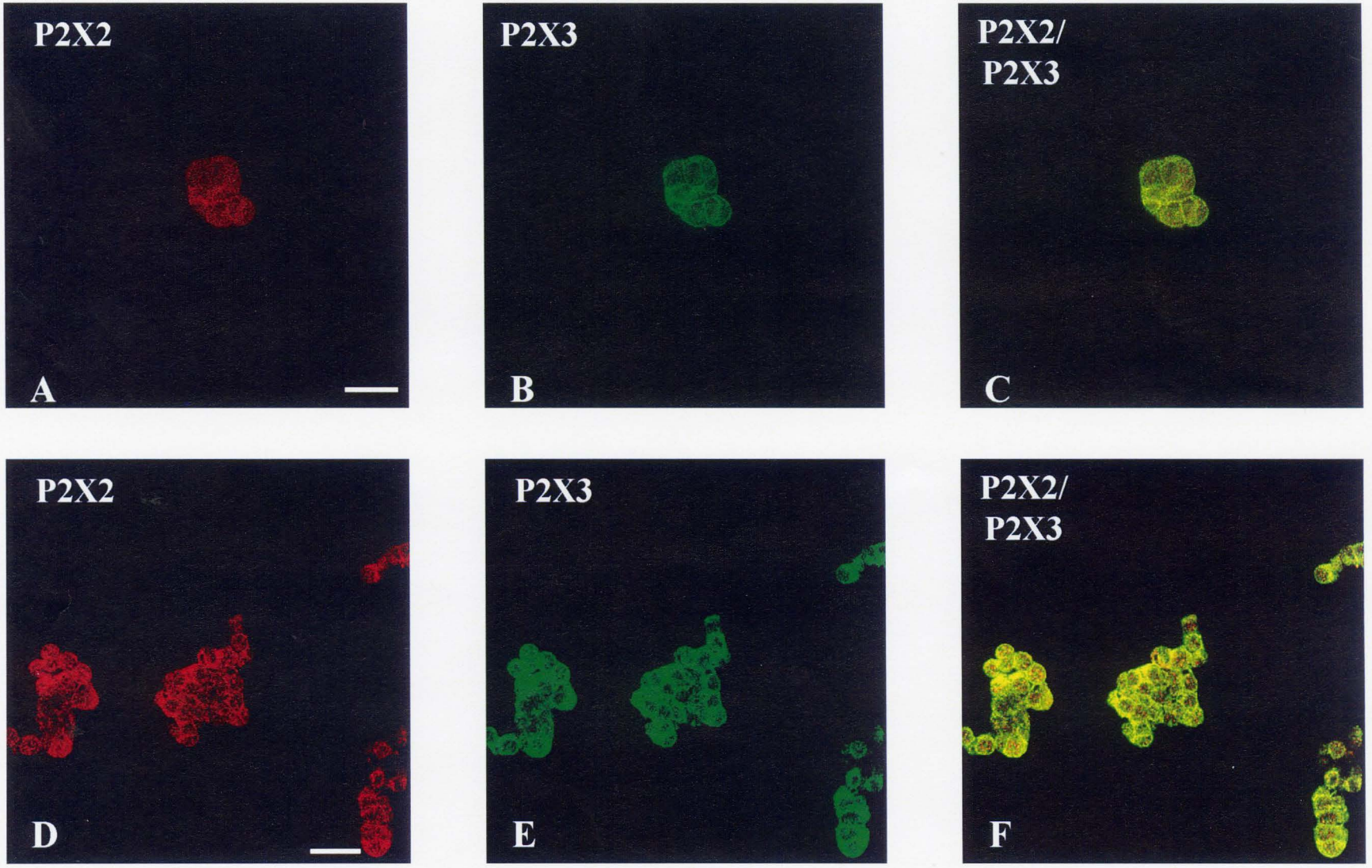
P2X2
A
P2X3
B
P2X2/
P2X3
C
P2X2
D
P2X3
E
P2X2/
P2X3
F

Table A.1 Expression of P2X2 and P2X3 subunits in various cell types

The table lists the expression profiles of P2X2 and P2X3 receptor subunits in various cell populations. The plus sign indicates the intensity for the bands observed on a 2% agarose gel stained with ethidium bromide; + very faint; ++ faint; +++ bright. The band intensities indicated are dependent on typical reactions performed on each of these cell types (n = 2). **RAMCC** – rat adrenal medullary chromaffin cells; **MAH** - immortal cell line derived from embryonic day 14 sympathoadrenal chromaffin precursor cells.

Table A.1 Expression of P2X2 and P2X3 subunits in various cell types

Cell Type	ß- Actin	P2X2	P2X3
Petrosal Ganglion P-9	+++	+++	+++
Carotid Body P-9	+++	+++	+++
Type I cell clusters P-0	+++	+++	++
Type I cell clusters P-9	+++	++	+
Nodose P-9	+++	+++	+++
RAMCC P-0	+++	+++	++
MAH	+++	+++	+++

+++ = bright band
++ = faint band
+ = very faint band

REFERENCES

AFEWORK M, BURNSTOCK G. (1999) Distribution of P2X receptors in the rat adrenal gland. *Cell Tissue Research* 298:449-56.

AFEWORK M, BURNSTOCK G. (2000) Age-related changes in the localization of P2X (nucleotide) receptors in the rat adrenal gland. *International Journal of Developmental Neuroscience* 18: 515-20.

HOLLINS B, IKEDA SR. (1997) Heterologous expression of a P2x-purinoceptor in rat chromaffin cells detects vesicular ATP release. *Journal of Neurophysiology.* 78:3069-76.

LIU M, DUNN PM, KING BF, BURNSTOCK G. (1999) Rat chromaffin cells lack P2X receptors while those of the guinea-pig express a P2X receptor with novel pharmacology. *British Journal of Pharmacology* 128:61-8.